Optimization Strategies for the Synthesis / Design of Highly Coupled, Highly Dynamic Energy Systems

Jules Ricardo Muñoz Guevara

Dissertation Submitted to the Faculty of
Virginia Polytechnic Institute and State University
in partial fulfillment of the requirements for the degree of

DOCTOR OF PHILOSOPHY
in
Mechanical Engineering

Dr. Michael von Spakovsky, Chair
Dr. Walter O'Brien
Dr. Michael Ellis
Dr. Peter King
Dr. Benoît Olsommer

Blacksburg, VA

September 29, 2000

Keywords: optimization, decomposition, thermoeconomics, exergy, MDO

Abstract

In this work several decomposition strategies for the synthesis / design optimization of highly coupled, highly dynamic energy systems are formally presented and their implementation illustrated. The methods are based on the autonomous optimization of the individual units (components, sub-systems or disciplines), while maintaining energy and cost links between all units, which make up the overall system. All of the approaches are designed to enhance current engineering synthesis / design practices in that: they support the analysis of systems and optimization in a modular way, the results at every step are feasible and constitute an improvement over the initial design state, the groups in charge of the different unit designs are allowed to work concurrently, and permit any level of complexity as to the modeling and optimization of the units.

All of the decomposition methods use the Optimum Response Surface (ORS) of the problem as a basis for analysis. The ORS is a representation of the optimum objective function for various values of the functions that couple the system units[1]. The complete ORS or an approximation thereof can be used in ways, which lead to different methods. The first decomposition method called the Local Global Optimization (LGO) method requires the creation of the entire ORS by carrying out multiple unit optimizations for various combinations of values of the coupling functions. The creation of the ORS is followed by a system-level optimization in which the best combination of values for the coupling functions is sought

The second decomposition method is called the Iterative Local Global Optimization (ILGO) scheme. In the ILGO method an initial point on the ORS is found, i.e. the unit optimizations are performed for initial arbitrary values of the coupling

[1] Note that when these coupling functions are represented by descrete variables, multiple ORSs may exist.

functions. A linear approximation of the ORS about that initial point is then used to guide the selection of new values for the coupling functions that guarantee an improvement upon the initial design. The process is repeated until no further improvement is achieved. The mathematical properties of the methods depend on the convexity of the ORS, which in turn is affected by the choice of thermodynamic properties used to charecterize the couplings. Examples in the aircraft industry are used to illustrate the application and properties of the methods.

A mi Abuelita en el cielo

Acknowledgements

This work would not have been possible without the help of numerous people. Firstly, I would like to thank my advisor, Dr. Michael von Spakovsky, for providing me the opportunity to come to Virginia Tech and conduct this research. Dr. von Spakovsky's trust and faith in my capabilities were invaluable. Many thanks to Drs. Walter O'Brien, Michael Ellis, Benoît Olsommer, Peter King, and Yehia El-Sayed for serving in my committee and for the valuable input they have given me over the course of this research. The conversations Dr. Olsommer and I had during these last years were very illuminating.

I am indebted to Tom Cunningham who helped a great deal in putting the engine model together, and to Richard Smith and Roland Watts of AFRL who helped in the painstaking labor of gathering information for constructing the ECS models. Many thanks are due to Mike Tong of NASA of Glenn Research Center for his help with the implementation of WATE. The comments and suggestions made by Jim Louviere of LMTAS are greatly appreciated. I would also like to thank Honeywell Engines and Systems for allowing us to use their excellent FAST software.

The list of people in my family and friends who have helped me throughout the years is just too long to write in detail. I have been blessed with good people who have been with me in good and bad times. They should share the pride I feel because they are a big part of what I have been able to accomplish.

This work was conducted under the sponsorship of the U.S. Air Force Office of Scientific Research.

Table of Contents

List of Figures

List of Tables

Nomenclature

A	Speed of sound	*LPT*	Low pressure turbine
A	Area	M	Mach number
AAF	Air-to-Air Fighter	*mil*	Military
BCA	Best cruise altitude	*mmn*	Maximum Mach number
BCM	Best cruise Mach Number	*MINLP*	Mixed integer non-linear programming problem
bleed	ECS bleed	*MILP*	Mixed integer linear programming problem
BP	Bleed port	N	Number of turns
C	Objective function, cost	n	Load factor
$\dot{C}$	Cost rate	O	Number of operational variables
cac	Combat acceleration	P	Product
C_L	Lift coefficient	$p\ \dot{p}$	Product rate
C_D	Drag coefficient	$p, \vec{p}$	Forward feedback function, product vector
C_{D0}	Drag coefficient at zero lift	*PPAY*	Permanent payload
ct_1	Combat turn 1	*PR*	Pressure ratio
ct_2	Combat turn 2	*PS*	Propulsion Sub-system
d	Number of design variables	q	Load factor
D	Drag	R	External input, resource,
E	Exergy, energy	r	Intermediate resource

ECS	Environmental Control Sub-System
EPAY	Expendable payload
esc	Escape dash
f	Objective function, feedback vector
F	"Uninstalled" thrust
g	Acceleration of gravity
G, g	Vector of inequality constraints
h	Altitude
H,h	Vector of inequality constraints
HX	Heat exchanger
HPC	High pressure compressor
HPT	High pressure turbine
HX	Heat exchanger
ILGO	Iterative Local-Global Optimization
K	Constant
K	Constant
LCC	Life cycle cost
loi	Loiter
R	Additional or "parasitic" drag
Re	Reynolds number
RFP	Request for proposal
S	Wing planform area
SL	Sea level
Sp	Vehicle speed in kilonots
SS	Structures Sub-system
t	Time
T	"Installed" thrust, total time for the set of load/environmental conditions
V	Velocity
u	Coupling function
WATE	Weight Analysis of Turbine Engines
v	Vector of flow and thermodynamic variables
w	Vector of geometrical variables
x	Vector of design variables
y	Vector of operational variables
Z	Capital function (weight, cost)

Greek

Superscripts

α	Step size, thrust fraction, engine bypass ratio
β	Weight fraction
δ	Design point
ε	Small number
ϕ	Inlet and nozzle drag coefficients
γ	Specific heat ratio, input function
Γ	Vector or inequality constraints for dynamic energy systems
H	Vector or equality constraints (analysis system of equations) for dynamic systems
φ	Stall margin (%)
λ, Λ	Marginal cost, vector of marginal costs
π	Leg weight ratio
τ	Number of time segments into which the set of load/environmental conditions is divided
ξ	Value of a coupling function
ψ	Value of a coupling function
Y	Vector or operational decision variables for dynamic energy systems
ζ	Cost function

o	Reference, initial value
**	Optimum
p	Capital
*	Restricted optimum
◊	Feasible and “promising” solution

Subscripts

decs	ECS drag
f	Fuel
it	Inlet temperature
o	Reference, initial value
wecs	ECS weight
0	Ambient
*	Optimum

Chapter 1

Introduction

As the level of interaction between the various sub-systems of energy systems has increasingly become complex, the more important the need has become to carry out the synthesis / design of the system in a completely integrated fashion in order that the demands imposed by all the sub-systems be accommodated in the best way possible. Unfortunately, when developing new systems or operating existing ones, the lack of comprehensive synthesis / design tools forces today's engineer to rely heavily on rules-of-thumb, individual experience and a fairly non-integrated, non-interdisciplinary approach of basic calculations, i.e. simple *trade-off analysis.* In cases where optimization is considered, partially due to the fact that new and more powerful computers have become available and optimization tools more popular, it is seen as a straightforward mathematical problem, which for large-scale, highly non-linear optimization problems can be very limiting to say the least. Even significant increases in computational power are not sufficient to offset the ever increasing complexity of energy systems and the ensuing synthesis / design problem. Therefore, the need for methods that permit effective solutions of large-scale optimization problems is still an area of research, which generates great interest.

The need for more complex, efficient, and cost effective systems makes it imperative not only to analyze a greater number of possible configurations and technologies but also to synthesize / design systems in a way which optimizes these

systems taking into account load and environmental variations over time. This contrasts with the common practice of designing a system for a single design point (typically chosen to be close to the most demanding operating point) followed by a verification of proper operation at off-design.

In formulating the entire synthesis / design problem (i.e. identifying all the interacting sub-systems, choosing the possible configurations and decision variables, and defining the physical constraints), it may turn out that solving the entire problem as a single problem (as opposed to solving a set of multiple problems) is simply impractical. The reasons are multiple:

- The number of decision variables involved may be simply be too large for an efficient solution. In fact, given the current state of mathematical optimization, a solution may not be obtainable at all in the most complex cases.
- A single group of engineers may not possess all the expertise required for dealing with the technologies, sub-systems, and components involved in the problem.
- The integration of different computer codes, which simulate different aspects of the system, may be difficult. This is even more the case if such codes are written on entirely different platforms. In addition, these codes may not be available for use to all the members of the entire team (i.e. not all sub-teams may have access).
- Even in cases when code integration is possible, the overhead is simply too great to make the optimization viable. This is especially the case if the simulation tools are computationally expensive to use (e.g., as is often the case with CFD codes).
- The synthesis / design of the different sub-systems may, in many cases, be done at different stages and times, crossing company lines. Furthermore, it is not uncommon to have design teams that are not located entirely at one facility, which added to cultural differences, complicates the task at hand even further.

1.1 OBJECTIVES

Based on the discussion presented above, it is clear that there exists a need for a general methodology that will permit the integrated synthesis / design optimization of energy systems. The required method should not only allow for the solution of the overall synthesis / design problem by dividing it into smaller sub-problems but facilitate as well the difficult task of sub-system integration. The objective of this work is to fill that void by developing a decomposition optimization strategy for energy system synthesis / design that has the following required features:

- is capable of using dissimilar modeling codes, possibly written on different platforms;
- effectively deals with the synthesis problem (i.e. deals with the presence of integer and binary variables) so that advanced optimization algorithms to solve the complex mixed-integer problem (typically non-linear) are supported;
- is modular so that analyses and optimizations can be divided to the greatest extent possible into clearly separated tasks assigned to specialty organizations;
- permits geographically dispersed organizations to carry out optimization tasks aimed at optimizing the entire system; thus, the method must allow for each organization to influence the other organizations' tasks while retaining responsiblities for its own objectives;
- requires the minimum possible number of repetitions (i.e. re-optimizations);
- supports concurrent and parallel tasks;
- integrates as many parameters as possible within each sub-problem but not so many that it cannot be adequately defined and solved;
- is sufficiently general to handle systems in both stationary or aircraft/aerospace applications;

- supports multiple design points (i.e. can be used in dynamic systems);
- guarantees, in the event of a premature halt in the process, a solution which is an improvement over the initial synthesis / design.

In addition to the above set of requirements, the proposed methodology should shed some light on the usefulness of 2nd Law quantities for optimization purposes (Newberry, 2000; Bejan, 2000; Paulus and Gaggioli, 2000).

Finally, it is assumed in what follows that system modeling requires a high level of detail (and is, therefore, expensive to simulate and optimize) and involves large numbers of independent continuous and discrete variables. In this work, the synthesis / design problem is set up in a general way so that streams and feedback may be represented by energy (or exergy) or by any other relevant quantity, depending on which better facilitates the interface between energy as well as non-energy sub-systems.

1.2 ORIGINAL CONTRIBUTIONS / PRACTICAL IMPACT

The originality of the proposed research is that it will provide the mathematical foundations for a completely general approach to the use of deomposition in large-scale optimization applied to the dynamic MINLP problem, irrespective of whether a system is energy-based or not. This will have an immediate practical impact on the way energy systems in general and aircraft/aerospace energy systems in particular are synthesized, designed and operated in that it will

- advance the state-of-the-art beyond simple trade-off analysis, bringing the power of real optimization to the complex synthesis / design problem of dynamic energy systems;
- allow for the decomposed optimization of sub-systems and components, thus simplifying the optimization problem without compromising the number of degrees of freedom possible;

- effectively deal with the complex problem of sub-system integration;
- incorporate the highly dynamic nature of energy systems operation into the synthesis / design process through appropriate modeling and decomposition tools;
- provide the framework to naturally incorporate advanced simulation tools (e.g., CFD analyses) into the synthesis / design problem, allowing, for example, detailed analyses of the influence of different sources of irreversibilities on the synthesis and design of components, sub-systems and systems;
- establish the necessary and sufficient conditions for system level synthesis / design optimization
- easily be implemented into existing synthesis / design environments.

Chapter 2

Background

This chapter deals with the mathematical, algorithmic, and computational tools that are required to transform a set of synthesis / design requirements into a workable and eventually optimum energy system.

2.1 NONLINEAR CONSTRAINED OPTIMIZATION

A focus of this work is the solution of nonlinear optimization problems with equality and inequality constraints. These problems are of the form

Minimize $f(\vec{x})$ (2.1)

with respect to $\vec{x}$ and subject to the following equality and inequality constraints:

$$\vec{h}(\vec{x}) = \vec{0} \tag{2.1.1}$$

$$\vec{g}(\vec{x}) \leq \vec{0} \tag{2.1.2}$$

Note that an inequality constraint $g_j \leq 0$ is active if $g_j = 0$. By definition all equality constraints are active.

The first order necessary conditions for a point to be a local minimum are called the Karush-Kuhn-Tucker or Kuhn-Tucker conditions. The conditions are stated in the following theorem:

2.1.1 The Lagrange Multiplier Theorem

Let $\vec{x}^*$ be local minimizer for problem (2.1). Then there exist vectors $\vec{\lambda}^*$ and $\vec{\mu}^*$ such that

1. $\vec{\mu}^* \geq \vec{0}$ (2.1.3)

2. $\nabla f(\vec{x}^*) + \vec{\lambda}^{*T} \nabla \vec{h}(\vec{x}^*) + \vec{\mu}^{*T} \nabla \vec{g}(\vec{x}) = \vec{0}$ (2.1.4)

3. $\vec{\mu}^{*T} \vec{g}(\vec{x}) = \vec{0}$ (2.1.5)

We normally refer to $\vec{\lambda}^*$ and $\vec{\mu}^*$ as the Lagrange multiplier vectors of equality and inequality constraints. In the literature, $\vec{\mu}^*$ is sometimes called the Karush-Kuhn-Tucker multipliers.

In addition to these first order necessary conditions for a local minimum, first order sufficiency conditions, which guarantee that the local minimizer $\vec{x}^*$ is a global minimizer, also exist. These additional conditions place certain restrictions of convexity or concavity on the objective function $f(\vec{x})$ and the equality and inequality functions $\vec{h}(\vec{x})$ and $\vec{g}(\vec{x})$, respectively. For a detailed discussion of these conditions and others, the reader is referred to Floudas (1995).

All of the conditions briefly outlined above lay the foundations of optimality for the non-linear optimization (programming) problem, problem (2.1). In practice, these conditions, expecially those for sufficiency, are oftentimes difficult if not impossible to meet. Thus, an effective search of the space of all possible solutions is fraught with the uncertainties of knowing where the global optimum or a set of near-global optimums lie(s).

2.2 BASIC ELEMENTS OF ENERGY SYSTEM OPTIMIZATION

The synthesis / design problem comprises two major elements: posing the problem as a set of mathematical statements amenable to solution and defining a strategy for solving the problem after it has been posed.

2.2.1 Modeling of an Energy System

The modeling of an engineering system typically begins with the selection of a number of degrees of freedom represented by parameters which can be varied at will within acceptable limits. These independent parameters or variables, hereby represented by a vector $\vec{x}$, are then used to create two systems of equations to represent the system, i.e.

$$\vec{H} = \begin{Bmatrix} \vec{h}_1(\vec{x}) \\ \vec{h}_2(\vec{x}) \\ \vec{h}_3(\vec{x}) \\ \vdots \\ \vec{h}_n(\vec{x}) \end{Bmatrix} = \vec{0} \tag{2.2}$$

$$\vec{G} = \begin{Bmatrix} \vec{g}_1(\vec{x}) \\ \vec{g}_2(\vec{x}) \\ \vec{g}_3(\vec{x}) \\ \vdots \\ \vec{g}_n(\vec{x}) \end{Bmatrix} \leq \vec{0} \tag{2.3}$$

The vector of equality constraints $\vec{H}$ is composed of sub-vectors $\vec{h}_i$ each of which mathematically describes a phenomenon usually within the realm of a particular discipline. The elements of the sub-vectors $\vec{h}_i$ are known as the *state* equations. For energy systems, a number of different disciplines are represented by $\vec{H}$, the most

common being the thermal sciences, materials, controls, and economics[2]. The vector of inequality constraints $\vec{G}$ represents natural or artificial limitations imposed upon the system.

Any arbitrary vector $\vec{x}$ may not satisfy the constraints imposed by equations (2.2) and (2.3). The residuals in the state equations are the elements of the vectors $\vec{r}_1$ and $\vec{r}_2$. In this case, equations (2.2) and (2.3) act as system *evaluators*. A feasible solution is one that has a vector of independent variables that identically satisfies equations (2.2) and (2.3), and, therefore, has no residuals. The process of finding a vector that leads to a feasible solution is typically iterative. The speed of this process is typically slow because in practical systems the size of $\vec{x}$ is large and the systems of equations (2.2) and (2.3) are highly non-linear. A system evaluator coupled to the iterative scheme just described is called a system *analyzer*.

The representation of the relevant phenomena is accomplished by means of the software implementation of the mathematical models of the system. For obvious practical reasons, different "codes" are developed with each representing a particular aspect of the system. Thus, it is common to talk about thermodynamic, sizing, CFD, or costing codes, although some exceptions exist. Examples of the latter are codes that are capable of blending in a single analysis fluid mechanics, heat transfer and stress analysis. In addition, for reasons having to do with company organization, codes for different types of technologies, multi-disciplinary or not, are dissagregated. It is, therefore, common to have an engine code, a structures code, and so on.

It becomes evident that creating a complete model of an energy system requires solving the *organizational problem* that the codes mentioned above may pose (Sobieszczanski-Sobieski and Haftka, 1997). In addition, the couplings between

[2] In this work, the thermal sciences and economics are used directly. Controls are implicitly involved in the synthesis / design whenever there is a need for adjusting certain parameters over time. Physical limitations on the components or materials used are incorporated in the models by constraints.

disciplines and/or technologies normally require large amounts of data flow, which may lead to costly overhead. The organizational challenge is exacerbated even further by the need to couple software from different sources and possibly written on different platforms. The solution of this organizational problem, which is very often overlooked, is critical to being able to successfully carry out any synthesis / design effort and has a profound effect on how the optimization problem is formulated and solved as will be seen in the chapters that follow.

2.2.2 Basic Formulations for Energy System Analysis and Optimization[3]

Consider the energy system of Figure 2.1, which is composed of two units[4] or two disciplines.

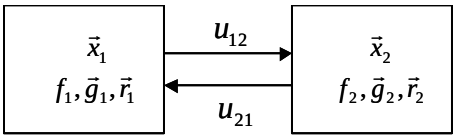

Figure 2.1 A simple system.

In the above figure, the $\vec{g}_i$ (i=1,2) are the vectors representing the limits or constraints imposed upon the units or disciplines; and the r_i are the residuals in the state equations. The vectors $\vec{u}_{12}$ and $\vec{u}_{21}$ are the coupling or linking functions. The two unit or discipline analyzers may be executed in parallel if values are set for the coupling functions, say $\vec{u}_{12}^{\,o}$ and $\vec{u}_{21}^{\,o}$.

In some cases, it is possible to define multiple objective functions simultaneously. The optimization is then carried out by assigning weights to each of them in order to obtain a unique objective. An area of mathematical optimization specializes in this type of multi-objective problems. In energy systems, one is typically concerned with a single objective function (e.g., cost, thermodynamic efficiency, fuel consumption, specific fuel

[3] In this section some of the terminology compiled by Balling and Sobieszczanski-Sobieski (1996) is used.

consumption, etc.). In this work the optimization problems are defined using one objective function. The scalars f_1 and f_2 are the contributions of units or disciplines 1 and 2 to the overall objective function f. Other objectives (e.g., range, acceleration, etc.) are then cast as constraints. The optimization problem is, therefore, stated as minimizing $f = f_1 + f_2$.

Assuming that the unit or discipline evaluators or analyzers are run independently of each other, a number of formulations are possible depending on whether a single or multiple level optimization is defined or a system evaluator or analyzer is used. Some of those combinations are presented below.

Single Level Optimization Type A

In the first combination, an optimizer is directly tied to all of the system evaluators

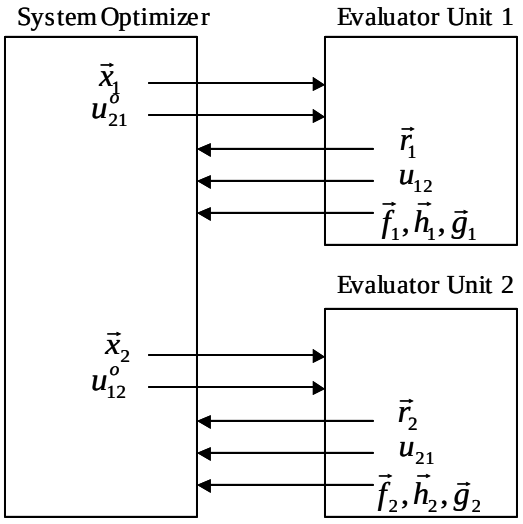

Figure 2.2 Single level optimization type A.

(see Figure 2.2). Thus, the synthesis / design problem is formally stated as

Minimize $f = f_1 + f_2$ (2.3)

---

[4] A unit refers to either a component or a sub-system.

w.r.t. $\vec{x}_1, \vec{x}_2$

subject to

$$\vec{G} = \begin{Bmatrix} \vec{g}_1 \\ \vec{g}_2 \end{Bmatrix} \leq \vec{0} \tag{2.4.1}$$

and $\vec{u}_{12} = \vec{u}_{12}^{\,o}, \qquad \vec{u}_{21} = \vec{u}_{21}^{\,o}$ (2.4.3)

$$\vec{r}_1 = \vec{0}, \qquad \vec{r}_2 = \vec{0} \tag{2.4.4}$$

For this combination, the system level optimizer is in charge of resolving the coupling between units and ensures the feasibility of the solutions (equations (2.4.4)). The implementation of the method is difficult if the size of the residual vectors or coupling functions is large or if more than two units / disciplines are involved.

Single Level Optimization Type B

For this combination, unit analyzers instead of evaluators are used (see Figure 2.3).

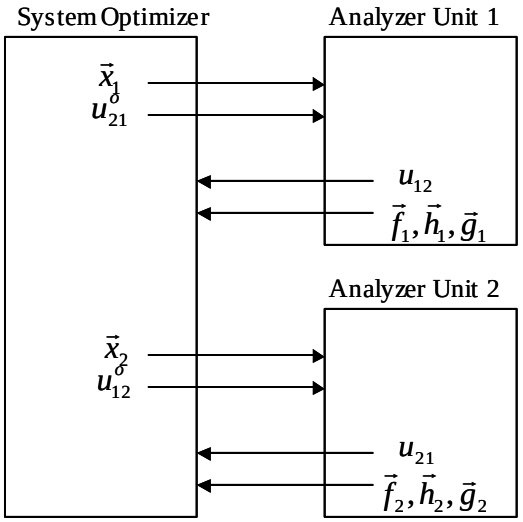

Figure 2.3 Single level optimization type B.

The problem formulation is identical to the previous combination with the exception of constraint (2.4.4), which does not apply in this case.

The two combinations just presented can be interpreted as an optimizer "wrapped around" the unit analyzers or evaluators. Practically speaking, a single group of analysts would need to maintain and operate all the elements of the system as well as the optimizer. Both approaches can be considered "all-at-once" approaches, which may pose additional difficulties if the number of independent variables is large.

Bi-Level Optimization Type A

This alternative formulation or combination uses a two-level optimization scheme as shown in Figure 2.4 below.

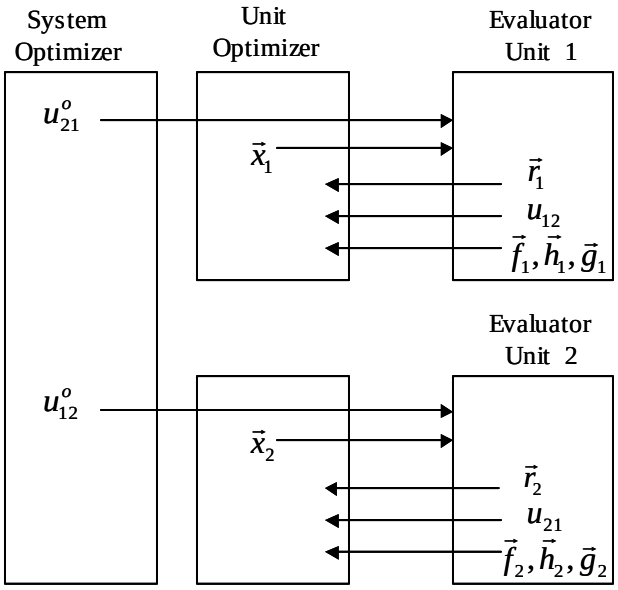

Figure 2.4 Bi-level optimization type A.

The system level problem is to

Minimize $f = f_1^* + f_2^*$ (2.4)

w.r.t. $\vec{u}_{12}, \vec{u}_{21}$

subject to $\vec{G} = \begin{Bmatrix} \vec{g}_1 \\ \vec{g}_2 \end{Bmatrix} \leq \vec{0}$ (2.5.1)

where, for example, f_1^* is the solution to the unit- or discipline-level problem given by

Minimize f_1 (2.5)

w.r.t. $\vec{x}_1$

subject to

$\vec{g}_1 \leq \vec{0}$ (2.5.1)

$\vec{r}_1 = \vec{0}$ (2.5.3)

Bi-Level Optimization Type B

The fourth possibility is identical to the previous one except that a unit analyzer is used instead of a unit evaluator (see Figure 2.5).

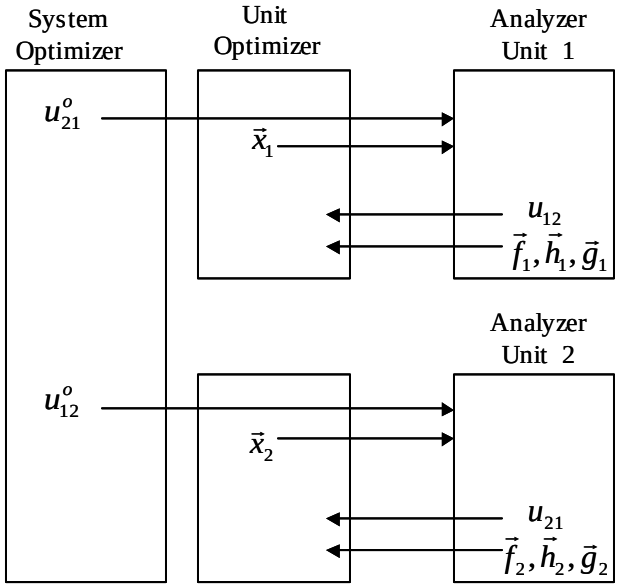

Figure 2.5 Bi-level optimization type B.

There are many possible implementations of the above combinations and they constitute the basis for the optimization algorithms developed in this work and presented in Chapter 4.

2.3 OPTIMIZATION ALGORITHMS

The optimization algorithm or optimization technique to be employed to solve the problems posed above depends on the type of optimization problem at hand. There are many possible ways of classifying optimization problems. The following is one such classification (Rao, 1996):

- Classification Based on the Existence of Constraints: any optimization problem may be classified as constrained or unconstrained, depending on whether or not constraints exist in the problem
- Classification Based on the Nature of the Decision (Independent) Variables: if the decision variables can be treated as parameters, the problem is classified as a static or parameteric optimization problem. If, on the other hand, the decision variables are represented by functions, the problem is called a trajectory optimization problem.
- Classification Based on the Nature of the Equations Involved: according to this classification, optimization problems can be linear, non-linear, geometric or quadratic programming problems. A problem is geometric if the objective function can be expressed as the sum of power terms (i.e. a polynomial). A quadratic problem is a non-linear programming problem with a quadratic objective function and linear constraints.
- Classification Based on the Permissible Values of the Independent Variables: depending on the values permitted for the decision variables, optimization problems can be classified as integer, real valued or mixed integer programming problems

- Classification Based on the Deterministic Nature of the Independent Variables: optimization problems can be classified as stochastic or deterministic programming problems.
- Classification Based on the Separability of the Functions: optimization problems can be classified as separable or nonseparable depending on whether the objective function or constraints functions can be written as the sum of n functions.
- Classification Based on the Number of Objective Functions: optimization problems can be classified as single and multi-objective programming problems

Most energy system synthesis / design optimization problems are single-objective, mixed integer, non-linear, deterministic optimization problems. Here we focus on techniques specifically developed to solve these types of problems. These techniques will be broadly divided into two categories: gradient-based algorithms and non-gradient-based algorithms.

2.3.1 Gradient-Based Algorithms

The gradient-based algorithms of optimization are a class of search methods for real-valued functions. These methods use the gradient of a given function as well as function values. Although most energy system synthesis / design problems are constrained, it is useful to start with a general description of the methods for unconstrained problems

Consider the unconstrained optimization problem

Minimize $f(\vec{x})$ (2.6)

w.r.t. $\vec{x}$

It can be shown (see, for example, Chong and Zak, 1996) that

$$f(\vec{x}^o - \alpha \nabla f(\vec{x}^o)) < f(\vec{x}^o) \quad (2.7)$$

for a sufficiently small step-size α. The resulting iterative algorithm is given by

$$\vec{x}^{k+1} = \vec{x}^{k} - \alpha_k \nabla f(\vec{x}^{k}) \tag{2.8}$$

One has the option of either taking very small steps and reevaluating the gradient at every step or taking large steps at any given point. The first approach results in a laborious method of reaching the system-level optimum, whereas the second may result in a more zigzag path for the optimizer. The choice of the step-size α_k leads to a number of algorithms: the steepest descent method, Newton and quasi-Newton methods (e.g., the Fletcher and Powell and the BFGS methods), conjugate direction methods (e.g., the methods of Fletcher-Reeves, Polar-Ribiere, and Hestenes-Stiefel).

A constrained optimization problem is defined as

Minimize $f(\vec{x})$ (2.9)

w.r.t. $\vec{x}$

subject to

$$\vec{g} \leq \vec{0} \tag{2.9.1}$$

A number of gradient-based methods exist for solving non-linear programming problems such as the one given above. Optimization methods that handle the constraints explicitly are known as direct methods. Indirect methods attempt to find an optimum by solving a sequence of unconstrained problems. Examples of the latter are the Interior ands Exterior Penalty and the Augmented Lagrange Multiplier methods. Examples of direct methods are the Sequential Linear and Quadratic programming methods, the Method of Feasible Directions (MFD), the Generalized Reduced Gradient Method, and the Rosen Projection Method. Two of the most popular methods are briefly described below.

Method of Feasible Directions (MFD)

The iterative algorithm that results from this method begins by choosing a feasible starting point and moving to a better point according to the iterative formula

$$\vec{x}^{k+1} = \vec{x}^{k} + \alpha \cdot \vec{S}^{k} \tag{2.10}$$

where $\vec{x}^{k}$ is the starting point, $\vec{S}^{k}$ is the direction of movement, and α is the step length. The value of α is chosen so that $\vec{x}^{k+1}$ lies in the feasible region. The search direction $\vec{S}^{k}$ is found such that (1) a small move in that direction does not violate any constraint and (2) the value of the objective function decreases in that direction. A vector $\vec{S}$ is a usable feasible direction if (Chong and Zak, 1996)

$$\frac{d}{d\alpha} f(\vec{x}^{k} + \alpha \cdot \vec{S})\Big|_{\alpha=0} = \vec{S}^{T} \nabla f(\vec{x}^{k}) < 0 \tag{2.11}$$

$$\frac{d}{d\alpha} g_{j}(\vec{x}^{k} + \alpha \cdot \vec{S})\Big|_{\alpha=0} = \vec{S}^{T} \nabla g_{j}(\vec{x}^{k}) \leq 0 \tag{2.12}$$

In the Zoutendijk's implementation of the method, the usable feasible direction is taken as the negative of the gradient direction if the initial point of the iteration lies in the interior, i.e.

$$\vec{S}^{k} = \nabla f(\vec{x}^{k}) \tag{2.13}$$

Otherwise, equations (2.12) and (2.13) are used to find an adequate search direction.

Sequential Quadratic Programming (SQP)

The SQP method has a theoretical basis that is related to the solution of a set of nonlinear equations using Newton's method and the derivation of simultaneous nonlinear equations using the Kuhn-Tucker conditions, which form the Lagrangian of

the constrained optimization problem. For a complete derivation of the method, see for example Rao (1996).

Algorithmically SQP is identical to equation (2.11) where the feasible search direction, $\vec{S}$, is found from solving the following quadratic problem, i.e. find the $\vec{S}$ which minimizes

$$Q(\vec{S}) = \nabla f(\vec{x})^T \vec{S} + \frac{1}{2}\vec{S}^T [\vec{H}]\vec{S} \tag{2.14}$$

subject to

$$\beta_j g_j(\vec{x}) + \nabla g_j(\vec{x})^T \vec{S} \le 0 \tag{2.15}$$

$$\beta_j h_j(\vec{x}) + \nabla h_j(\vec{x})^T \vec{S} = 0 \tag{2.16}$$

where $[\vec{H}]$ is a positive definite matrix that is taken initially as the identity matrix and is updated in subsequent iterations so as to converge to the Hessian matrix of the Lagrangian of the original problem (2.10). The last two constraints are linearized by taking $\beta_j = 1$ if $g_j(\vec{x}) \le 0$ and $\beta_j = 0.9$ if $g_j(\vec{x}) > 0$. Problem (2.14) is then easily solved using a linear quadratic programming algorithm.

2.3.2 Nongradient-Based Optimization Algorithms

Most practical energy system synthesis / design problems are characterized by mixed continuous-discrete variables, and discontinuous and nonconvex design surfaces. If standard nonlinear programming techniques such as the ones presented above are used exclusively for this type of problem, they will be inefficient and in most cases find a relative optimum that is closest to the starting point (i.e. a local minimum). In addition

to this, gradient-based methods can not use discrete variables since gradients with respect to integer numbers are not defined .

A number of methods circumvent the above problems by means of specialized search schemes. These types of algorithms specialize in performing a complete search of the entire synthesis / design space and as a consequence are often referred to as global search algorithms. Among these are rule-based expert systems and their more advanced implementations such as Tabu search and Hybrid expert systems. The latter are heuristic methods and have received considerable attention lately. However, the most popular and most developed methods for global search are Neural Networks, Simulated Annealing and Genetic Algorithms. Here we briefly describe the last two methods.

Simulated Annealing (SA)

Simulated Annealing is a combinatorial optimization technique based on random evaluations of the objective function in such a way that transitions out of a local minimum are possible. Although the method usually requires a large number of function evaluations to find the optimum solution, it will find the global optimum with a high probability even for ill-conditioned functions with numerous local minima. The name of the method is derived from the simulation of the thermal annealing of critically heated solids.

The implementation of the method typically starts with a feasible solution given by $\vec{x}_k$ and an associated value of the objective function f_k. A random walk is then made along each coordinate axis so that a new feasible solution with independent variables $\vec{x}_{k+1}$ is found. If the new value of the objective, f_{k+1}, is lower than f_k then the new point is immediately accepted. If that is not the case, the new point is accepted or rejected according to a criterion known as the Metropolis criterion (Kirkpatrick et al., 1983), which establishes that the probability of accepting the point is given by

$$P(\Delta f) = e^{-\Delta f / kT} \tag{2.17}$$

where $\Delta f = f_{k+1} - f_k$, k is a scaling factor analogous to the "Boltzmann constant" and T is a parameter analogous to "temperature". The algorithm starts with a high "temperature". A sequence of design vectors is generated until "thermal equilibrium" is reached, i.e. the value of f remains at a stable value as the iteration process progresses. Once "thermal equilibrium" is reached, a new sequence is started with the optimum value from the previous sequence and a lower "temperature". The process is repeated until a sufficiently low "temperature" is reached, at which stage no additional improvement can be expected. The choice of "temperatures" and scaling factors depend on a predetermined "cooling schedule". A number of cooling schedules have been studied in the literature (e.g., Hajek, 1988)

Genetic Algorithms (GAs)

Genetic Algorithms (GAs) are based on the principles of genetics and Darwin's theory of natural selection. The basic elements of natural genetics - crossover, mutation and selection - are used in the genetic search procedure. In Holland's original algorithm, GAs are characterized by bit string representations (chromosomes) of possible solutions to a given problem and by transformations used to vary those coded solutions. The algorithm is based on an elitist reproduction strategy where the individuals considered most fit are allowed to reproduce, thus, strengthening the chromosomal makeup of the new generation. Although many schemes to represent syntheses / designs as chromosome-like strings are possible (Hajela, 1999), the most popular is to use binary quantities[5]. Thus, each synthesis / design variable is represented as strings of 0s and 1s, with the string length defining the desired precision. A number of such strings constitute a population of syntheses / designs. The recommended number of individuals in a

[5] Note, that depending on the application, other representations, e.g., floating point numbers, maybe more appropriate or useful than using a binary representation. An example of this is found in Olsommer et al. (1999a).

population is in the range 2n to 4n, where n is the number of independent variables (Rao, 1996). Each has a corresponding fitness value, F_v. The fitness value could be the objective function in a maximization problem (or its inverse in a minimization problem).

Once a chromosomal representation of the synthesis / design variables for a given population is available, the evolutionary mechanisms of selection, crossover and mutation are applied. One simplistic approach to selecting members of a population is to eliminate the individuals whose fitness value is below the average for the entire population. The selection proceeds by making copies of the fittest individuals so that the size of the new generation is equal to the original. The crossover process allows for an exchange of synthesis / design characteristics among members of a population. From the many ways in which crossover can be done (Goldberg, 1989), the most widely used approach is to randomly select two mating parents followed by a swap of binary numbers at a random position. Mutation safeguards[6] the search from a premature loss of information during reproduction and crossover. The fundamental idea is to choose a few members of the population using a probabilistic scheme and then switch a 0 to a 1 or vice-versa at a random place on the string. The GA then proceeds from generation to generation until no further improvements in the fitness function are achieved.

[6] This is only true up to a point. Additional considerations such as the chromosomal representation (see footnote 5 above) as well as the methods of selection and crossover can have significant impacts on assuring that there is no significant loss of information too early in the search process (see Olsommer et al., 1999).

Chapter 3

State of the Art of Energy System Synthesis/Design

The synthesis / design of complex energy systems requires that sophisticated methodologies and tools be developed and applied. In fact, a number of these with varying degrees of sophistication have been the subject of research since the 1950s. Of these, probably the most common and the least sophisticated is the system / component simulation package which aids the engineer in the synthesis / design process but forces the engineer, nonetheless, to rely heavily on rules-of-thumb and experience. More structured tools exist, however. One can broadly classify the latter depending on the fundamental purpose for which they are used. Thus, one can distinguish between methodologies and tools for Energy System Analysis and those for Energy System Synthesis/Design Optimization. Analysis methodologies and tools are typically used to gain a fundamental understanding of a process or system. The information is then used to rationally define a set of possible configurations or a mode of operation. Optimization is then applied to refine the synthesis / design so that a figure of merit is maximized or minimized. A description of both types of methodologies / tools and their variations follow.

3.1 Energy System Analysis

3.1.1 Pinch Technology

Pinch Technology (e.g., Linnhoff, 1993; Boland and Linhoff, 1979) is a systematic approach without a comprehensive operational research base used primarily in the process industry for reducing costs. It does this by minimizing the number of heat exchangers in a heat exchanger network, i.e. the network's costs, and determining the placement of heat pumps and power generation cycles with respect to this network. Although it has not by any means gained wide acceptance in this industry, it has, nevertheless, gained more of a foothold than all of the mathematically based modeling, analysis and optimization methods that have been or are being developed in the research domain.

Pinch technology requires the creation of temperature vs. enthalpy rate difference diagrams. In applications with various hot and cold streams it is necessary to combine the thermal characteristics of the hot and cold streams into a hot composite curve and a cold composite curve, respectively. The location of the minimum temperature difference (the pinch) can then be found by inspection. Naturally, during the design process, the pinch can be varied to make the two composite curves approach closer or move farther away on the temperature-enthalpy difference plane. A set of simple rules can be applied to guide the selection of a near optimum heat exchanger network. These rules simply stated are: do not transfer heat across the pinch, use a hot stream above the pinch and use a cold stream below the pinch.

It has been claimed that pinch technology is a tool that can be used for process design (Linhoff, 1989). However, based on the results of a challenge problem solved in the early 1990's (Linhoff and Alanis, 1991; Gaggioli et al, 1991), it would appear that exergy analysis as applied by an expert may be superior for that purpose, a fact which is not surprising since exergy analysis is 2nd Law-based and more complete as an overall

analysis tool. An interesting (and spirited) comparison between pinch technology and exergy analysis is given by Sama (1995)

3.1.2 Exergy Analysis

Exergy is defined as the maximum theoretical useful work[7] that can be obtained as a system is allowed to interact with a second idealized system called the *reference environment* (or *"dead state"*). Exergy is in fact a measure of the departure of the state of the system from that of the reference environment.

It is common practice to break down the quantity of exergy into several components in order usually to facilitate cost assignment. Several options are available for this purpose: First, exergy may be split into thermomechanical exergy and chemical exergy (Moran, 1982). A second method (Tsatsaronis et al. 1989) is to break exergy into four constituents: thermal, mechanical, reaction, and environmental exergies.

The method of choice here (Kestin, 1980) is to divide the total exergy, E_x, of a mixture of n constituents into four components (provided other effects such as magnetic, surface tension, and nuclear are absent): physical, kinetic, potential and chemical exergy, thus

$$E_x = E_x^{ph} + E_x^{kn} + E_x^{pt} + E_x^{ch} \tag{3.1}$$

where

$$E_x^{ph} = (U - U_o) + P_o(V - V_o) - T_o(S - S_o) \tag{3.2}$$

$$E_x^{kn} = \frac{1}{2} m V^2 \tag{3.3}$$

[7] More generally it is described as the maximum potential for change or "departure from equilibrium" with the reference environment ("dead state").

$$E_x^{pt} = mgz \tag{3.4}$$

$$E_x^{ch} = \sum_{i=1}^{n} \left(\mu_i^o(T_o, P_o) - \mu_{0,i}(T_o, P_o)\right) N_i \tag{3.5}$$

where $\mu_i^o(T_o, P_o)$, are the chemical potentials of the constituents at the reference temperature T_o and pressure P_o. In this case, the mixture is said to be at the restricted dead state. The last term in equation (3.5), $\mu_{0,i}(T_o, P_o)$, corresponds to the chemical potentials of the corresponding constituents in the reference or dead state, i.e. when they are in thermal, mechanical, *and* chemical equilibrium with the environment. Therefore, the chemical part of the exergy is seen to be the component of exergy associated with the departure of the chemical composition of a system from that of the reference environment. In order to calculate the chemical exergy of the system, no chemical reactions should take place between the environmental components. Because of the complexity of the calculations of chemical exergies, Szargut and his coworkers (1965,1988) introduced the concept of standard chemical exergy. This is calculated on the assumption that the environmental temperature and pressure have standard values. According to this concept, the environment is regarded as composed of a set of reference substances with standard concentrations to be determined by convention.

It is impractical to define many equilibrium "environments" or reference states for the chemical exergy calculations. The criteria for the selection of appropriate reference points have been given by Fratzcher and Gruhn (1965) and later by Wepfer and Gaggioli (1978). There is general agreement that the model of the environment must fulfill three basic conditions: First, it must satisfy the thermodynamic equilibrium requirements; second, it must be practical from a technical standpoint; and third, it must be consistent with the theory of economics. These conditions require that all dead streams in a thermal or chemical system must have positive or zero exergy values. This becomes possible if the reference substances and conditions form a dead system, which means that all mixtures and compounds that do not belong to the reference system must have positive exergy values. Furthermore, the reference environment should be as close

as possible to the natural environment. However, the natural environment is not exactly in thermodynamic equilibrium, since its temperature, pressure and composition change both spatially and with time. It was observed that calculations to establish the dead state lead to a reference system, which is not close to the real environment (Ahrendts, 1980). In order for the reference environment to be practical, the exergy of streams going to the environment should have zero values. A final condition for the model of the environment is that it should be capable of providing an economic indicator for the exergy values. Thus, substances abundant in nature should have lower exergies than scarce ones. It is apparent that the simultaneous fulfillment of all the conditions defined above is not easily attainable in a single model and as a consequence many models have been proposed. A critical review of those models is given in Muñoz and Michaelides (1999).

As with pinch technology, exergy analysis is a systematic but less structured way of analyzing alternative synthesis / design options for energy systems and components. Though less structured than pinch technology or other First Law approaches, it does provide a more complete picture and a greater number of insights into the overall synthesis, design and operation problem since it accounts both for the quantity and quality of all energy conversions present in a process. Furthermore, it is not primarily centered on heat exchange or mass exchange networks. It uses a set of common sense guidelines (Sama, 1995; Sama et al., 1989) to detect and avoid or remove Second Law errors in synthesis, design and operation in order to guarantee a more efficient and possibly cost effective system. The objective of this type of analysis is the judicious expenditure of exergy (availability)[8] to reduce not just fuel costs but total costs.

[8] The terms *exergy* and *availability* are interchangeable. Either combines the notions of the *quantity* of energy resulting from the 1st Law and the *quality* of energy resulting from the 2nd Law into a single entity which can be used to assess the real thermodynamic losses which occur within, to and from a system.

3.1.3 Expert Systems

Unlike the two systematic approaches just described, expert systems are not a type of analysis but a form of artificial intelligence which organizes and efficiently and quickly makes available the knowledge and experience of more than one expert. This knowledge and experience takes the form of rules-of-thumb and/or the same set of guidelines used by exergy and/or pinch analyses. This is accomplished by reproducing the engineer's decisional path via a knowledge-based computer code that uses synthesis and design data to devise a process or operations data to run a process in much the same way that an engineer or engineering team would (e.g., Sciubba, 1998; Sciubba 1995).

3.2 Energy System Synthesis / Design Optimization

There are significant limitations as to what can be done with the analysis methodologies / tools described in the previous sections. Approaches for overcoming these limitations are mathematically based. They simultaneously model the thermodynamic and/or economic aspects of a system and its components. This permits the use of optimization algorithms whether deterministic or heuristic which search the solution space of all possible solutions for the optimum synthesis, design and/or operation of the system and its components.

The use of optimization for the synthesis / design optimization of stationary energy systems has been widespread during the last thirty years. A large number of researchers are involved in this field. The applications that can be found range from relatively simple NLP problems (e.g., Valero et al, 1994) to very complex MINLP problems (e.g., Olsommer et al, 1999a,b).

Energy system synthesis / design, at least at the conceptual stage, typically employs two disciplines: the thermal sciences and economics. Other disciplines such as material

science and controls are handled indirectly. For example, stress considerations are treated as constraints and controls are included by using so-called operational variables.

Based on the above, one may classify the work on stationary energy system synthesis / design optimization based on the disciplines used to formulate the optimization problem. Thus, one can have purely thermodynamic problems or combined thermodynamic and cost problems, i.e. *thermoeconomic* problems. Another possible classification is mathematically based. The leading optimization methods for stationary energy systems are presented below using a classification based on disciplines

3.2.1 Discipline-based Optimization Methods

The most established and well-developed discipline-based optimization methods are Entropy Generation Minimization and Thermoeconomics. The former uses purely thermodynamic objective functions and the latter combines cost and thermodynamic principles.

Entropy Generation Minimization (EGM)

Entropy Generation Minimization - EGM (Bejan, 1995; Bejan et al, 1996), is a 2^{nd}-Law-based *thermodynamic* modeling and optimization approach which

- explicitly identifies and calculates the physical causes of entropy generation;
- relates "thermodynamic non-ideality" to physical mechanisms (i.e. finite temperature differences, friction, etc);
- minimizes the generation of entropy through design changes to the physical characteristics of the system.

The main advantages of EGM are that it

- couples detailed (e.g., computational fluid dynamics (CFD) based) heat transfer and mass transfer analyses with thermodynamic analyses;
- highlights locations of high entropy production (e.g., using entropy production contours);
- provides information, which can be used to influence component designs.

Its disadvantages are that it may require too much experimental verification and be too computationally intensive (i.e. requires CFD for modeling both the heat and mass transfer of each component), particularly when the interest of the designer extends beyond the individual component level to both the sub-system and system levels. This is particularly true as component, sub-system and system complexity and/or the number of degrees of freedom for the integrated optimization of all of these increases. Thus, EGM

- lacks a natural way (i.e. one without expert intervention) of integrating the component synthesis / design optimizations with that of the sub-system and system as a whole; this poses a significant barrier to the *integrated* *decomposition* of the synthesis / design problem and, thus, to the number of degrees of freedom that can be optimized simultaneously;
- lacks built-in limitations (i.e. those built directly into the objective minimized) on the extensive size parameters (e.g., mass, volume, area, length) of each sub-system component (i.e. an inherent economic size limitation is missing); using constraints instead will not necessarily and more than likely not lead to the same results;
- lacks a common basis for easy comparison of a very diverse set of parameters (e.g., entropy generations, specific fuel consumption, take-off gross weight (TOGW), range, weight, volume, etc.).

Thermoeconomics

Thermoeconomics was originally meant to signify the combination of exergy analysis and economic principles for the purpose of improving energy systems. Today,

however, it is generally accepted that thermoeconomics may use 1st Law quantities combined with cost and the word exergoeconomics is reserved for the version that uses 2nd Law quantities and cost.

The fact that thermoeconomics blends two very different fields: thermodynamics and economics, makes it particularly suitable for the design of energy systems. This is due to the natural trade-off between efficiency (usually translated into fuel consumption or the cost of operation) and capital cost. Thus, Thermoeconomics addresses some of the inherent drawbacks of EGM (von Spakovsky and Evans, 1984; Evans and von Spakovsky, 1993; von Spakovsky, 1994; El-Sayed, 1996; Olsommer et. al 1999a,b; Frangopoulos, 1994; Valero et al., 1994a,b; Tsatsaronis and Pisa, 1994)[9] in that it:

- directly incorporates the size constraint through component costing equations
- addresses the component, sub-system, and system synthesis / design *integration* problem through the use of both decomposition and large-scale optimization schemes;
- incorporates component synthesis / design models as well as sub-system and system models;
- distinguishes between and employs both *thermodynamic* variables (e.g., power, mass rate, heat rate, exergy rate, pressure, temperature, composition, enthalpy, entropy, specific volume, pressure loss, heat loss, temperature difference, adiabatic efficiency, heat exchanger effectiveness, extent of reaction, stoichiometric excess, etc.) and *design* and *manufacturing* variables (e.g., volume, length, area; mass, strength, etc.);
- dynamically develops information (e.g., build component costing functions during the modeling and optimization process) used to optimally influence component syntheses / designs consistent with overall sub-system and/or system optimums;

[9] Note that each of the alternatives appearing in this list of key thermoeconomic references does not necessarily employ all of the items listed.

- is able to simultaneously optimize a higher number of degrees of freedom when decomposition is used, i.e. higher than is possible with non-decomposition approaches (e.g., EGM);
- is able to effectively deal with the mixed-integer, non-linear programming problem of synthesis / design where synthesis in this case is not restricted to the geometry and material characteristics of components but also includes the existence / non-existence or on / off behavior of system components[10];
- permits a consideration of off-design behavior and the influence of this behavior on system synthesis and design over time.

A drawback to most thermoeconomic approaches is that there is less specificity about exactly where locations of high entropy generation occur (e.g., entropy generation contours) since CFD modeling of both the heat and mass transfer of each component is not typically employed. This is due to the fact that the optimizations involved are already sufficiently complex and computationally intensive to make direct use of CFD much too computationally burdensome. Of course, developing this information on entropy generation indirectly in a completely separate step through CFD and/or experimental modeling and then incorporating it using, for example, regression analysis, directly into a thermoeconomic approach is a way around this drawback. The level of detail, which can, thus, be used in a thermoeconomic approach at the component level, specially one in which decomposition is employed, can be quite high.

[10] Once again note that *synthesis* refers to changes in system configuration while *design* here refers exclusively to, for example, the nominal (full load or design point) capacity and performance of a given component or technology.

3.2.2 Decomposition Methods

To facilitate energy system synthesis / design optimization decomposition is used. Strictly speaking two forms of decomposition are possible. The first is a disciplinary decomposition in which thermodynamics and cost are de-coupled and each discipline is optimized independently. Another possibility is to decompose the system across unit (components or sub-systems) boundaries. For dynamic problems it is also possible to divide the independent variables into *synthesis / design* (those which remain constant over time) and control or *operational* (those that can be varied in time) variables. This breakdown is often called time decomposition.

Disciplinary Decomposition

The decision variables in energy system synthesis / design may be broken down into purely thermodynamic and flow variables ($\vec{v}$) and others which are purely geometrical ($\vec{w}$). Thermodynamic variables are for example component adiabatic efficiencies, pressures and temperatures. Geometric variables are, for instance, the physical dimensions of a heat exchanger, the number of blades in a turbine, the technology level of a component (including the choice of material).

With the above considerations in mind, it is possible to define a two-level optimization problem. At the highest level, the problem could be to minimize the amount of fuel required to perform a given task. Typically, thermodynamic variables ($\vec{v}$) are chosen by the high-level optimizer. These values are set as boundary parameters for each of the units in the system. The material (cost or weight) used in each component is then minimized. The latter set of problems uses geometry, technology, and material choice as decision variables. Examples of the use of this type of approach are given in El-Sayed (1986) and Zimering (1999).

Physical (unit) Decomposition

Unit decomposition, as opposed to disciplinary decomposition, tries to isolate the influence that each of the units that form a system has in terms of the overall objective function. The unit's impact may be multi-disciplinary as shown below. To illustrate the fundamental differences between the leading decomposition methods for energy system synthesis / design, consider the simple two-unit system of Figure 3.1.

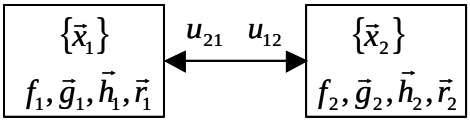

Figure 3.1. A simple two-unit energy system.

In Figure 3.1, $\vec{x}_1$ and $\vec{x}_2$ are the decision variables, $\vec{g}_1$ and $\vec{g}_2$ are the functions that describe the physical processes, $\vec{g}_1$ and $\vec{g}_2$ are the constraints imposed upon each of the units, $\vec{r}_1$ and $\vec{r}_2$ are the residuals of the analysis system of equations, and u_{12} and u_{21} are the functions (or in the general case the vector of functions) that couple the two units.

The typical objective function, *f*, is written as the sum of the contributions of each of the units. In turn, the contribution of each unit is composed of two terms as indicated below:

$$f_1 = k_1 R_1 + Z_1 \tag{3.6}$$

for given values of $\vec{u}_{12}$ and $\vec{u}_{21}$. In equation (3.6), *R* is some external resource used by the unit (typically fuel) and *Z* is a function related to the size of the unit (weight or cost) while k_1 is a conversion factor. In a thermoeconomic problem, *Z* is the capital cost. In a thermodynamic problem *Z* is ignored altogether.

The Evans-El Sayed Formalism

The Evans and El-Sayed formalism (1970) is without a doubt the single most influential work in thermoeconomics. Many of the leading cost assignment and optimization methods such as Engineering Functional Analysis (von Spakovsky and Evans, 1993; Evans and von Spakovsky, 1993); Thermoeconomic Functional Analysis (Frangopoulos, 1994), Structural Analysis (Valero et al., 1994) and others (e.g., Tsatsaronis and Pisa, 1994) are to a certain extent variations of the original Evans and El-Sayed method. The original version of the method used the Lagrange theorem of optimization (see Chapter 2) to show the possibility of decomposing the system into units. However, to present the method here, a more direct approach is used.

Consider the simple energy system of Figure 3.2. The system is composed of two units (components or subsystems). In the original formulation, the coupling functions (u_{12} and u_{21}) as well as the external resources are given in terms of exergy. Unit 1 uses an external resource R_1 (fuel) expressed in exergy terms (E_f). Unit 2 does not use any external resources. The fuel is used to produce a product E_o, which is assumed constant. Additionally the capital functions Z_1 and Z_2 are in fact capital costs Z_1^p and Z_2^p, respectively.

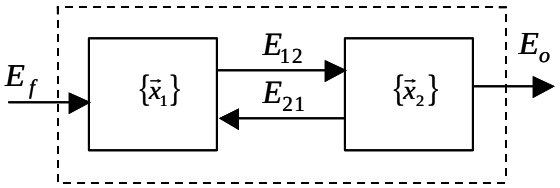

Figure 3.2 A simple two-unit energy system for illustrating the Evans-El-Sayed formalism.

In Figure 3.2, the vectors $\vec{x}_1$ and $\vec{x}_2$ are the independent variables for both units. To begin with, assume that no variable is common to both units. For each unit, the input exergy is assumed to be a function of the exergy of the stream leaving the unit and the unit's independent variables. Thus,

$$E_f = E_1 = E_1(\vec{x}_1, E_{12}) \tag{3.7}$$

$$E_{12} = E_{12}(\vec{x}_2, E_{21}, E_2) = E_{12}(\vec{x}_2, E_{21}, E_o) = E_{12}(\vec{x}_2, E_{21}) \tag{3.8}$$

$$\vec{E}_{21} = E_{21}(\vec{x}_1, E_{12}) \tag{3.9}$$

where E_o drops out of equations (3.8) and (3.9) since it is constant. In addition, the cost of unit *i*, Z_i^p (capital), is assumed to have the same functional behavior as equations (3.7) and (3.9) so that

$$Z_1^p = Z_1(\vec{x}_1, E_{12}) \tag{3.10}$$

and

$$Z_2^p = Z_2(\vec{x}_2, E_{21}) \tag{3.11}$$

The design optimization problem objective is formulated as

$$\text{Minimize } C_T = k_1 E_f + Z_1^p + Z_2^p \tag{3.12}$$

where k_1 is a conversion factor from exergy to monetary units. The fact that problem (3.12) uses both capital cost and thermodynamic functions makes it a "thermoeconomic" problem. If a purely thermodynamic problem is desired, one could neglect the capital cost terms and set the conversion factor k_1 to 1.

Before attempting the optimization problem given above, let us assume that a workable solution, i.e. one that satisfies the equality and inequality constraints associated with equation (3.12), is known either from experience or by solving the state equations iteratively. The workable solution thus obtained has vectors of independent variables $\vec{x}_1^o$ and $\vec{x}_2^o$ and an associated cost C_T^o.

Now, assume a small deviation in the value of the independent variables about the reference solution. The associated increase in cost due to such a deviation is

$$dC_T = k_1 dE_1 + dZ_1 + dZ_2 \tag{3.13}$$

which with equations (3.7), (3.10) and (3.11) becomes

$$dC_T = k_1\left(\frac{\partial E_1}{\partial x_1}dx_1 + \frac{\partial E_1}{\partial E_{12}}dE_{12}\right) + \left(\frac{dZ_1}{dx_1}dx_1 + \frac{dZ_1}{dE_{12}}dE_{12}\right) + \left(\frac{dZ_2}{dx_2}dx_2 + \frac{dZ_2}{dE_{21}}dE_{21}\right) \tag{3.14}$$

From equations (3.8) and (3.9)

$$dE_{12} = \frac{\partial E_{12}}{\partial x_2}dx_2 + \frac{\partial E_{12}}{\partial E_{21}}dE_{21} \tag{3.15}$$

$$dE_{21} = \frac{\partial E_{21}}{\partial x_1}dx_1 + \frac{\partial E_{21}}{\partial E_{12}}dE_{12} \tag{3.16}$$

Combining equations (3.14), (3.15) and (3.16) and after much manipulation, one finally arrives at

$$dC_T = \gamma_1 dx_1 + \gamma_2 dx_2 \tag{3.17}$$

where

$$\gamma_1 = \gamma_1\left(\vec{x}_1, \vec{x}_2, E_{21}, E_{12}\right) = k_1\frac{dE_1}{dx_1} + \frac{\partial Z_1}{dx_1} + \frac{dE_{21}}{dx_1}\left[\frac{\frac{\partial Z_2}{dE_{21}} + \frac{\partial E_2}{dE_{21}}\left(k_1\frac{dE_1}{dE_{12}} + \frac{\partial Z_1}{dE_{12}}\right)}{1 - \frac{\partial E_{21}}{dE_{12}}\frac{\partial E_2}{dE_{21}}}\right] \tag{3.18}$$

and

$$\gamma_2 = \gamma_2\left(\vec{x}_1, \vec{x}_2, E_{21}, E_{12}\right) = \frac{\left[\frac{\partial Z_2}{dx_2} + \frac{dE_{12}}{dx_2}\right]\left[\frac{\partial Z_2}{dE_{21}}\frac{dE_{21}}{dE_{12}} + k_1\frac{dE_1}{dE_{12}} + \frac{\partial Z_1}{dE_{12}}\right]}{1 - \frac{\partial E_{21}}{dE_{12}}\frac{\partial E_{12}}{dE_{21}}} \tag{3.19}$$

One of the expectations of the above formulation was that it would provide the necessary framework for decomposing the units so that individual optimization

problems for each unit could be defined. The basis of the proposed decomposition was the fact that equation (3.17) states mathematically that a change in, say, dx_1 would cause a change in the total cost by an amount proportional to dx_1. The proportionality factor being the function that multiplies dx_1, i.e. γ_1. The values of such coefficients would indicate where design changes would need to be made in order to achieve better system cost. Large changes in x_1 and x_2 could be made if the coefficients were linear over the ranges of those changes. If such linearity were not observed then an iterative procedure could be defined in which piece-wise linear approximations would be used.

The resulting algorithm (Gaggioli and El-Sayed, 1989) would begin with a workable solution, followed by the calculation of γ_1 and γ_2. A decision regarding a change in x_1 and x_2 would then be made depending on the magnitude of the coefficients (provided that they are different than zero) and any known information about the behavior of the coefficients. With no information available, only small changes in the independent variables would be allowed. With new updated values for x_1 and x_2, the process is restarted until a limit on the independent variables is reached or until γ_1 and γ_2 take a value of zero.

It has been claimed (Gaggioli and El-Sayed, 1989) that equation (3.17) indicates that the two units are ‘isolated’ in the sense that the first term of the right hand side of equation (3.17) is related to unit 1 and the second to unit 2. Close inspection, however, shows that the capital cost function of unit 1 appears in the second term and the capital cost function of unit 2 appears in the first term. This fact shows that an “inner coupling” exists. This poses a great problem for decomposing systems as proposed. Such coupling could be avoided if the capital cost functions were linear with respect to the internal exergy flows (couplings), i.e.

$$\frac{\partial Z_1}{dE_{12}} = \text{constant} \tag{3.20}$$

and

$$\frac{\partial Z_2}{dE_{21}} = \text{constant} \tag{3.21}$$

There are many examples in which the capital cost equations have been derived specifically so that equations (3.20) and (3.21) are verified.

The prospect of being able to decompose the system in the manner described above led to an enormous amount of enthusiasm in the 2nd Law academic community (e.g., von Spakovsky, 1986, 1994; Frangopoulos, 1983, 1984, 1989; Tsatsaronis, 1985; Tsatsaronis and Winhold, 1984). Such enthusiasm was explicitly or implicitly based on the hope and the expectation that the coefficients γ_1 and γ_2 were approximately constant from iteration to iteration, thus, facilitating the decomposition. A number of works have been devoted to analyzing and creating conditions for achieving the required isolation by introducing linear approximations and "functional analysis" (Evans and coworkers). The resulting methods, however, are cumbersome and based (in some cases) on rather arbitrary "rules" and, thus, are difficult to implement. Note that even if the conditions given by equations (3.20) and (3.21) are met, the behavior of the functions γ_1 and γ_2 is unknown. Typically the functions relating exergy of a stream entering a unit and that of a stream leaving is highly non-linear. Close examination of γ_1 and γ_2 does not seem to reveal any special trend as to their magnitude or even their sign, particularly when several independent variables are considered. Thus, these functions could conceivably vary very widely in magnitude and sign, thus, hindering the iterative process that was mentioned above. An additional implication is that it would be easy to get trapped in a local minimum, due to the fact that changes in the coefficients' sign could lead the procedure to prematurely stop because a value of zero for the coefficients γ_1 and γ_2 is found.

The fact that the Evans and El-Sayed formalism and the methods that have been derived from it along with the necessary iterative procedure needed to implement them heavily depend on the (at least piece-wise) constant behavior of the coefficients γ_1 and γ_2 poses many potential problems. This and a number of other issues have hindered the

widespread acceptance of the method among practitioners. The drawbacks of the method are summarized as follows

- The method in its original form presupposes that exergy[11] is the property of choice to represent the streams of the system. Regrettably, exergy and in general Second Law-based thermodynamic analysis are not concepts clearly understood or widely used in industry. That is not likely to change unless substantial advantages to their use can be found. As will be seen later such advantages may be claimed for analysis purposes but not necessarily for optimization purposes.
- A problem related to the previous item is the need to have functions that relate capital and operational costs to exergy terms. These costs (usually sparse) are typically not correlated in a form amenable to the decomposition described above (equations (3.2)). Much work is usually needed to do so.
- The above formulation was developed using exergy. However, energy or other properties can be used. For example "negentropy" has been used in the past (von Spakovsky, 1994; Frangopoulos, 1994) and relative free energy has been proposed as well (Valero et al., 1993). There are some indications that the use of one or more of these additional 2nd Law based quantitites positively affect the behavior of γ_1 and γ_2, but there are no indications to believe that the choice of one or more of these quantities will solve all of the problems mentioned above related to successfully decomposing the optimization problem for complex systems.
- An additional practical disadvantage of the method is that it leaves little room for the use of commodities different from energy or exergy-based quantities. In modern, highly integrated systems, energy-based sub-systems must interact with non energy-based sub-systems. An example is an aircraft where aerodynamics, structures,

[11] In subsequent forms of the method (e.g., Frangopoulos, 1983, 1994; von Spakovsky, 1986, 1994), other 2nd Law quantities such as negentropy were introduced in order to positively affect the behavior of γ_1 and γ_2.

weapons, propulsion and other subsystems must work in concert to provide the system-level objectives.

- The Evans and El-Sayed method was developed for systems with a unique design point. As will be seen later, relatively well-behaved functions that describe the coefficients accompanying dx_1 and dx_2 are needed not only at design conditions but at all the other operating conditions, i.e. at off-design.

Other Second Law-based Decomposition Methods

An alternative 2nd Law-based decomposition method was proposed by El-Sayed (1996). The formulation results from combining equation (3.12) with an exergy balance around each unit. The resulting optimization problem for each unit, say unit *i*, is to

$$\text{Minimize } C_i = c_d E_D + Z_i^p \tag{3.22}$$

where E_D is the exergy destruction, Z_i^p is the capital cost, and c_d is the cost of the exergy destruction in the unit. In El-Sayed's method, the cost assignment for the exergy destruction, i.e. the value of c_d, is arbitrary. When the product of the unit is constant, c_d takes a value equal to the cost of the fuel; and when the amount of resources used by the unit is constant, c_d takes a value equal to the cost of the products. This cost is assigned externally.

The method in its original form has multiple drawbacks, all of them having to due with the value of c_d:

- The method does not provide for ways of calculating the exergy destruction cost when the different components of exergy destruction are dissagregated
- None of the two conditions above (i.e. those related to the assignment of cost) may apply to the case of "internal" units. For such units neither resources used nor products produced are necessarily constant.

- The method is ambiguous when multiple resources are going into or multiple products are leaving the unit[12].

A more rational way for assigning cost to exergy destruction has been given by Muñoz and von Spakovsky (1999). The method uses the marginal costs of each of the sources of exergy destruction or entropy generation to account for their system-level impact. Although this method is not considered here, the reader is invited to consult the original reference.

[12] Of course, in the past some authors have handled this problem through the use of "Thermoeconomic Functional Analysis" (Frangopoulos, 1983, 1994) or "Engineering Functional Analysis" (von Spakovsky and Evans, 1993; Evans and von Spakovsky, 1993; von Spakovsky, 1986, 1994) in which each unit is uniquely assigned a specific function, i.e. production of a single product.

Chapter 4

General Mathematical Foundation for Physical Decomposition

Consider a general non-hierarchical[13] engineering system[14] composed of three units (sub-systems, components, disciplines or simply black-boxes) as shown in Figure 4.1. Three is a sufficiently large number to visualize the features of the methods and to present the necessary mathematics in a compact way. The results of this chapter can be routinely extended to systems with more than three units. In Figure 4.1 the functions u_{ij} are called coupling, compatibility, interdisciplinary, linking or connecting functions or parameters. The coupling functions can also be considered intermediate forward and backward feedback functions. Each unit has its own vector of decision variables $\vec{x}_i$ and has a local contribution, f_i, to the overall objective function, f. The objective function is often called the cost function. The coupling functions are in general written as

$$u_{ij} = u_{ij}(\vec{x}_i, \vec{x}_j) \tag{4.1}$$

---

[13] A non-hierarchical system is one in which each decision, even a localized decision, may influence the rest of the system.

[14] In order to be as general as possible, the term "system" is used here to refer to any engineering system whether energy based or not.

In Figure 4.1, the contribution of any unit, say unit 1, to the overall objective function, *f*, is given by

$$f_1 = f_1(\vec{x}_1, u_{21,} u_{31}, u_{12,} u_{13}) \tag{4.2}$$

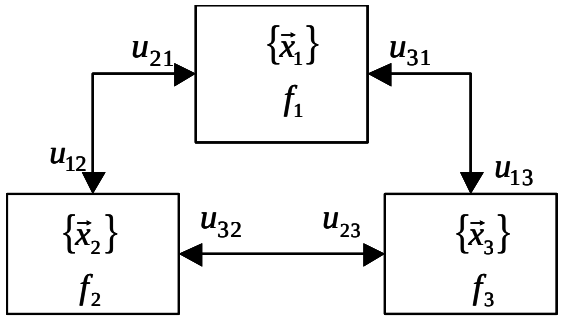

Figure 4.1. A coupled non-hierachical system.

The system-level problem is the sum of the contributions of all units, i.e.

$$\text{Minimize} \quad \begin{aligned} f = {} & f_1(\vec{x}_1, u_{21,} u_{31}, u_{12,} u_{13}) + f_2(\vec{x}_2, u_{12,} u_{32}, u_{21,} u_{23}) \\ & + f_3(\vec{x}_3, u_{13,} u_{23}, u_{31,} u_{32}) \end{aligned} \tag{4.3}$$

w.r.t. $\vec{x}_1, \vec{x}_2, \vec{x}_3$

subject to

$$\vec{H} = \begin{bmatrix} \vec{h}_1 \\ \vec{h}_2 \\ \vec{h}_3 \end{bmatrix} = \vec{0} \tag{4.3.1}$$

$$\vec{G} = \begin{bmatrix} \vec{g}_1 \\ \vec{g}_2 \\ \vec{g}_3 \end{bmatrix} \leq \vec{0} \tag{4.3.2}$$

where each of the three terms to the right of the equals in equation (4.3) is called a *local* or *unit-based* objective function. The vectors of independent (or decision) variables, $\vec{x}_i$, can be real or integer valued. The vectors $\vec{H}$ and $\vec{G}$ in expressions (4.3.1) and (4.3.2) constitute the physical description of the units and are known as the *analysis* system of equations. $\vec{H}$ and $\vec{G}$ are hereby called the *primary* constraints.

Numerous solution approaches exist for the solution of the problem at hand. First of all, the solution of problem (4.3) can be attempted using a conventional technique for solving mixed integer non-linear programming (MINLP) problems. However, this approach has the following practical drawbacks:

- In general each unit may represent a different discipline. In this case, the difficult problem of *analysis integration* needs to be solved. This implies putting together discipline analyzers of perhaps a different nature and written for different platforms.
- The total number of independent variables may grow to be very large. This may pose a significant penalty in terms of the time required to achieve the solution or the ability to even arrive at the solution.
- The previous item is added to the fact that the unit (discipline) analyzers (equations (4.3.1) and (4.3.2)) need to be solved not only at each iteration of the optimization but for computing derivatives as well, a fact, which makes the method extremely expensive. If discrete variables are present, the need for artificial intelligence-based algorithms makes the problem even worse computationally.
- The method is not immune to failure because the choice of independent variables may lead to values of intermediate feedback (or coupling), which are not realistic. This is equivalent to generating points that cannot be analyzed by each discipline.

4.1 Decomposition: Local-Global Approach

In the Local-Global Optimization (LGO) approach, the units (disciplines) are decomposed and the resulting problems are solved for different values of the unit couplings. The optimum results are used by a system-level optimization problem, which is optimized with respect to the coupling functions.

Now, consider a modified version of the MINLP problem (equations (4.3)), i.e.

$$\text{Minimize} \quad \begin{aligned} f = {} & f_1(\vec{x}_1, u_{21,} u_{31}, u_{12,} u_{13}) + f_2(\vec{x}_2, u_{12,} u_{32}, u_{21,} u_{23}) \\ & + f_3(\vec{x}_3, u_{13,} u_{23}, u_{31,} u_{32}) \end{aligned} \tag{4.4}$$

w.r.t. $\vec{x}_1, \vec{x}_2, \vec{x}_3$

subject to

$$\vec{H} = \begin{bmatrix} \vec{h}_1 \\ \vec{h}_2 \\ \vec{h}_3 \end{bmatrix} = \vec{0} \tag{4.4.1}$$

$$\vec{G} = \begin{bmatrix} \vec{g}_1 \\ \vec{g}_2 \\ \vec{g}_3 \end{bmatrix} \leq \vec{0} \tag{4.4.2}$$

and the additional (secondary) constraints

$$u_{ij} - \xi_{ij} = \vec{0} \tag{4.4.3}$$

Constraints (4.4.3) simply state that the coupling functions, u_{ij}, are forced to take the values ξ_{ij} such that

$$u_{ij_{\min}} \leq \xi_{ij} \leq u_{ij_{\max}} \tag{4.4.4}$$

Since the values of u_{ij} are fixed, one can easily decompose problem (4.4) into three *local sub-problems*, one for each of the units. For unit 1, the local sub-problem is to

Minimize $f_1 = f_1(\vec{x}_1, \xi_{21,}\xi_{31}, \xi_{12,}\xi_{13})$ (4.5)

w.r.t. $\vec{x}_1$

subject to

$\vec{h}_1 = \vec{0}$ (4.5.1)

$\vec{g}_1 < \vec{0}$ (4.5.2)

For unit 2, the local sub-problem is to

Minimize $f_2 = f_2(\vec{x}_2, \xi_{12,}\xi_{32}, \xi_{21,}\xi_{23})$ (4.6)

w.r.t. $\vec{x}_2$

subject to

$\vec{h}_2 = \vec{0}$ (4.6.1)

$\vec{g}_2 \leq \vec{0}$ (4.6.2)

and for unit 3 to

Minimize $f_3 = f_3(\vec{x}_3, \xi_{13,}\xi_{23}, \xi_{31,}\xi_{32})$ (4.7)

w.r.t. $\vec{x}_3$

subject to

$\vec{h}_3 = \vec{0}$ (4.7.1)

$\vec{g}_3 \leq \vec{0}$ (4.7.2)

Decomposition effectively makes the dimensionality of problems (4.5) to (4.7) much smaller than that of the original MINLP problem (4.4).

The local sub-problems need to be solved numerous times for different combinations of values of the functions u_{ij} within the ranges given by the physical limits, i.e. expressions (4.4.4). The assumption clearly used here is that there are different sets of independent variables $\vec{x}_1$, $\vec{x}_2$, and $\vec{x}_3$ capable of producing the desired values of u_{ij}. If that is not the case, the solution to problems (4.5) to (4.7) is trivial.

The different solutions to problems (4.5) to (4.7) for the various combinations of u_{ij} lead to a set of *restricted* optimum solutions with corresponding optimum values of the sub-problem objectives, f_i^*. For unit 1, for example, the restricted optimum solution has the form

$$f_1^* = \min\left(f_1(\vec{x}_1, \xi_{21,}\xi_{31}, \xi_{12,}\xi_{13})\right) \tag{4.8}$$

The restricted optimum independent variables $\vec{x}_1^*$ are such that

$$f_1^* = f_1(\vec{x}_i^*, \xi_{21,}\xi_{31}, \xi_{12,}\xi_{13}) \tag{4.9}$$

A vector of restricted optimum values, f^*, for the system-level objective function results from combinations of the sum of the restricted optimum solutions found by solving the local problems, problems (4.5) to (4.7), i.e.

$$f^* = \sum_{i=1}^{3} f_i^* \tag{4.10}$$

It is possible to construct a surface of f^* versus the coupling functions u_{ij}. This hyper-surface constructed from the unit optimums is called the optimum *response*

surface[15] of the overall synthesis / design problem. The optimum response surface is then used to define the system-level problem given by

$$\text{Minimize } f = f_1^* + f_2^* + f_3^* \tag{4.11}$$

w.r.t. $\xi_{ij} \quad i, j = 1,2,3 \qquad i \neq j$

subject to

$$\vec{G} = \begin{bmatrix} \xi_{ij} - \xi_{ij\,\max} \\ -\xi_{ij} + \xi_{ij\,\min} \end{bmatrix} \leq \vec{0} \tag{4.11.1}$$

In other words, the system-level problem is one of finding the optimum combination of values for the intermediate feedback (coupling) functions. The restricted optimum solutions have functional relationships such as the one given by Eq. (4.9). In problem (4.11), the unit (discipline) independent variables are not used as decision variables in the system-level optimization. This is because there (supposedly) are unique restricted optimum values $\vec{x}_i^*$ for every combination of ξ_{ij}.

The LGO method formulated above may be implemented in two different ways:

- Real Time Local-Global Optimization (RT-LGO): In this case the system optimization problem, i.e. problem (4.11), is defined at the highest or controlling level. Once the system-level optimizer selects a combination of values for ξ_{ij}, the local (unit) optimizations take place. The process is repeated until the entire objective function-feedback space is searched.

[15] The optimum response surface may be a graphical representation of the restricted minimum cost versus the coupling (intermediate feedback) functions, or it could also be a lookup table from which restricted optimum solutions can be obtained by interpolation, curve-fitting or other means. Furthermore, multiple response surfaces exist any time an intermediate feedback is represented by a discrete instead of a continuous variable. However, in order to simplify our presentation, the singular tense will be used throughout even though more than one of these hyper-surfaces may be present for any given optimization problem.

- Off-line Local-Global Optimization (OL-LGO): In this case the local (unit) level optimizations takes place off-line before the system-level problem is solved. The restricted optimum solutions are then stored and used by the system-level optimizer at a later time.

The LGO technique has the important advantage that if a sufficiently large number of combinations of the coupling functions is used to solve the unit optimizations, the optimum response surface constitutes a true representation of the optimum design space. The main drawback is that even though the unit problems are smaller than the overall MINLP problem, the number of times they need to be solved (i.e. optimized) can be quite large. This could happen if the range of u_{ij} is big and/or if the u_{ij} are in fact vectors of functions. Another problem which can occur (as in the original MINLP problem) is the need for expensive unit (discipline) analyzers, which hinder the numerous optimizations suggested by problems (4.5) to (4.7). The required use of, for example, heuristic algorithms to deal with integer variables may also cause creation of the optimum response surface to be very expensive.

4.2 Decomposition: Iterative Local Global Approach A

In order to deal with the inherent limitations of LGO, an Iterative Local-Global Optimization (ILGO) approach is proposed. ILGO uses a first order Taylor expansion to locally approximate the optimum response surface, effectively reducing the number of unit optimizations needed. The procedure typically begins with the selection of an initial set of values for u_{ij}, i.e. ξ_{ij}. The units are then optimized for those specific values. The optimization progresses by selecting a new combination of ξ_{ij} that guarantees an improved restricted optimum solution. This selection is done intelligently by studying the local behavior of the optimum response surface. The process is guided by the partial derivatives of the local (unit) objective functions. A formal presentation of Approach A of this method (i.e. ILGO-A) follows:

Consider a modified version of problems (4.5) to (4.7), i.e.

Sub-problem 1:

Minimize $f_1 = f_1(\vec{x}_1, \xi_{21}^o, \xi_{31}^o, \xi_{12}^o, \xi_{13}^o)$ (4.12)

w.r.t. $\vec{x}_1$

subject to

$\vec{h}_1 = \vec{0}$ (4.12.1)

$\vec{g}_1 \leq \vec{0}$ (4.12.2)

Sub-problem 2:

Minimize $f_2 = f_2(\vec{x}_2, \xi_{12}^o, \xi_{32}^o, \xi_{21}^o, \xi_{32}^o)$ (4.13)

w.r.t. $\vec{x}_2$

subject to

$\vec{h}_2 = \vec{0}$ (4.13.1)

$\vec{g}_2 \leq \vec{0}$ (4.13.2)

Sub-problem 3:

Minimize $f_3 = f_3(\vec{x}_3, \xi_{13}^o, \xi_{23}^o, \xi_{31}^o, \xi_{32}^o)$ (4.14)

w.r.t. $\vec{x}_3$

subject to

$\vec{h}_3 = \vec{0}$ (4.14.1)

$$\vec{g}_3 \le \vec{0} \tag{4.14.2}$$

In problems (4.12) to (4.14), the coupling functions, u_{ij}, have been fixed at some arbitrary initial values, ξ_{ij}^o. The resulting restricted values for the optimum solutions are $\left(f_1^*\right)^o$, $\left(f_2^*\right)^o$ and $\left(f_3^*\right)^o$ with corresponding $\left(\vec{x}_1^*\right)^o$, $\left(\vec{x}_2^*\right)^o$ and $\left(\vec{x}_3^*\right)^o$. The superscript *o* that accompanies the restricted optimum solutions serves as a remainder that they are calculated at the initial or reference point.

A Taylor series expansion of the unit-level objective functions is performed about the ORS reference point and the linear term is taken so that, for example, for unit 1

$$f_1 = (f_1^*)^o + \left(\frac{\partial f_1^*}{\partial u_{12}}\right)^o \Delta u_{12} + \left(\frac{\partial f_1^*}{\partial u_{13}}\right)^o \Delta u_{13} + \left(\frac{\partial f_1^*}{\partial u_{21}}\right)^o \Delta u_{21} + \left(\frac{\partial f_1^*}{\partial u_{31}}\right)^o \Delta u_{31} \tag{4.15}$$

Using a more compact notation, equation (4.15) reduces to

$$f_1 = (f_1^*)^o + \lambda_{12}^1 \Delta u_{12} + \lambda_{13}^1 \Delta u_{13} + \lambda_{21}^1 \Delta u_{21} + \lambda_{31}^1 \Delta u_{31} \tag{4.16}$$

and for units 2 and 3

$$f_2 = (f_2^*)^o + \lambda_{21}^2 \Delta u_{21} + \lambda_{23}^2 \Delta u_{23} + \lambda_{12}^2 \Delta u_{12} + \lambda_{32}^2 \Delta u_{32} \tag{4.17}$$

$$f_3 = (f_3^*)^o + \lambda_{31}^3 \Delta u_{31} + \lambda_{32}^3 \Delta u_{32} + \lambda_{13}^3 \Delta u_{13} + \lambda_{23}^3 \Delta u_{23} \tag{4.18}$$

where

$$\lambda_{ij}^i = \left(\frac{\partial f_i^*}{\partial u_{ij}}\right)^o \tag{4.19}$$

The partial derivatives (the λ's) are a measure of the relative importance of the coupling functions in terms of the overall system-level objective. In ILGO-A, the λ's guide the selection of a new set of values for u_{ij} since equations (4.16) to (4.20) show

that depending on the sign and absolute value of the partial derivatives, it is possible to obtain improved restricted optimum values for each of the local objective functions by changing the desired value of the coupling functions. Thus, for example, negative partial derivatives indicate that an increase in the corresponding coupling function may lead to a decrease of the objective function. Geometrically they represent the direction (on the ORS) in which an improvement in the system-level objective function is achieved. The new values are chosen so that the linear representation of the objective functions is valid.

An algorithm for ILGO-A follows:

1. Obtain an initial point on the ORS with the value of the coupling functions, u_{ij}, equal to ξ_{ij}^{o} by solving the optimization problems (4.12) to (4.14).

2. Calculate the partial derivatives (λ_{ij}^{i}) of the restricted optimum functions f_i^* with respect to the u_{ij}.

3. Update the values of ξ_{ij}^{o} based on the following algorithm:

$$\left(\xi_{ij}^{o}\right)_{new} = \left(\xi_{ij}^{o}\right)_{old} - \alpha_o \left(\frac{\partial f_m^*}{\partial u_{ij}}\right)^o = \left(\xi_{ij}^{o}\right)_{old} - \alpha_o \lambda_{ij}^{m} \tag{4.20}$$

where

$$\lambda_{ij}^{m} = \lambda_{ij}^{1} \text{ if } \left|\left(\frac{\partial f_1^*}{\partial u_{ij}}\right)^o\right| \geq \left|\left(\frac{\partial f_2^*}{\partial u_{ij}}\right)^o\right| \text{ and } \left|\left(\frac{\partial f_1^*}{\partial u_{ij}}\right)^o\right| \geq \left|\left(\frac{\partial f_3^*}{\partial u_{ij}}\right)^o\right| \tag{4.21}$$

$$\lambda_{ij}^{m} = \lambda_{ij}^{2} \text{ if } \left|\left(\frac{\partial f_2^*}{\partial u_{ij}}\right)^o\right| > \left|\left(\frac{\partial f_1^*}{\partial u_{ij}}\right)^o\right| \text{ and } \left|\left(\frac{\partial f_2^*}{\partial u_{ij}}\right)^o\right| > \left|\left(\frac{\partial f_3^*}{\partial u_{ij}}\right)^o\right| \tag{4.22}$$

$$\lambda_{ij}^{m} = \lambda_{ij}^{3} \text{ if } \left| \left(\frac{\partial f_3^*}{\partial u_{ij}} \right)^o \right| > \left| \left(\frac{\partial f_1^*}{\partial u_{ij}} \right)^o \right| \text{ and } \left| \left(\frac{\partial f_3^*}{\partial u_{ij}} \right)^o \right| > \left| \left(\frac{\partial f_2^*}{\partial u_{ij}} \right)^o \right| \tag{4.23}$$

4. Steps 1 through 3 are repeated until no improvement in the unit optimizations is achieved or until the coupling functions have reached the minimum or maximum allowable value.

Equations (4.21) to (4.23) specifically deal with the typical competing tendencies, which local objective functions tend to have. Geometrically, they indicate that the search is conducted in the direction of greatest decrease of the overall system-level objective function. Thus, the algorithm given in steps 1 to 4 above can be characterized by equation (4.20) as a gradient descent algorithm (see Chapter 2) in the objective-coupling function domain, i.e. on the Optimum Response Surface of the problem. Therefore, the speed and convergence properties of ILGO-A are the same as any gradient-based optimization algorithm and depend on the general behavior of the Optimum Response Surface, the starting point, and the step size α. The particular descent properties of the algorithm when applied to energy systems are addressed below.

The above algorithm may result in a better way of exploring the optimum response surface than the LGO algorithm in its original form. As in any gradient-based algorithm, one has the option of either taking very small steps and reevaluating the gradient at every step or taking large steps at any given point. The first approach results in a laborious method of reaching the system-level optimum, whereas the second may result in a more zigzag path for the optimizer. Obviously very small steps will require a large number of solutions of the unit optimization problems, defeating the purpose of the method altogether.

4.3 Decomposition: Iterative Local Global Approach B

The previous version of the ILGO technique (ILGO-A) makes explicit use of the assumption that there exists a set of vectors $\vec{x}_i^*$ that minimizes equations (4.12) to (4.14), and satisfies the unit (or discipline) constraints and the additional constraint that the coupling functions take the values ξ_{ij}^o. In some systems, however, not every combination of the ξ_{ij} leads to a feasible solution (much less to an optimum solution), i.e. one that satisfies the equality and inequality constraints imposed by the unit analyzers. As a matter of fact, it is possible to have cases where ILGO-A may point towards a simultaneous increase in the u_{ij} (because their associated partial derivatives are negative); but due to the characteristics of the units this is not physically possible. That would be the case of a system with competing effects of u_{ij}. For such cases, an alternative version of the approach (ILGO-B) is proposed.

Recalling the functional relationships given by expression (4.1), one can write that

$$\Delta u_{ij} = \nabla_{x_i}\left(u_{ij}\right)^T \cdot \Delta\vec{x}_i \quad + \nabla_{x_j}\left(u_{ij}\right)^T \cdot \Delta\vec{x}_j \tag{4.24}$$

where

$$\nabla_{x_i}\left(u_{ij}\right)^T \Delta\vec{x}_i = \frac{\partial u_{ij}}{\partial x_{i1}}\Delta x_{i1} + \cdots + \frac{\partial u_{ij}}{\partial x_{in}}\Delta x_{in} \tag{4.25.1}$$

and n is the size of the vector of independent variables $\vec{x}_i$, and, for example,

$$\Delta x_{i1} = x_{i1} - \left(x_{i1}^*\right)^o \tag{4.25.2}$$

This relationship (equation (4.25)) shows the effect that the unit decision variables, $\vec{x}_i$ and $\vec{x}_j$, have on the coupling functions (i.e. intermediate feedbacks).

Based on equation (4.15), the system-level optimization problem (4.3) can be rewritten as

Minimize

$$
\begin{aligned}
f \;=& \sum_{k=1}^{3}\left(f_k^*\right)^o + \left(\frac{\partial f_1^*}{\partial u_{12}}\right)^o \Delta u_{12} + \left(\frac{\partial f_1^*}{\partial u_{13}}\right)^o \Delta u_{13} + \left(\frac{\partial f_1^*}{\partial u_{21}}\right)^o \Delta u_{21} + \left(\frac{\partial f_1^*}{\partial u_{31}}\right)^o \Delta u_{31} \\
&+ \left(\frac{\partial f_2^*}{\partial u_{12}}\right)^o \Delta u_{12} + \left(\frac{\partial f_1^*}{\partial u_{32}}\right)^o \Delta u_{32} + \left(\frac{\partial f_2^*}{\partial u_{21}}\right)^o \Delta u_{21} + \left(\frac{\partial f_2^*}{\partial u_{23}}\right)^o \Delta u_{23} \\
&\left(\frac{\partial f_3^*}{\partial u_{13}}\right)^o \Delta u_{13} + \left(\frac{\partial f_3^*}{\partial u_{23}}\right)^o \Delta u_{23} + \left(\frac{\partial f_3^*}{\partial u_{32}}\right)^o \Delta u_{32} + \left(\frac{\partial f_3^*}{\partial u_{31}}\right)^o \Delta u_{31}
\end{aligned}
\tag{4.26}
$$

or in more compact form using equations (4.16) to (4.18) as

$$
\text{Minimize } f = \sum_{k=1}^{3}\left(f_k^*\right)^o + \sum_{k=1}^{3}\left(\sum_{i=1,i\neq k}^{3}\lambda_{ik}^k \Delta u_{ik} + \sum_{i=1,i\neq k}^{3}\lambda_{ki}^k \Delta u_{ki}\right) \tag{4.27}
$$

w.r.t. $\vec{x}_1, \vec{x}_2, \vec{x}_3$

subject to the same constraints as the original MINLP, i.e. problem (4.4).

Combining equations (4.25) and (4.28), the system-level optimization problem can be written as

$$
\begin{aligned}
\text{Minimize } & f = \sum_{k=1}^{3}\left(f_k^*\right)^o + \sum_{k=1}^{3}\sum_{i=1,i\neq k}^{3}\lambda_{ik}^k\left(\nabla_{x_i}\left(u_{ik}\right)^T \cdot \Delta\vec{x}_i \;+ \nabla_{x_k}\left(u_{ik}\right)^T \cdot \Delta\vec{x}_k\right) \\
& + \sum_{k=1}^{3}\sum_{i=1,i\neq k}^{3}\lambda_{ki}^k\left(\nabla_{x_i}\left(u_{ki}\right)^T \cdot \Delta\vec{x}_i \;+ \nabla_{x_k}\left(u_{ki}\right)^T \cdot \Delta\vec{x}_k\right)
\end{aligned}
\tag{4.28}
$$

w.r.t. $\vec{x}_1, \vec{x}_2, \vec{x}_3$

subject to the same constraints as the original MINLP, i.e. problem (4).

Equation (4.29) states mathematically *the fundamentally important concept that in any system a variation in the local (unit) independent variables has an impact on the local objective function and on the objective functions of all the other units (the rest of the system)*. For example, in Figure 4.1, a perturbation on $\vec{x}_1$ about an arbitrary point creates changes in u_{12}, u_{13}, u_{21} *and* u_{31} that translates into a variation in the optimum

value of the local objective function of unit 1 *and* units 2 and 3. The contribution of each of the local variables can be disaggregated to create a set of decomposed optimization sub-problems at the system level, which for unit 1 takes the form

Minimize

$$f^{(1)} = \sum_{k=1}^{3} \left(f_k^*\right)^o + \left(\frac{\partial f_1^*}{\partial u_{12}}\right)^o \Delta u_{12}^{(1)} + \left(\frac{\partial f_1^*}{\partial u_{13}}\right)^o \Delta u_{13}^{(1)} + \left(\frac{\partial f_1^*}{\partial u_{21}}\right)^o \Delta u_{21}^{(1)} + \left(\frac{\partial f_1^*}{\partial u_{31}}\right)^o \Delta u_{31}^{(1)} + \left(\frac{\partial f_2^*}{\partial u_{12}}\right)^o \Delta u_{12}^{(1)} + \left(\frac{\partial f_2^*}{\partial u_{21}}\right)^o \Delta u_{21}^{(1)} + \left(\frac{\partial f_3^*}{\partial u_{13}}\right)^o \Delta u_{13}^{(1)} + \left(\frac{\partial f_3^*}{\partial u_{31}}\right)^o \Delta u_{31}^{(1)} \tag{4.29}$$

w.r.t. $\vec{x}_1$

subject to the same constraints as in problem (4.14)

and where, for example,

$$\Delta u_{21}^{(1)} = \nabla_{x_1}\left(u_{21}\right)^T \Delta \vec{x}_1 \tag{4.30}$$

that is, $\Delta u_{21}^{(1)}$ is the change in the coupling function u_{21} due to a variation in $\vec{x}_1$ *only*. In general,

$$\Delta u_{ji}^{(i)} = \nabla_{x_i}\left(u_{ji}\right)^T \Delta \vec{x}_i \tag{4.31}$$

The above problem (equation (4.29)) can also be written as

Minimize

$$f^{(1)} = f_1 + f_2^* + f_3^* + \lambda_{12}^2 \Delta u_{12}^{(1)} + \lambda_{21}^2 \Delta u_{21}^{(1)} + \lambda_{13}^3 \Delta u_{13}^{(1)} + \lambda_{31}^3 \Delta u_{31}^{(1)} \tag{4.32}$$

w.r.t. $\vec{x}_1$

subject to the same constraints as in problem (4.14)

Problem (4.32) is not strictly speaking a local problem for unit 1 because in addition to the contribution f_1 of unit 1 to the overall objective function f, it includes the effect

that changes in the local (unit 1) independent variables have on the local contributions f_2 and f_3 of units 2 and 3, respectively. This impact is taken into account via the coupling functions. The variation in local decision variables propagates into other units by means of the partial derivatives (the λ's) and ends up affecting the system-level objective. In this work problems such as problem (4.29) are called *unit-based system-level optimization problems*.

The unit-based system-level optimization problems for units 2 and 3 are

Minimize

$$f^{(2)} = f_2 + f_1^* + f_3^* + \lambda_{12}^1 \Delta u_{12}^{(2)} + \lambda_{21}^1 \Delta u_{21}^{(2)} + \lambda_{23}^3 \Delta u_{23}^{(2)} + \lambda_{32}^3 \Delta u_{32}^{(2)} \tag{4.33}$$

w.r.t. $\vec{x}_2$ and subject to the same constraints as in problem (4.14), and

Minimize

$$f^{(3)} = f_3 + f_1^* + f_2^* + \lambda_{13}^1 \Delta u_{13}^{(3)} + \lambda_{31}^1 \Delta u_{31}^{(3)} + \lambda_{23}^2 \Delta u_{23}^{(3)} + \lambda_{32}^2 \Delta u_{32}^{(3)} \tag{4.34}$$

w.r.t. $\vec{x}_3$ and subject to the same constraints as in problem (4.14)

The above sub-problems have the advantage that only values of the independent variables close to $\left(\vec{x}_i^*\right)^o$, which lead to feasible solutions, are allowed to participate in the optimization. Each set of possible feasible solutions is evaluated based on its impact on the overall system-level objective in terms of the coupling functions. As in the first version of the algorithm, the partial derivatives provide the direction (in the optimum response surface domain) in which changes in u_{ij} lead to better solutions.

The above discussion indicates that the local (unit) decision variables are allowed to take arbitrary values that satisfy the primary constraints. Such freedom may cause significant changes in the coupling functions, so in general, the additional or secondary constraints

$$\Delta u_{ij} - \varepsilon \cdot \Delta u_{ij\,\max} \leq 0 \tag{4.35}$$

are imposed. In equation (4.35), the $\Delta u_{ij\,\max}$ are the maximum allowable values for changes in the coupling functions and the factor ε is added to ensure that linear Taylor series expansions (equations (4.16) to (4.18)) are a good local representation of the optimum response surface. It should be obvious that if the partial derivatives are constant over wide ranges of u_{ij}, very rapid jumps in the optimum objective-coupling function domain can be made. If the nature of the optimum response surface is such that it does not permit large jumps from one point to the other, i.e. it is highly non-linear, it will be necessary to iterate. The higher the non-linearity is, the larger the number of iterations will be.

The algorithm for ILGO-B (approach B of the ILGO technique) is as follows:

1. Obtain an initial point of the optimum response surface for an initial reference value of the coupling functions, i.e. u_{ij} equal to ξ_{ij}^{o}, by solving the optimization problems (4.12) to (4.14)
2. Calculate the partial derivatives (λ_{ij}^{i}) of the restricted optimum functions f_i^* with respect to u_{ij} at the initial point.
3. Estimate the maximum allowable values of u_{ij} and the corresponding factor ε. If no information is available, assume that the partial derivatives are constant over most of the optimum response surface.
4. Solve problems (4.32) to (4.34) subject to the additional constraint on the coupling functions u_{ij} (expression (4.35)).
5. Use the solutions from the previous step to update $\left(\vec{x}_i^*\right)^o$ and ξ_{ij}^{o}. Repeat the procedure (steps 2 to 5) until no improvement is achieved or until the u_{ij} have reached the minimum or maximum allowable values.

4.4 Special Cases

4.4.1 Systems with units having common independent variables.

Consider an energy system (see Figure 4.2) in which, in addition to the local variables, $\vec{x}_i$, the units share a common decision variable x. In this case, the relation-

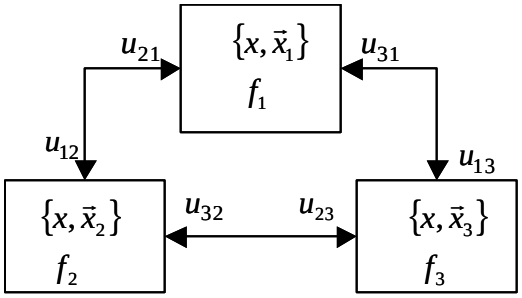

Figure 4.2. A coupled energy system with common independent variables.

ship given for say unit 1 is restated as

$$f_1 = f_1(x, \vec{x}_1, u_{21,} u_{31}, u_{12,} u_{13}) \tag{4.36}$$

The resulting restricted values for the optimum solutions are $\left(f_1^*\right)^o$, $\left(f_2^*\right)^o$ and $\left(f_3^*\right)^o$ with corresponding $\left(\vec{x}_1^*\right)^o$, $\left(\vec{x}_2^*\right)^o$ and $\left(\vec{x}_3^*\right)^o$.

A Taylor series expansion of the unit-level objective functions is performed about the ORS reference point with the independent variables $\left(\vec{x}_1^*\right)^o$, $\left(\vec{x}_2^*\right)^o$, $\left(\vec{x}_3^*\right)^o$, and $\left(x^*\right)^o$ and the linear term is taken so that for unit 1

$$\begin{aligned} f_1 = (f_1^*)^o + \left(\frac{\partial f_1^*}{\partial x}\right)^o \Delta x + \left(\frac{\partial f_1^*}{\partial u_{12}}\right)^o \Delta u_{12} + \left(\frac{\partial f_1^*}{\partial u_{13}}\right)^o \Delta u_{13} \\ + \left(\frac{\partial f_1^*}{\partial u_{21}}\right)^o \Delta u_{21} + \left(\frac{\partial f_1^*}{\partial u_{31}}\right)^o \Delta u_{31} \end{aligned} \tag{4.37}$$

where the first partial derivative is defined in general terms as

$$\lambda_x^i = \left(\frac{\partial f_i^*}{\partial x} \right)^o \tag{4.38}$$

It becomes clear that it is possible to make the assumption that a hypothetical "unit" has been added to the original system of Figure 4.1 with independent variable *x*. Under this assumption one can then define a "unit-based" system-level optimization problem such that

Minimize

$$f^{(x)} = \left(f^* \right)^o + \left(\lambda_x^1 + \lambda_x^2 + \lambda_x^3 \right) \Delta x \tag{4.39}$$

w.r.t. x and subject to the same constraints as in problem (4.14)

Clearly problem (4.38) is one of minimizing the effect of the common variables in terms of the overall system-level objective. Note that an extension of the method to the case when the common variables form a vector is trivial.

4.4.2 Problems with discrete variables

The methodology presented here heavily relies on the existence of the partial derivatives $\partial f_i^* / \partial u_{ij}$. Obviously, this means that a necessary condition for the implementation of the methods is that the objective function is differentiable with respect to the coupling functions. This implies that at the very least the ORS is continuous over some ranges of u_{ij}. However, the partial derivatives $\partial u_{ij} / \partial x_i$ and $\partial u_{ij} / \partial x$ were introduced in order to illustrate the inner workings of the method and are not required. This supports the use of non-gradient based algorithms such as genetic algorithms (GAs) or simulated annealing (SAs) to solve the unit-based system-level optimization problems.

4.5 Comments

The descent properties of the ILGO algorithm indicate that, at the very least, a local minimum will be found. This important finding leads to the conclusion that if the cost function is convex and smooth with respect to the coupling functions, then the ILGO approach points towards a global optimum (e.g., the local minimum of a smooth convex function is the global minimum). In the worst case, the ILGO method only leads to a local minimum in which case the process must be repeated with different workable starting points (i.e. feasible syntheses / designs) until confidence in the solution as a global optimum is achieved. Despite the obvious time penalty that this may cause, the ILGO may still be the most if not the only practical optimization scheme that can be applied to a highly complex, highly dynamic energy system synthesis and design.

Chapter 5

Decomposition Strategies for the Synthesis and Design Optimization of Highly Dynamic Energy Systems

Dynamic energy systems have special attributes and pose great challenges to the practical application of any of the decomposition methods outlined above. To begin with, consider the non-hierarchical energy system of Figure 5.1, which is composed of m units.

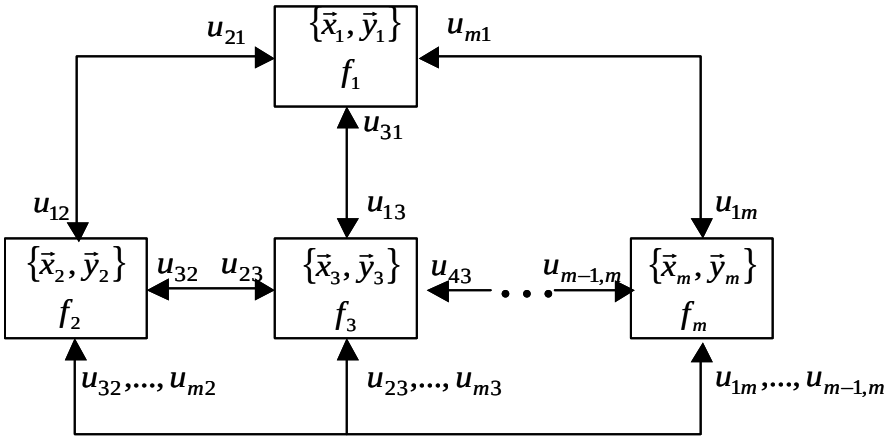

Figure 5.1. A coupled non-hierarchical energy system.

As in the previous chapter each unit, *i*, has a contribution f_i to the overall objective or cost function *f*. In typical energy systems each unit's contribution to the overall objective function has the form

$$f_i = k_i R_i + Z_i \tag{5.1}$$

where the functions R_i $(i = 1,...,m)$ represent the external resources (e.g., fuel) used to perform the required tasks. These tasks are assumed known. The functions Z_i are related to the physical dimensions and material and technology choice for the unit and can, therefore, be given in terms of mass, area, volume, and/or capital cost. The Z_i will, thus, be called the *capital* functions. The constant k_i is an appropriate conversion factor.

One of the features of dynamic energy systems is that the amount of external resources can be varied at different instants in time. Likewise, under certain circumstances, the capital functions can take different values over time. One such circumstance is when the capital function represents costs that may be influenced by operating conditions (e.g., maintenance costs). Another feature of energy systems is that the coupling functions u_{ij} may be interpreted as intermediate products of unit *i* but in turn become intermediate resources for unit *j*. In some cases, the coupling functions can be considered as attributes of *j* that are passed back to *i*, i.e. they effectively act as intemermediate feedback functions.

Time variations in the local objective functions are accomplished by the definition of independent synthesis / design and operational variable vectors $\vec{x}_i$ and $\vec{y}_i$, respectively, for each unit. The synthesis / design variables, $\vec{x}_i$, typically correspond to geometric parameters (physical dimensions of components), design flow rates, design pressure ratios, and in a wider sense some discrete (e.g., material or technology choice) or binary (e.g., existence or nonexistence of a unit in the system configuration) parameters. By definition synthesis / design variables remain constant in time. Operational variables, $\vec{y}_{i_t}$, are parameters which can be controlled over time so that off-

design operation is at an optimum. Operational variables can be continuous variables (flow rates, valve settings) or binary variables (e.g., units on or off).

Given the dynamic nature of the problem, it is often convenient to work with objective functions in rate form. The functional relationships for the local objective functions at an instant *t* are then given by

$$\begin{aligned} \dot{R}_1 &= \dot{r}_1\left(\vec{x}_1, \vec{y}_{1t}, u_{12}, ..., u_{1m}, u_{21}, ..., u_{m1}\right) \\ &\vdots \\ \dot{R}_m &= \dot{r}_m\left(\vec{x}_m, \vec{y}_{mt}, u_{m1}, ..., u_{m\,m-1}, u_{1,}, ..., u_{m-1\,m}\right) \end{aligned} \tag{5.2}$$

$$\begin{aligned} \dot{Z}_1 &= \dot{Z}_1\left(\vec{x}_1, \vec{y}_{1t}, u_{12}, ..., u_{1m}, u_{21}, ..., u_{m1}\right) \\ &\vdots \\ \dot{Z}_m &= \dot{Z}_m\left(\vec{x}_m, \vec{y}_{mt}, u_{m1}, ..., u_{m\,m-1}, u_{1,}, ..., u_{m-1\,m}\right) \end{aligned} \tag{5.3}$$

and

$$\begin{aligned} \dot{f}_1 &= \dot{f}_1\left(\vec{x}_1, \vec{y}_{1t}, u_{12}, ..., u_{1m}, u_{21}, ..., u_{m1}\right) \\ &\vdots \\ \dot{f}_m &= \dot{f}_m\left(\vec{x}_m, \vec{y}_{mt}, u_{m1}, ..., u_{m\,m-1}, u_{1,}, ..., u_{m-1\,m}\right) \end{aligned} \tag{5.4}$$

At an instant *t*, the coupling functions are in general given by

$$u_{ij_t} = u_{ij}(\vec{x}_i, \vec{x}_j, \vec{y}_{it}, \vec{y}_{j_t}) \tag{5.5}$$

With this in mind and after choosing the independent variables, the system-level synthesis / design problem is formulated as

$$\text{Minimize} \quad f = \int_{time} \left(\sum_{i=1}^{m} \dot{f}_{it} \right) dt \tag{5.6}$$

w.r.t. $\vec{X}^T = \{\vec{x}_1, \vec{x}_2, \cdots, \vec{x}_m\}$, $\vec{\mathrm{Y}}^T = \{\vec{Y}_t\}^T = \{\vec{y}_{1t}, \vec{y}_{2t}, \cdots, \vec{y}_{mt}\}$

subject to

$$\vec{\mathrm{H}} = \left\{\vec{H}_t\right\} = \begin{Bmatrix} \vec{h}_{1t} \\ \vdots \\ \vec{h}_{mt} \end{Bmatrix} = \vec{0}$$
$$\vec{\Gamma} = \left\{\vec{G}_t\right\} = \begin{Bmatrix} \vec{g}_{1t} \\ \vdots \\ \vec{g}_{mt} \end{Bmatrix} \le \vec{0} \qquad (5.6.2)$$

where

$$\dot{f}_i = k_i \dot{R}_i + \dot{Z}_i \qquad (5.6.3)$$

The vectors of equality and inequality constraints at various instants of time, $\vec{H}_t$ and $\vec{G}_t$, respectively, represent the thermodynamic, physical, and cost models (i.e. the analysis system of equations) and the restrictions imposed on the synthesis / design. One such restriction is the desired product for each of the units. Thus, the n_{th} element of any vector of equality constraints $\vec{h}_i$ at any instant *t* is given by

$$h_{i,n_t} = \dot{P}_{i_t} - \dot{P}^{o}_{i\ t} \qquad (5.6.4)$$

where $\dot{P}_{i_t}$ is the actual product rate and $\dot{P}^{o}_{i\ t}$ the product rate required for unit *i*.

In most cases it is advisable to discretize the time integral by taking time segments (independent of each other or not[16]) over the entire load and/or range of environmental conditions. The number of these segments depends on the nature of the load and the level of detail desired. A discretized version of equation (5.6) can be written as

$$\text{Minimize } f = \sum_{t=1}^{\tau} \left(\sum_{i=1}^{m} \dot{f}_i \right) \Delta t_t \qquad (5.7)$$

[16] A problem with dependent time segments is one where transient effects are important.

w.r.t. $\vec{X}^T = \{\vec{x}_1, \vec{x}_2, \cdots, \vec{x}_m\}$ $\vec{\mathrm{Y}}^T = \{\vec{Y}_t\}^T = \{\vec{y}_{1t}, \vec{y}_{2t}, \cdots, \vec{y}_{mt}\}$ $t = 1,..., \delta,..., \tau$

subject to

$$\vec{\mathrm{H}} = \{\vec{H}_t\} = \begin{Bmatrix} \vec{h}_{1t} \\ \vdots \\ \vec{h}_{mt} \end{Bmatrix} = \vec{0} \qquad t = 1,..., \delta,..., \tau \tag{5.7.1}$$

$$\vec{\Gamma} = \{\vec{G}_t\} = \begin{Bmatrix} \vec{g}_{1t} \\ \vdots \\ \vec{g}_{mt} \end{Bmatrix} \leq \vec{0} \qquad t = 1,..., \delta,..., \tau \tag{5.7.2}$$

Here the subscript *t* refers to the τ different segments into which the load/environmental conditions have been divided. Note that in equation (5.7), the time segments can have different durations.

Now, assume that the sizes of the synthesis / design and operational variable vectors are *d* and *o*, respectively. The total number of variables is, therefore, $d+o\tau$. For complex, highly dynamic energy systems, which may require high levels of detail or have large numbers of units, the total combined number of variables, discrete and continuous may grow very large. In addition, the fact that the response of energy system components and subsystems is typically highly nonlinear and the nature of the synthesis / design space non-contiguous (due to the presence of discrete variables) make the problem very expensive computationally and in some cases, even impossible to be solved with existing optimization algorithms. In fact, the resulting mixed-integer, non-linear programming (MINLP) problem has a known solution only under very special, restricted conditions (Floudas, 1995; Bruno et al., 1998).

The alternatives normally considered are to reduce the number of independent variables either by varying only a few synthesis / design variables at a time (trade-off analysis), considering a severely limited number of synthesis / design variables while accounting for only one of the operating conditions (one-point design), and/or linearizing the problem in order to transform it into a mixed integer linear programming

(MILP) or linear programming (LP) problem. These alternatives can be avoided through the use of decomposition so that the solution to the original problem does not compromise the quality of the final synthesis / design.

However, as mentioned above, the purpose of decomposition is not just to decrease the size of the synthesis / design problem. An equally important reason is to facilitate the difficult task of sub-system and, in some cases, discipline integration. In many existing industrial design processes, the synthesis/design of units are carried out by different groups and oftentimes different departments within a company or even different companies. The different design philosophies, tools and procedures are in many cases not compatible with each other, making the solution of the entire problem as a single block simply impractical. These difficulties are only worsened by the fact that the synthesis / design of the different units is done at different times.

Therefore, in many practical settings, decomposition is an absolute necessity. In this work, two types of decomposition are considered. The first is *time decomposition* and the second *physical* (i.e. unit) *decomposition*. Physical or unit decomposition uses the mathematical concepts for LGO and ILGO defined in the previous chapters.

5.1 Time Decomposition

Time decomposition exploits the fundamental differences that exist between the design and operational variables to create a set of hierarchical problems each with a lower dimensionality than the overall system-level problem. Different types of time decomposition can be defined.

The most common time decomposition schemes (e.g., Frangopoulos (1989), Olsommer, et al (1999a,b)) are depicted in Figure 5.2. In both cases the synthesis / design variables are selected by a high-level optimizer. Once the synthesis / design variables ($\vec{X}$) are fixed they are used by a low-level optimizer to find the optimum operational decision variables ($\vec{Y}_t$). This second step can be done taking all of the time segments into which the load/environmental conditions have been divided and using

them in a single problem as illustrated in Figure 5.2a. If the number of operational decision variables (e.g., the size of vector $\vec{Y}$) and/or the number of time segments is large, it may be advisable to define a set of τ optimization problems, one for each of the time segments (each with respect to the instantaneous operational variables ($\vec{Y}_t$) as indicated in Figure 5.2b). Once the low-level problems are solved, the optimum values of the objective functions corresponding to the given synthesis / design variables, indicated in Figure 5.2 as f_x^*, are sent back to the high-level optimizer for analysis. The high-level optimizer is in charge of finding the optimum values for the synthesis / design variables.

Time decomposition effectively reduces the size of the overall problem from $d+o\tau$ variables by solving two problems of size d and $o\tau$, respectively, in the case of Figure 5.2a. In the case of Figure 5.2b, the original problem is replaced by one problem of size d and τ problems of size o/τ.

The main disadvantages of the time decomposition approaches outlined above are

- the very large expense of the nested optimizations that result from applying either approach (i.e. all the time segments as a single problem or each time segment as an individual problem).
- the size of the sub-problems may still be too large even with time decomposition.
- other forms of decomposition, e.g., physical decomposition, are difficult to implement at the synthesis / design level.
- it is likely that a large number of combinations of the synthesis / design variables X when used in the low-level problem(s) (to find the optimum $\vec{Y}_t$) will not lead to feasible solutions.

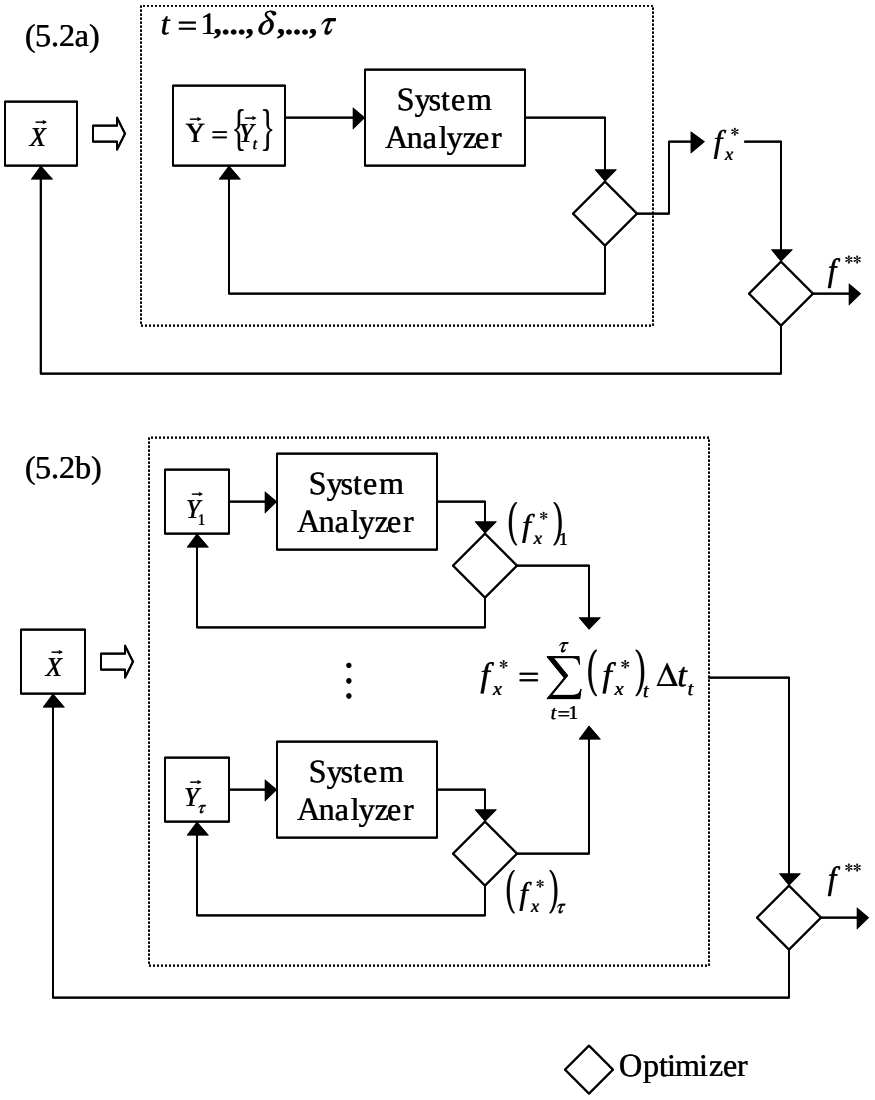

Figure 5.2. Variable-based time decomposition schemes.

Other than the third disadvantage above, all of these drawbacks are alleviated somewhat by the fact that both approaches are easily parallelized in various ways. Thus, for example, multiple processors may simultaneously handle different combinations of the synthesis / design variables along with the optimizations with respect to the operational

variables. Another possibility is to have multiple processors execute the optimizations at different time segments as shown in Figure 5.2b.

To get around the disadvantages listed above and in particular the third one, the type of time decomposition that is proposed and used in this work is depicted in Figure 5.3. The approach, which is not based on a nested scheme, consists of selecting one time segment, say segment δ, which has the most demanding[17] load requirements and/or environmental conditions[18], as the synthesis / design point[19]. The system is then synthesized / designed for this point by solving the restricted problem:

$$\text{Minimize } f_\delta = \left[\left(\sum_{i=1}^{m} \dot{f}_i \right) \cdot \Delta t \right]_\delta \tag{5.8}$$

w.r.t. $\vec{X}^T = \{\vec{x}_1, \vec{x}_2, \cdots, \vec{x}_m\}$ $\vec{Y}^T = \{\vec{Y}_\delta\}^T = \{\vec{y}_{1\delta}, \vec{y}_{2\delta}, \cdots, \vec{y}_{m\delta}\}$

subject to

$$\vec{H}_\delta = \begin{Bmatrix} \vec{h}_{1\delta} \\ \vdots \\ \vec{h}_{m\delta} \end{Bmatrix} = \vec{0} \tag{5.8.1}$$

$$\vec{G}_\delta = \begin{Bmatrix} \vec{g}_{1\delta} \\ \vdots \\ \vec{g}_{m\delta} \end{Bmatrix} \leq \vec{0}$$

[17] The most demanding segment could be the one that uses the greatest amount of external resources and/or poses the greatest challenges in terms of meeting the system analyzer equations including the external demand for the system's products.

[18] Actually, more than one segment could be chosen especially if a priori it were not clear which segment is the most demanding or if two or more segments are relatively close in significance. Of course, each additional segment complicates the process and too many defeats the purpose of this type of time decomposition all together.

[19] A single reference condition is normally called the synthesis / design point. In this context, such a designation is somewhat misleading since one is trying to obtain the synthesis / design that minimizes the cost over the entire load.

where Δt is the length of time considered for time segment δ and m the number of units in the system. The subscript δ refers to the segment chosen for the "synthesis / design" of the system.

The result obtained from solving equation (5.8) for a single synthesis / design is a set of feasible solutions[20] (some optimal with respect to equation (5.8) and others not) that satisfies the constraints given by equations (5.8.1). These solutions have a corresponding set of vectors $\vec{X}_\delta$ and $\vec{Y}_\delta$. The most promising of these feasible solutions (indicated in Figure 5.3 as having decision variables $\vec{X}_\delta^{\,fp}$ and $\vec{Y}_\delta^{\,fp}$, and corresponding objective function value $f_\delta^{\,\Diamond}$) are then used to minimize the total cost over the entire load/environmental profile for each of these feasible solutions, i.e.

$$\text{Minimize } f = \left[\left(\sum_{i=1}^{m} \dot{f}_i\right)\cdot \Delta t\right]_\delta^{fp} + \sum_{t=1}^{\tau-1}\left(\sum_{i=1}^{m} \dot{f}_i\right)\Delta t_t \tag{5.9}$$

$$\text{w.r.t.} \quad \vec{\mathrm{Y}}^T = \left\{\vec{Y}_t\right\}^T = \left\{\vec{y}_{1t}, \vec{y}_{2t}, \cdots, \vec{y}_{mt}\right\} \qquad t = 1,\ldots,\delta-1,\delta+1,\ldots,\tau \tag{5.9.1}$$

subject to

$$\vec{\mathrm{H}} = \left\{\vec{H}_t\right\} = \begin{Bmatrix} \vec{h}_{1t} \\ \vdots \\ \vec{h}_{mt} \end{Bmatrix} = \vec{0} \qquad t = 1,\ldots,\delta-1,\delta+1,\ldots,\tau \tag{5.9.2}$$

$$\vec{\Gamma} = \left\{\vec{G}_t\right\} = \begin{Bmatrix} \vec{g}_{1t} \\ \vdots \\ \vec{g}_{mt} \end{Bmatrix} \le \vec{0} \qquad t = 1,\ldots,\delta-1,\delta+1,\ldots,\tau$$

and $$\vec{X} - \vec{X}_\delta^{\,fp} = \vec{0} \tag{5.9.3}$$

[20] This presupposes a means for generating these feasible solutions, which can be done with a heuristic approach such as a genetic algorithm or conventional gradient-based method.

This type of decomposition uses the implicit assumption that only a relatively few number of sets of synthesis / design variables $\vec{X}$ are likely to lead to an optimum solution when the entire load profile is included. The first term on the right of equation (5.9) is known from solutions to equation (5.8). It is furthermore assumed that the best solution(s) for the reference (synthesis / design) point used with equation (5.8) is not necessarily the best when integrated over the various off-design conditions. To this end, as indicated by constraint (5.9.3), the values of the synthesis / design variables are set equal to the various synthesis / design variable values associated with the promising feasible solutions obtained from solving problem (5.8).

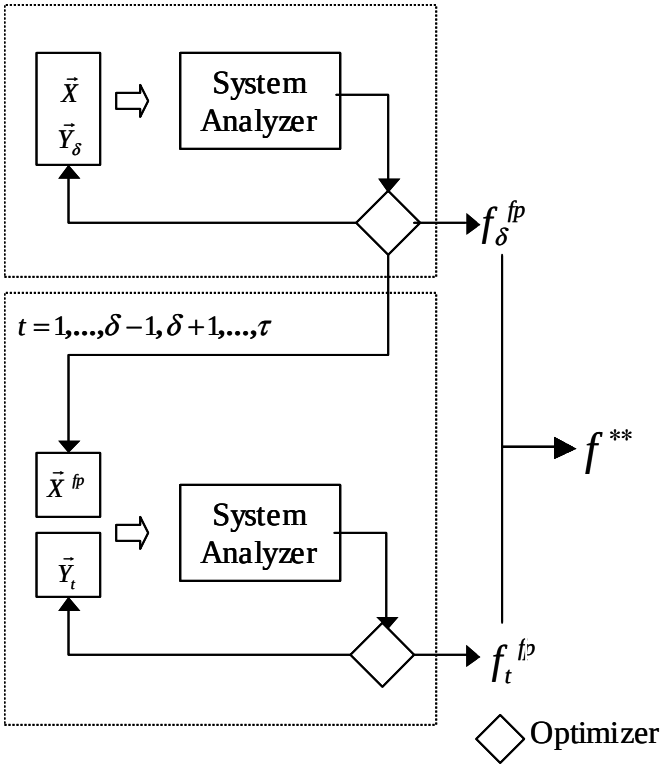

Figure 5.3. Design/Off-design time decomposition scheme.

The type of time decomposition proposed effectively transforms a problem with $d+o\tau$ variables into two problems (one of synthesis / design and the other of operation), the latter of which can be divided further into τ-1 problems since one can define (τ-1) off-design optimization problems (implemented in parallel) with respect to the

instantaneous operational decision variables ($\vec{Y}_t$). The synthesis / design problem will, thus, have *d+o* decision variables while each of the operational or off-design problems will have *o* decision variables. The reduced number of variables for the decomposed problem, however, comes at the expense of possibly having to carry out the optimization problem given by problem (5.9) for several possible feasible (but promising) solutions found by solving the reduced problem given by problem (5.8). An obvious advantage over the nested time decomposition schemes described earlier (Figure 5.2) is that no time is spent on solutions that i) are infeasible or ii) do not meet the most stringent demand and operating conditions.

The solution of the synthesis / design problem (5.8) may be problematic, however, if the number of variables (*d+o)* is still very large. In this case, time decomposition reduces the number of variables for each decomposed operational problem but does not completely facilitate the solution of the overall problem. Thus, an additional decomposition is necessary.

5.2 Physical (Unit) Decomposition

Physical decomposition relies on the premise that energy systems can be divided into components or sub-systems with clearly defined coupling functions which in energy systems can be considered as products, resources, or feedback functions. Under certain conditions, the resulting units could then be optimized independently while maintaining the energy and cost flow connections between them. The resulting set of decomposed problems would, as with time decomposition, have a much smaller size than the overall problem making it possible to take into account a large number of variables. Depending on the size of the problem (number of units, number of inputs/outputs of each unit, number and nature of the independent variables), two of the approaches presented in the previous chapter can be considered for solving the overall problem using physical decomposition. The first is the Local-Global Optimization (LGO) and the second the Iterative Local-Global Optimization (ILGO) applied to

energy systems. Both approaches use certain desirable properties of the marginal costs associated with the energy and cost flow couplings between units to facilitate the optimization and the convergence of the process. In order to apply any of these methods, let us consider the three-unit energy system of Figure 5.4. Three is considered a small enough number to understand the features of the methods yet large enough to reveal patterns and facilitate the use of compact mathematics.

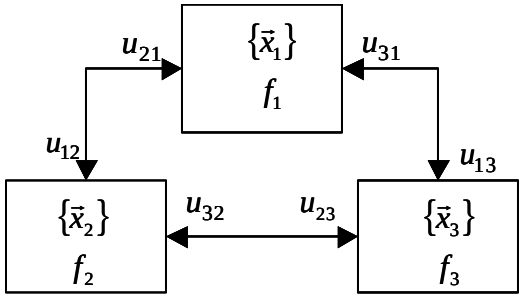

Figure 5.4. A highly coupled three-unit energy system.

The synthesis / design problem for this system is to

$$\text{Minimize } f = \sum_{t=1}^{\tau} \left[\begin{array}{c} \dot{f}_1\left(\vec{x}_1, \vec{y}_{1t}, \left(u_{21,}u_{31}, u_{12,}u_{13}\right)_t\right)\Delta t_t + \dot{f}_2\left(\vec{x}_2, \vec{y}_{3t}, \left(u_{12,}u_{32}, u_{21,}u_{23}\right)_t\right)\Delta t_t \\ + \dot{f}_3\left(\vec{x}_3, \vec{y}_{3t}, \left(u_{13,}u_{23}, u_{31,}u_{32}\right)_t\right)\Delta t_t \end{array} \right] \quad (5.10)$$

$$\text{w.r.t. } \vec{X}^T = \{\vec{x}_1, \vec{x}_2, \vec{x}_3\} \quad \vec{\mathrm{Y}}^T = \left\{\vec{Y}_t\right\}^T = \{\vec{y}_{1t}, \vec{y}_{2t}, \vec{y}_{3t}\} \qquad t = 1,..., \delta,..., \tau$$

subject to the primary constraints

$$\vec{\mathrm{H}} = \left\{\vec{H}_t\right\} = \begin{Bmatrix} \vec{h}_{1t} \\ \vec{h}_{2t} \\ \vec{h}_{3t} \end{Bmatrix} = \vec{0} \qquad t = 1,..., \delta,..., \tau$$

$$\vec{\Gamma} = \left\{\vec{G}_t\right\} = \begin{Bmatrix} \vec{g}_{1t} \\ \vec{g}_{2t} \\ \vec{g}_{3t} \end{Bmatrix} \le \vec{0} \qquad t = 1,..., \delta,..., \tau \quad (5.10.1)$$

5.3 Local-Global Optimization (LGO) for Energy Systems

In order to apply the LGO approach presented in the previous chapter to the synthesis / design optimization of the energy system of Figure 5.4, it is assumed that the coupling functions $u_{ij,}$ i.e. the intermediate feedbacks, are kept at a constant value ξ_{ij} at each instant of time, i.e.

$$\left\{u_{ij}\right\}_t = \left\{\xi_{ij}\right\}_t \qquad t = 1,...,\delta,...,\tau \tag{5.11}$$

Given the functional relationships for the coupling functions given by equations (5.5), it is clear that decision variable vectors $\vec{x}_i$ and $\vec{y}_i$ are strictly local and that the u_{ij} are the only link between unit *i* and the rest of the system. The fact that u_{ij} are kept fixed allows one to define a local optimization problem for unit 1 and a different one for units 2 and 3 combined or two different ones for units 2 and 3 as separate entities[21]. For example, as mentioned above, the following local (unit) synthesis / design problem for unit 1 could be defined:

$$\text{Minimize } f_1 = \sum_{t=1}^{\tau} \dot{f}_1\left(\vec{x}_1, \vec{y}_{1t}, \left(\xi_{21,}\xi_{31}, \xi_{12,}\xi_{13}\right)_t\right)\Delta t_t \tag{5.12}$$

w.r.t. $\vec{x}_1,\ \vec{y}_{1t} \qquad t = 1,...,\delta,...,\tau$

subject to

$$\vec{h}_{1t} = \vec{0} \qquad t = 1,...,\delta,...,\tau \tag{5.12.1}$$

$$\vec{g}_{1t} \le \vec{0} \qquad t = 1,...,\delta,...,\tau \tag{5.12.2}$$

[21] Further decompositions are, of course, also possible of each of the units.

The requirement imposed by equation (5.11) on the values for the coupling functions may be overly restrictive, particularly if the values of the coupling functions at different instants are dependent on each other. In such cases, it is advisable to use the time decomposition scheme proposed above and solve the problem in two sequential steps. In the first step, problem (5.12) and the corresponding ones for units 2 and 3 are solved at one load/environmental condition, δ, judged to be the most critical so that it becomes the synthesis / design condition. The most promising solutions from these problems are then used to minimize the sum of the local (unit) rate forms of the objective functions at all the other (off-design) conditions.

The solutions obtained from solving problem (5.12) and similar problems defined for units 2 and 3 are the restricted local (unit-based) optimum cost rates at different times $\left\{\dot{f}_{i\ t}^{\ *}\right\}$ and their corresponding restricted total values f_i^* as well as the optimum operational decision variables at all instants of time $\left\{\vec{y}_{i\ t}^{\ *}\right\}$ and the optimum synthesis / design variables $\vec{x}_i^*$. The restricted optimum values for the objective function and their corresponding coupling function values constitute a point on the Optimum Response Surface (ORS) for the problem. The entire ORS can then be created by varying the values of ξ_{ij} within specified ranges and solving the local (unit) problems for those values.

In addition to the unit-based sub-problems, the system-level problem is to

$$\text{Minimize } f = \sum_{t=1}^{\tau} \left(\dot{f}_1^* + \dot{f}_2^* + \dot{f}_3^*\right)\Delta t_t \tag{5.13}$$

w.r.t. $\xi_{ij_t} \qquad t = 1,...,\delta,...,\tau$

subject to

$$\vec{H}_t = \begin{bmatrix} \xi_{ij} - \xi_{ij\ \max} \\ -\xi_{ij} + \xi_{ij\ \min} \end{bmatrix}_t \leq \vec{0} \qquad t = 1,...,\delta,...,\tau \tag{5.13.1}$$

The local (unit) optimizations (e.g., problem (5.12)) can be performed at the same time the system-level problem is being solved (RT-LGO approach). A second alternative is to store the results from the sub-problems and use them later in the global system-level optimizer (OL-LGO approach). In both cases, the optimum results for the unit syntheses / designs form the ORS of the system.

It should be pointed out that the coupling function u_{ij} going from unit i to unit j may in fact be a vector of multiple products (e.g., electricity, steam, compressed air). It is clear then that a multi-unit, multi-product system may require a very large number of optimization runs (i.e. problems such as problem (5.12) would need to be solved innumerable times for many different combinations of the elements of the vectors u_{ij}). The potential problem caused by the large amount of computational and analysis time, which would be involved, is exacerbated by two facts:

- Each unit may need to be optimized using time decomposition (as described above).
- The synthesis / design problem in its entirety requires the use of binary, discrete, and continuous variables. The optimization algorithms needed to deal with the resulting mixed-integer non-linear programming problems (MINLPs) are usually of the artificial intelligence type (e.g., Genetic Algorithm and Simulated Annealing). Although these algorithms are effective when properly developed and conditioned, they impose a serious computational burden on finding the solution.

Thus, the application of the LGO approach for complex highly integrated, highly dynamic energy system synthesis / design can require a large number of optimizations to create the optimum response surface. The amount of computational time required to do this may simply be impractical. A possible solution to these difficulties is the use of the ILGO approach presented in the previous chapter.

5.4 Iterative Local-Global Optimization (ILGO) Applied to Energy Systems

As shown in the previous chapter, the ILGO method uses the linear term of a Taylor series expansion to guide the selection of values for the coupling functions that makes the system-level cost lower than that of some reference solution. Versions A and B of ILGO start with finding an arbitrary initial point on the optimum response surface. This initial or reference solution is obtained by setting $u_{ij_t} = \xi^o_{ij_t}$ and solving a set of unit-level problems, which for unit 1 take the form

$$\text{Minimize } f_1 = \sum_{t=1}^{\tau} \dot{f}_1\left(\vec{x}_1, \vec{y}_{1t}, \left(\xi^o_{21,}\xi^o_{31}, \xi^o_{12}, \xi^o_{13}\right)_t\right) \cdot \Delta t_t \tag{5.14}$$

$$\text{w.r.t. } \vec{x}_1,\ \vec{y}_{1t} \qquad t = 1,...,\delta,...,\tau$$

subject to

$$\vec{h}_{1_t} = \vec{0} \qquad t = 1,...,\delta,...,\tau \tag{5.14.1}$$

$$\vec{g}_{1_t} \le \vec{0} \qquad t = 1,...,\delta,...,\tau \tag{5.14.2}$$

As before, time decomposition may be needed to solve the above problem. The solutions to the unit-level sub-problems are the restricted local (unit-based) optimum cost rates at different times $\left(\dot{f}_i^*\right)_t^o$ and their corresponding restricted total values $\left(f_i^*\right)^o$ as well as the optimum operational decision variables at various instants in time $\left(\vec{y}^*_{i\,t}\right)^o$ and the optimum synthesis / design variables $\left(\vec{x}_i^*\right)^o$ at the initial or reference point.

The initial value selection for the coupling functions can be made by different means. For example a largely simplified model of the system can be used to find a near optimum solution, which could then be used as the ORS reference point. Another possibility is to use any of the analysis techniques described in previous chapters to find

the coupling functions that cause the system to have a high Second Law efficiency, for example.

One of the most appealing features of ILGO is its ability to provide the information necessary to improve an existing synthesis / design. In fact, in engineering practice, the word optimization is often used not to indicate the search for an absolute global optimum but rather to find a solution which is *better* than some existing system. Any of the versions of ILGO excels at this task since one could use the existing synthesis / design (which is assumed to be "optimized") as the reference condition and start the iterative process from there.

Once a suitable initial or reference point in the ORS is found, a Taylor series expansion is performed about that point. After taking the linear terms, the local (unit-based) cost rate at an instant t can then be written for unit 1 as

$$\dot{f}_{1t} = (\dot{f}_1^*)_t^o + \left(\frac{\partial \dot{f}_1^*}{\partial u_{12}}\right)_t^o \Delta u_{12_t} + \left(\frac{\partial \dot{f}_1^*}{\partial u_{13}}\right)_t^o \Delta u_{13_t} + \left(\frac{\partial \dot{f}_1^*}{\partial u_{21}}\right)_t^o \Delta u_{21_t} + \left(\frac{\partial \dot{f}_1^*}{\partial u_{31}}\right)_t^o \Delta u_{31_t} \qquad (5.15)$$

The partial derivatives above are by definition the shadow prices or marginal costs of the coupling functions. Similar quantities, which have been defined in the past (von Spakovsky and Evans, 1993) form the basis of the calculus methods of thermoeconomics such as Thermoeconomic Functional Analysis (Frangopoulos, 1984, 1994), Engineering Functional Analysis (von Spakovsky and Evans, 1993; Evans and von Spakovsky, 1993; von Spakovsky, 1994) and the approach of El-Sayed (1989, 1996). The marginal costs used here are more general in that they are defined for arbitrary coupling functions, whether energy- or exergy-based or not. Furthermore the marginal costs in equation (5.15) are instantaneous and, thus, are allowed to take substantially different values at different instants in time.

Using the notation commonly found in the thermoeconomics literature, equation (5.15) is rewritten for units 1, 2, and 3 as

$$\dot{f}_{1t} = (\dot{f}_1^*)_t^o + \lambda_{12_t}^1 \Delta u_{12_t} + \lambda_{13_t}^1 \Delta u_{13_t} + \lambda_{21_t}^1 \Delta u_{21_t} + \lambda_{31_t}^1 \Delta u_{31_t} \qquad (5.16)$$

$$\dot{f}_{2t} = (\dot{f}_2^*)_t^o + \lambda_{21t}^2 \Delta u_{21t} + \lambda_{23t}^2 \Delta u_{23t} + \lambda_{12t}^2 \Delta u_{12t} + \lambda_{32t}^2 \Delta u_{32t} \tag{5.17}$$

$$\dot{f}_{3t} = (\dot{f}_3^*)_t^o + \lambda_{31t}^3 \Delta u_{31t} + \lambda_{32t}^3 \Delta u_{32t} + \lambda_{13t}^3 \Delta u_{13t} + \lambda_{23t}^3 \Delta u_{23t} \tag{5.18}$$

where the marginal costs based on the restricted local (unit-based) optimum cost rate at an instant of time *t* are defined as

$$\lambda_{ij}^i = \left(\frac{\partial \dot{f}_i^*}{\partial u_{ij}} \right)_t^o \tag{5.19}$$

Naturally "design" and "off-design" marginal costs are defined. The former are those with $t = \delta$ and the latter those with $t \neq \delta$.

The equations presented above contain a wealth of information that can be exploited with the purpose of improving the initial or reference synthesis / design. They provide a means of moving in the optimum system cost vs. coupling functions (intermediate products/feedback) space, i.e. the optimum response surface. The first feature of these equations is that they show the trade-off between the costs that are purely local and those, which are affected by synthesis / design and operational considerations in the rest of the system. The comparative magnitude of the λ's will indicate whether a decrease in intermediate coupling functions coming from unit *i* and the (likely) resulting increase in local cost of unit *j* will reduce the system-level cost. These marginal costs will, provided that they are not identically equal to zero[22], suggest synthesis / design changes that will make the system as a whole better from the standpoint of the cost objective. Thus, for example, negative marginal costs will point towards the need for higher values for the coupling functions (e.g., more intermediate products/feedbacks) and vice versa. Therefore, the optimizer would tend to favor

[22] This would indicate that the reference point is in fact already the optimum for the objective consistent with the optimum for the system as a whole.

syntheses / designs with greater values of the coupling functions with associated lower marginal costs.

In addition, the off-design marginal costs become a measure of how important the entire load/environmental profile is when compared to the most critical point in the load/environmental profile, i.e. the synthesis / design point. The marginal costs will help pinpoint syntheses / designs that may have a relatively poor performance at the design point but may perform better than the best solution at the design point when combined with all of the off-design conditions.

The step that follows the calculation of the marginal costs is problem dependent. In both versions of ILGO (A and B), the marginal costs indicate the changes in the coupling functions that need to be made in order to improve the reference solution. In ILGO-A, a new set of values for the coupling functions is chosen according to the descent algorithm

$$\left(\xi^{o}_{ij\,t}\right)_{new} = \left(\xi^{o}_{ij\,t}\right)_{old} - \alpha_o \left(\frac{\partial \dot{f}^{*}_{m\,t}}{\partial u_{ij}}\right)^{o} = \left(\xi^{o}_{ij\,t}\right)_{old} - \alpha_o \lambda^{m}_{ij\,t} \tag{5.21}$$

where the marginal cost used in the above equation is such that the greatest improvement in the objective function is achieved as shown in the previous chapter. The step size is chosen to ensure the descent properties of the algorithm.

The importance of equation (5.21) is that it shows the required changes in the coupling functions at all time steps so that both synthesis / design and operational variables can be adjusted accordingly. It may be necessary, particularly for large problems, to perform the changes sequentially by using time decomposition. Using ILGO-A, for example, a new set of values for the coupling functions at the synthesis / design point, i.e. $\left(\xi^{o}_{ij\,\delta}\right)_{new}$, can be chosen according to (5.21). An improved solution at the synthesis / design point can be found by solving the decomposed local (or unit-based) optimization problems. The resulting set of most feasible solutions are then fed into the off-design problems to find the optimum operational variables. It is apparent

that an implicit assumption in the use of ILGO-A is that there is enough confidence that an optimum solution can be obtained for the new values of the coupling functions $\left(\xi^{o}_{ij\ t}\right)_{new}$, which may require some prior knowledge about the system's behavior. If this assumption does not hold, ILGO-B instead of ILGO-A must be applied.

In the second version of the ILGO method, i.e. ILGO-B, the coupling functions are allowed to fluctuate within limits to preserve the validity of the Taylor series expansion (as opposed to forcing them to take fixed values $\left(\xi^{o}_{ij\ t}\right)_{new}$). ILGO-B improves upon the initial solution by solving a set of unit-based system-level sub-problems, which for unit 1 takes the form

Minimize

$$f^{(1)} = \sum_{t=1}^{\tau} \begin{pmatrix} \dot{f}_1^{\,*} + \lambda^1_{12_t}\Delta u^{(1)}_{12\ t} + \lambda^1_{13_t}\Delta u^{(1)}_{12\ t} + \lambda^1_{21_t}\Delta u^{(1)}_{21\ t} + \lambda^1_{31_t}\Delta u^{(1)}_{31\ t} \\ \dot{f}_2^{\,*} + \dot{f}_3^{\,*} + \lambda^2_{12_t}\Delta u^{(1)}_{12\ t} + \lambda^3_{13_t}\Delta u^{(1)}_{12\ t} + \lambda^2_{21_t}\Delta u^{(1)}_{21\ t} + \lambda^3_{31_t}\Delta u^{(1)}_{31\ t} \end{pmatrix} \Delta t_t \tag{5.22}$$

or

Minimize

$$f^{(1)} = \sum_{t=1}^{\tau} \left(\dot{f}_1 + \dot{f}_2^{\,*} + \dot{f}_3^{\,*} + \lambda^2_{12_t}\Delta u^{(1)}_{12\ t} + \lambda^3_{13_t}\Delta u^{(1)}_{12\ t} + \lambda^2_{21_t}\Delta u^{(1)}_{21\ t} + \lambda^3_{31_t}\Delta u^{(1)}_{31\ t} \right) \Delta t_t \tag{5.22.1}$$

w.r.t. $\vec{x}_1, \vec{y}_{1_t} \qquad t = 1,...,\delta,...,\tau$

subject to

$$\vec{h}_{1_t} = \vec{0} \qquad t = 1,...,\delta,...,\tau \tag{5.22.2}$$

$$\vec{g}_{1_t} \le \vec{0} \qquad t = 1,...,\delta,...,\tau \tag{5.22.3}$$

where for example

$$\Delta u^{(1)}_{12\ t} = \nabla_{x_1}\left(u_{12_t}\right)^T \Delta\vec{x}_1 + \nabla_{y_1}\left(u_{12_t}\right)^T \Delta\vec{y}_{1t} \tag{5.23}$$

In general the effect of the decision variables on the coupling functions is given by

$$\Delta u_{ij\ t}^{(i)} = \nabla_{x_i}\left(u_{ij\,t}\right)^T \Delta\vec{x}_i + \nabla_{y_i}\left(u_{ij\,t}\right)^T \Delta\vec{y}_{i\,t} \tag{5.24}$$

In addition to the above constraints, the additional constraints

$$\Delta u_{ij_t} - \varepsilon\ \Delta u_{ij_{t\max}} \le 0 \tag{5.25}$$

are imposed upon the problem. In expression (5.25), the $\Delta u_{ij_{t\,\mathbf{max}}}$ are the maximum allowable values for the coupling functions and the factor ε is added to ensure that the linear Taylor series expansions are a good local representation of the optimum response surface. It is readily seen that one of the advantages of ILGO-B over ILGO-A is that $\vec{x}_1$ *and* $\vec{y}_{1t}$ may be chosen so that the internal constraints (both the analysis system of equations and the desired unit's products or tasks) are met.

Problem (5.22) represents the minimization of the system-level objective function by varying the local (unit 1) decision variables only. The function to be minimized is composed of the local contribution (in this case f_1) to the overall objective *plus* the impact that the local decision variables ($\vec{x}_1, \vec{y}_{1t}$) have on the local objectives of the other units (2 and 3). This impact is made via the coupling functions.

5.5 Discussion / Comments

As discussed above, in energy systems, the coupling functions can be regarded as intermediate products/resources and/or feedbacks going to or coming from the units. Typically these functions can be expressed in terms of a thermodynamic or flow variables. In this work, however, non-energy functions are permitted.

As to the purely thermodynamic and flow connections between units, the previous discussion allows one to tackle in an informed way the question of what thermodynamic property should be used as the linking or coupling variable between sub-problems (i.e.

sub-systems or components) when physical decomposition is used for optimization purposes. Thus, the optimization methods presented above are shed some light on the on-going debate (Newberry, 2000; Paulus and Gaggioli, 2000; Bejan, 2000; Muñoz and von Spakovsky, 2000a,b,c) as to the property of choice for representing energy-based coupling functions. The answer depends on how the total objective behaves with respect to the system's coupling functions (i.e. the optimum response surface) when represented in terms of any of the candidate quantities (e.g., energy, exergy, thrust, negentropy, etc)[23]. In fact, Gaggioli and El-Sayed, two of the biggest proponents of exergy and Second Law analysis, state in their landmark article of 1989 (Gaggioli and El-Sayed, 1989) that, for optimization, which quantity (ies) is (are) best is an open question and will more than likely depend on the case at hand. Of course, in the past, a number of authors have observed advantages to using exergy as opposed to energy, advantages, which they believed, simplified decomposition and speeded up and possibly even ensured convergence (Frangoupolos and Evans, 1984; Frangopoulos, 1984; Gaggioli and El-Sayed, 1989; von Spakovsky and Evans, 1993; Evans and von Spakovsky, 1993; El-Sayed, 1989, 1996). These results cannot be directly compared to those for the ILGO approach presented here since they were obtained with the Evans and El-Sayed formalism or one of its derivatives. However, with respect to ILGO, exergy as the basis for the coupling functions between unit sub-problems is only justified[24] on the basis of how, as stated above, the total cost function behaves with respect to the system's coupling functions and, thus, aids decomposition and, in turn, optimization of the whole. In certain cases, it will be the quantity of choice. In others, as has been shown (Muñoz and von Spakovsky, 1999, 2000a; Frangopoulos, 1994; von Spakovsky, 1994), energy or some other quantity (e.g., thrust, negentropy, etc.) may work very well and be a better choice for any number of practical reasons.

---

[23] This has direct bearing on the associated marginal costs and their behavior.

[24] Of course, using exergy may add information which otherwise would not be there and could eventually aid in an interpretation of the optimization results. The argument made here, however, is that exergy is simply not necessarily required in order to obtain these results using decomposition.

Based on recent and past work by Muñoz and von Spakovsky (1999; 2000a,b,c) and by others, the determinant total cost function (overall system-level objective function) behavior with respect to intermediate products and feedbacks (the ORS) is summarized as follows:

- that this surface be smoothly convex (or concave) with respect to the coupling functions; this will ensure that the ILGO approach leads to the global optimum;
- that ideally this cost function be linear with respect to these coupling functions; this will increase the convergence speed of the algorithm; obviously since the cost function is the sum of resources (usually fuel) and capital, there is always the alternative of manipulating the latter to make the cost function linear or piecewise linear, a technique which has been used by a number of researchers (e.g., Frangopoulos, 1984, von Spakovsky, 1986). A linear cost function with respect to the coupling functions would produce a hyper-plane and the optimum solution would be expected to be at or close to one of the corners of that plane.

Finally, some additional observations as to the best choice of thermodynamic quantities for describing the coupling functions of a system can be made:

- Consider a single unit that uses a single resource R_1 to produce a single product P_1. The synthesis / design optimization will find the optimum vector of decision variables $\vec{x}_1^*$ and $\vec{y}_1^*$ that minimize the sum $k_1 R_1 + Z_1$ for a given value of P_1. Typically, if the quantity or quality of product P_1 increases, the best design will tend to have a higher value for the total cost function than that of a synthesis / design with a lower required P_1. This is valid regardless of the choice of thermodynamic property used to describe the product. The implication is that overall (total) cost functions have the tendency to be *monotonic* with respect to their products. This type of behavior will favor the convexity of the cost function. Problems arise, however, when the need to have a larger product forces changes in the technology being

employed. In this case the tendency may be inverted and even make the total cost function discontinuous. This obviously can occur when the overall optimization problem uses a discrete variable that represents various possible types of units (a vapor compression cycle vs. an absorption cycle, for example). Note, however, that discrete variables present in the local (unit) optimization problem (e.g., representing different types of material for a given component) do not pose this problem.

- Exergy has the important mathematical characteristic of combining temperature, pressure, chemical composition, velocity, mass flow rate, etc. in a single function. This conceptually poses an advantage for the calculation of the marginal costs. A fair amount of work has been devoted to the study of exergy-based marginal costs in stationary applications (Serra, 1994; Frangopoulos, 1994; von Spakovsky, 1994; Lazzaretto and Andreatto, 1995; etc.). However, there are practical difficulties for their calculation when models of real systems are used. For example, take the case of the design of a gas turbine, which in addition to shaft work produces compressed air for a process. The air is to be taken, say, from the last compressor stage. It is much easier to design the system for a given value of the air mass flow rate to be taken from the compressor than for a given exergy value. This is because the pressure and temperature of the air depend on a number of factors that are not easily controllable, including, among others, the position of the design point on the gas turbine maps, the maximum allowable temperature in the combustor, the technology used and some stability considerations.

- There is a need to remain open-minded to the possibility of using marginal costs based on commodities other than exergy or energy[26]. In some applications, the use of non-energy values may be necessary. For example, size (volume and mass) and thrust (force) are critical factors in aircraft design. Although some authors

[26] Other functions have been proposed and used in the past. For example, Valero et al. (1993) proposed the use of the relative free energy.

(Frangopoulos and von Spakovsky, 1993; von Spakovsky and Frangopoulos, 1994; Sciubba, 1999) may argue that one could relate exergy to a unit's mass via the manufacturing process, that option is replete with difficulties and pitfalls (Curti et al., 2000a,b) and will simply not be considered here.

Chapter 6

Application of the Local Global Optimization Approach (LGO)

The potential benefits of Second Law Analysis and decomposed optimization for large-scale optimization have recently attracted the attention of the aerospace/aircraft community. Aircraft, of course, are very complex systems that contain a myriad of sub-systems and components with different levels of interdependence and feedback. The requirements in terms of performance are very stringent and are usually in conflict with the physical characteristics (volume and weight) of its components and sub-systems. These characteristics added to the highly dynamic loads and a wide variety of environmental conditions to which an aircraft is subjected call for the use of systematic, rigorous, and practical approaches for their synthesis and design. The aerospace community has in the past used decomposition for the optimal design of aircraft systems typically applied to the problem of minimizing the total take-off weight of a system composed of two units[27]: structures and aerodynamics. However, the complete integrated synthesis and design optimization of these sub-systems and an aircraft's energy-based sub-systems (propulsion, air conditioning, thermal management, hydraulics, etc.) is still a wide-open field of research. Variations on existing methods for

[27] Units in this context refer to either sub-systems or components.

stationary applications may be ideal candidates for interfacing the various aircraft sub-system optimizations in order to arrive at an overall optimum synthesis and design for the aircraft system as a whole.

The Local-Global Decomposed Optimization Algorithm (LGO) was applied by Muñoz and von Spakovsky (1999, 2000a) to the design of an Environmental Control System (ECS) for an advanced military aircraft. In their application, it was assumed that the engine and airframe were given. In this chapter, a brief summary of their analysis and results is presented. In Chapter 7, an example application of the iterative version of the approach (ILGO) is presented.

6.1 Environmental Control System Description

There are a number of heat sources in aircraft including kinetic sources, solar radiation, avionics, hydraulics, generators, fuel pumps, people, engines and gearbox oil. The most commonly used cooling methods are environmental control sub-system (ECS) air bled from the main engine, ram air, fuel, oil, and refrigerants in a cooling cycle (Letton, 1976). The major air conditioning task for aircraft is the solution of the various cooling problems arising from high-speed flight, i.e. the dissipation of heat that is generated both external and internal to the aircraft. Heat is transferred from heat sources to a heat sink outside or within the aircraft. External heat sources result mainly from aerodynamic heating plus heat received through solar radiation. A major portion of this heat is prevented from transferring into the aircraft by use of thermal insulation. Internal heat sources include people and electronic, electrical, and mechanical equipment. Available heat sinks are the outside (ambient air) and the fuel. Ambient air may be in the form of either ram air or bleed air from the main engines.

There are two principal types of cooling systems: the air cycle based on a reverse Brayton cycle and the vapor compression cycle based on a reverse Rankine cycle. These systems operate independently or in combination as, for example, when a vapor-compression system is used to supplement an air cycle.

Two types of air cycles are possible:

- Open Cycles: Those in which the air is taken from the outside and rejected after being used in the cycle components.
- Closed Cycles: Those in which air is re-circulated continuously through the cycle components.

A survey of the many possible different configurations is given in the SAE Aerospace Applied Thermodynamics Manual (1969). The bootstrap system, however, is by far the most widely used, due to higher efficiency when compared to a simple air cycle. In the bootstrap system, performance is improved by using the turbine work output for increased compression of the air upstream of the turbine. Thus, a higher compression ratio is achieved with a correspondingly higher temperature drop across the turbine.

The conventional bootstrap system shown in Figure 6.1 is similar to the one used by the F-16 fighter. It provides conditioned air to the cockpit and avionics. Airflow to the ECS is from the pre-conditioning bleed-air subsystem. Flow into the ECS is varied by a pressure-modulating valve at the ECS inlet. This valve also limits maximum inlet pressure to the ECS's primary heat exchanger and bootstrap compressor.

Air is compressed and cooled in the bootstrap ECS. After compression, the air is cooled in a counter-flow, secondary heat exchanger using ram air from scoop inlets. Air from the secondary heat exchanger is then cooled in the regenerative heat exchanger, before it is cooled further by expansion in the bootstrap turbine. Most of the water condensed during cooling of air in the turbine is removed in a low-pressure water separator. For the application presented here, the combination of the two sub-systems constitutes the overall system being analyzed.

The ECS is closely coupled with the engine and aircraft flight conditions. Changes in engine power settings cause changes in bleed air pressures and temperatures, which in turn affect the performance of the ECS.

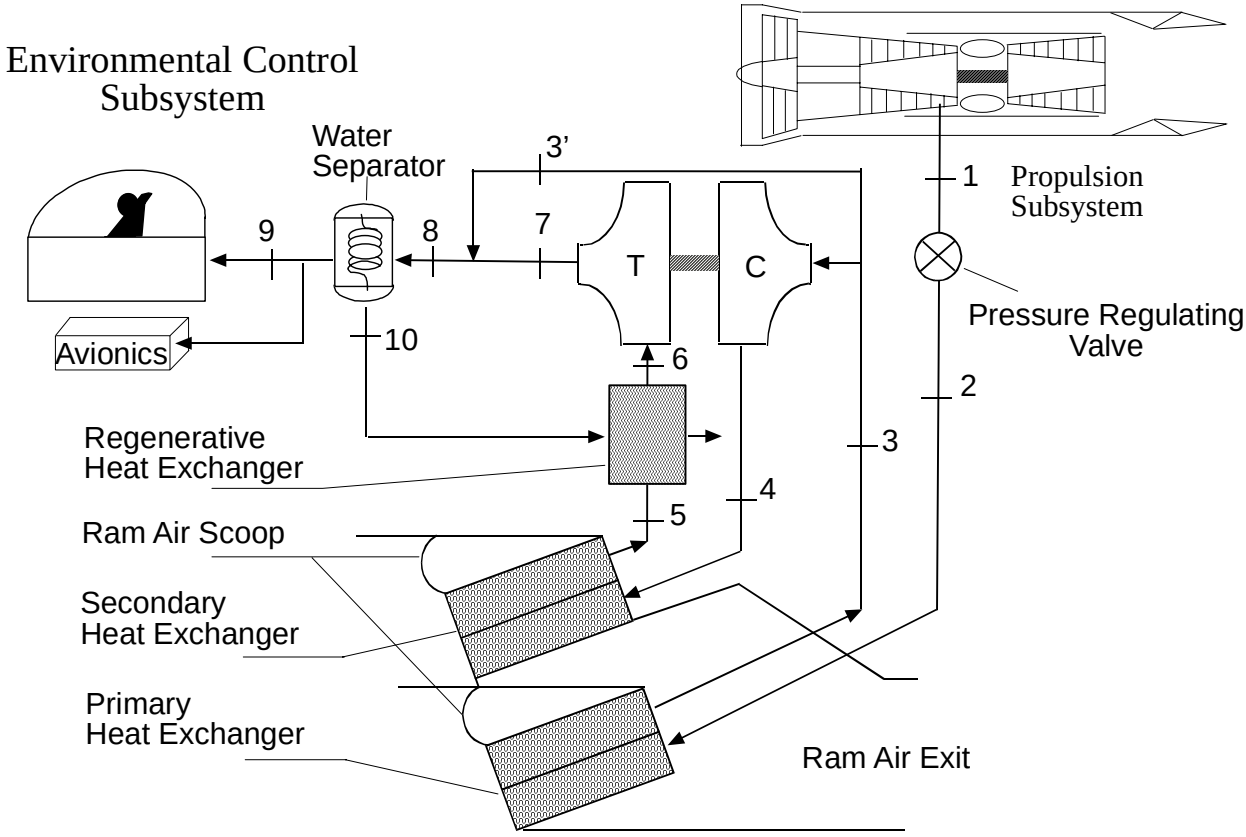

Figure 6.1. Schematic diagram of an ECS.

The mass flow rate and pressure of the bleed air will in general depend on the pressure and temperature at which the cold air must be delivered to the cockpit and avionics and the design of the ECS. Quite obviously, the energy or exergy of the air that can be had from the main engine compressor is not a continuous function but rather is limited by the fact that it can only be extracted from the discrete stages of the compressor. Typically, modern ECSs have a bleed port at a low and one at a high-pressure stage. Once the amount of bleed air needed (usually a unique value calculated

from the allowed inlet and outlet temperatures of the load (cabin and avionics) and the cooling load itself) and the stage at which air is bled are fixed, the energy of the bleed air can be calculated. It is then possible to estimate the amount of fuel required to produce the compressed air by means of, for example, an engine simulator.

As to the ram air inlet, it will create a penalty in the system, which is proportional to the drag force created by it. The basic principle is to decelerate the cooling airflow, pass it through the heat exchanger at low speed, and then accelerate it back to ambient pressure. Quantitatively, the drag force created by the inlet-heat exchanger-exit assembly is defined as the cooling airflow's rate of momentum change. In addition to this will be the profile drag of the inlet and exit and perhaps some 'interference' drag due to unfavorable interactions. The greater the pressure drop in the heat exchanger and ducts, the higher the momentum drag will be. Increasing the heat transfer rate in the heat exchanger has the opposite effect.

Turning now to the mass of the ECS and additional fuel, the amount of fuel necessary to carry the mass of the ECS or the fuel itself is a function of a number of factors including the flight conditions (altitude, Mach number, angle of attack, etc.) and the relative location of the ECS with respect to the center of gravity of the aircraft. Therefore, the fuel penalty due to weight is highly dependent on the aircraft being analyzed. This weight is part of the independent variable set which minimizes the objective and includes among others the pressure setting in the regulating valve, the mass flow rate of cooling air in the regenerative heat exchanger and the mass flow rate of bypass warm air necessary to obtain the pressure, temperature and mass flow rate schedules in the cabin and avionics. The available pressure of the bleed air is dependent on the altitude and Mach number of the aircraft. In this chapter, it is assumed that the bleed air is extracted from a fixed, high-pressure compressor stage with constant temperature and pressure characteristics.

Completing the definition of the problem are a set of physical constraints. With these, the energy (or exergy) of bleed air is calculated along with the drag created by the ram air. The weight of each component is also calculated according to physical models

created for that purpose. A simplified way of calculating the associated mass drag is used. A complete description of all of the models used, both thermodynamic and physical, is given in Muñoz and von Spakovsky (1999).

6.2 Objective Function Definition

When an ECS (and for that matter any other sub-system) is installed in an aircraft, additional fuel is required to:

- Overcome the additional drag associated with carrying the sub-system mass
- Supply power to the sub-system. This can be expressed as the amount of fuel required to meet the energy requirements of the ECS while maintaining constant net thrust. The energy extracted can be in the form of compressed (bleed) air or shaft power.
- Overcome any additional drag, which may result from installing a sub-system in the aircraft (e.g., the increase in profile drag and momentum drag caused by ram air induction for cooling purposes).
- Carry the quantity of fuel required for the previous items.

Additional fuel consumption in the main engine due to the ECS will now be chosen as the objective function[28]. If the amount of fuel needed to produce a differential increase in the intermediate product/feedback (bleed air) and thrust (to overcome drag due to ram and weight) are known, the total fuel consumed due to the ECS can be written as

$$d\dot{m}_f = \frac{\partial \dot{m}_f}{\partial E_b} dE_b + \frac{\partial \dot{m}_f}{\partial T_r} dT_r + \frac{\partial \dot{m}_f}{\partial T_w} dT_w \tag{6.1}$$

[28] Other objective functions will be considered in the next chapter.

where dE_b is the amount of exergy extracted from the compressor for use in the ECS and dT is the additional thrust T_r and T_w due to the drag caused by the ram air and the mass of the components in the ECS, respectively (see Figure 6.2). The fuel consumption due to the volume is assumed to be constant and is, therefore, not considered.

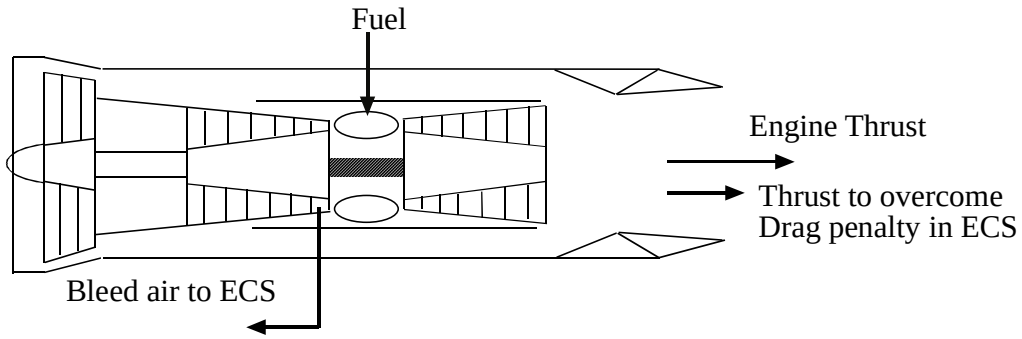

Figure 6.2 Propulsion sub-system and a depiction of the bleed air extraction as well as the additional thrust due to drag required.

Multiplying this differential increase in fuel consumption in the main engine by the unit cost of fuel c_f results in a differential increase in total cost (provided the capital costs are negligible), i.e.

$$d\dot{C}_T = \frac{\partial(c_f \dot{m}_f)}{\partial \dot{E}_b} d\dot{E}_b + \frac{\partial(c_f \dot{m}_f)}{\partial T_r} dT_r + \frac{\partial(c_f \dot{m}_f)}{\partial T_w} dT_w \tag{6.2}$$

Recalling the definition of marginal costs and integrating over time t as well as with respect to $\dot{E}_b$, T_r and T_w, the following alternative version of equation (6.2) is obtained:

$$\text{Minimize } C_T = \int_{time} \left(\lambda_{E_b} \dot{E}_b + \lambda_{T_r} T_r + \lambda_{T_w} T_w \right) dt \tag{6.3}$$

w.r.t. $\vec{x}$

subject to a set of constraints.

The marginal costs of bleed exergy and thrust[29] are given by:

$$\lambda_{E_b} = \frac{\partial \dot{C}_T}{\partial \dot{E}_b} \tag{6.4}$$

$$\lambda_{T_r} = \frac{\partial \dot{C}_T}{\partial T_r} \tag{6.5}$$

$$\lambda_{T_w} = \frac{\partial \dot{C}_T}{\partial T_w} \tag{6.6}$$

It was assumed that the marginal costs in equation (6.3) are approximately constant. The functions that describe the marginal costs of bleed air and thrust are dependent on flight conditions and on the aerodynamic and thermodynamic behavior of the main engine of the particular aircraft. When the marginal costs are calculated on a unit cost basis, i.e. in terms of mass flow rates of fuel, they can be seen as the penalties that the sub-system imposes on the overall aircraft system. Penalties are a common way of calculating the impact of fitting a sub-system into an aircraft. Although the methods for calculating them are proprietary to each manufacturer, some general methods are available in the open literature (see, for example, SAE AIR 1168/8 and Le Claire, 1976). These methods use values from average engines and employ overly simplified assumptions, and, therefore, fail to capture all the important factors involved.

As indicated in previous chapters, to fully achieve the benefits of decomposition, the marginal costs must have certain desirable properties. The assumption that the marginal costs are constant, facilitated writing the optimization problem in the form of equation (6.3). This assumption, however, had to be verified. To this end, the effect of bleed extraction and additional thrust required from a turbofan engine were studied. A computer simulation that accurately simulates engine performance was used. The model of a medium bypass turbofan engine was used to perform the calculations.

---

[29] Thrust is not a Second Law quantity. Thrust is used here, however, because, as opposed to kinetic energy, it is commonly used to specify the performance of aircraft. The units of the marginal cost for thrust is $/N-sec

Figure 6.3a shows the change in the non-dimensional total cost (in this case fuel) as a function of the additional drag crated by the ECS for two different flight conditions while keeping the exergy of the bleed air constant. Figure 6.3b shows the change in non-dimensional total cost (fuel in this case) as a function of the exergy of bleed air while keeping the thrust penalty constant. The exergy was calculated using the local[30] temperature and pressure as the reference thermodynamic state. The non-dimensional cost is defined as

$$C_f{}^* = \frac{C_f - C_{f_o}}{C_{f_o}} \tag{6.7}$$

where C_{f_o} is the cost of the fuel without bleed or extra thrust requirements and C_f is the fuel cost after including these penalties. The amount of bleed air and thrust were varied so that the maximum net thrust and bleed exergies in Figure 6.3 correspond to the maximum allowable values at the specified altitude and Mach number for a medium bypass ratio turbofan engine in the 1000-1500 lb thrust class.

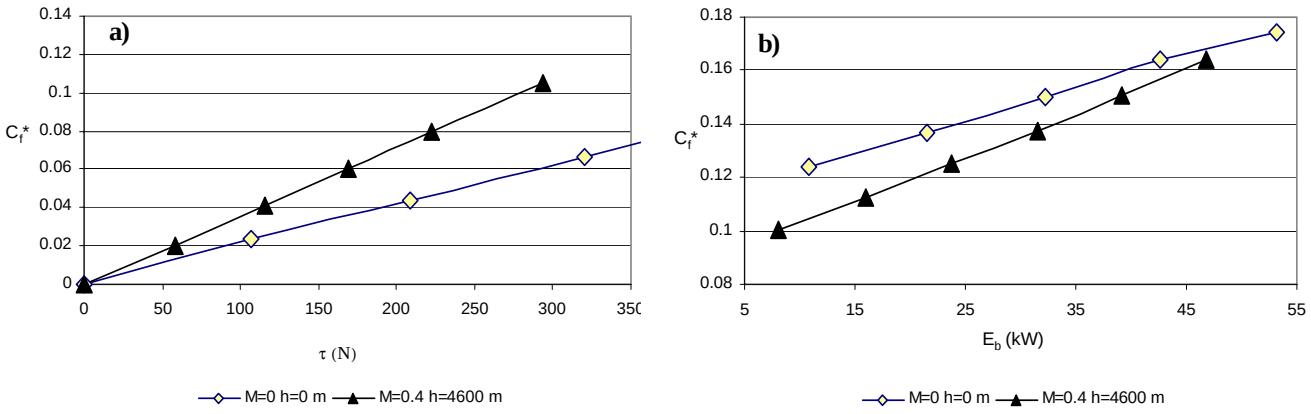

Figure 6.3. Non-dimensional cost versus a) drag penalty and b) bleed exergy extracted.

[30] Local refers to temperature and pressure at a given altitude

The slopes of the curves in Figure 6.3 correspond to the non-dimensional marginal costs of thrust and bleed air, respectively. Clearly the linearity assumption is fully justified in this case. Although this result is unique to a particular engine, results available in the literature seem to suggest that this is a general result (see, for example, Lykins et al, 1998). Prior knowledge of the functions describing the marginal costs as a function of altitude and Mach number allows one to effectively decompose the system and optimize the ECS without simultaneously simulating, during the optimization process, the propulsion sub-system.

6.3 LGO Implementation – Unit Based Sub-problems

To illustrate the use of the Local Global decomposed optimization technique (LGO) developed in previous chapters, two different sub-systems within the ECS are defined as indicated in Figure 6.4 below. The first sub-system is called the pre-conditioning sub-system and the second the bootstrap sub-system as indicated in that figure. Stream (3), connecting the sub-systems, provides the necessary thermodynamic and cost links between the two sub-systems. We choose the temperature of stream 3 as the function that describes the coupling stream. The main reason for this choice is twofold. Firstly, temperature is a convenient parameter for heat exchanger calculations; and secondly, the pressure drop in the heat exchangers has a minimal effect on the design. A more complete discussion is given in Muñoz and von Spakovsky (1999).

The design of the ECS heat exchangers, the air cycle machine (compressor and turbine assembly), and the ram air inlet, exit and ducts is carried out for a reference case, which has a Mach number and altitude of 2.0 and 18,000 m, respectively[31]. The valve is assumed to be fully open with negligible pressure drop. The water separator has a typical performance, which is reported by Muñoz and von Spakovsky (1999).

[31] A dynamic version of this problem for a multiple-segment mission has been solved by Muñoz and von Spakovsky (1999, 2000a).

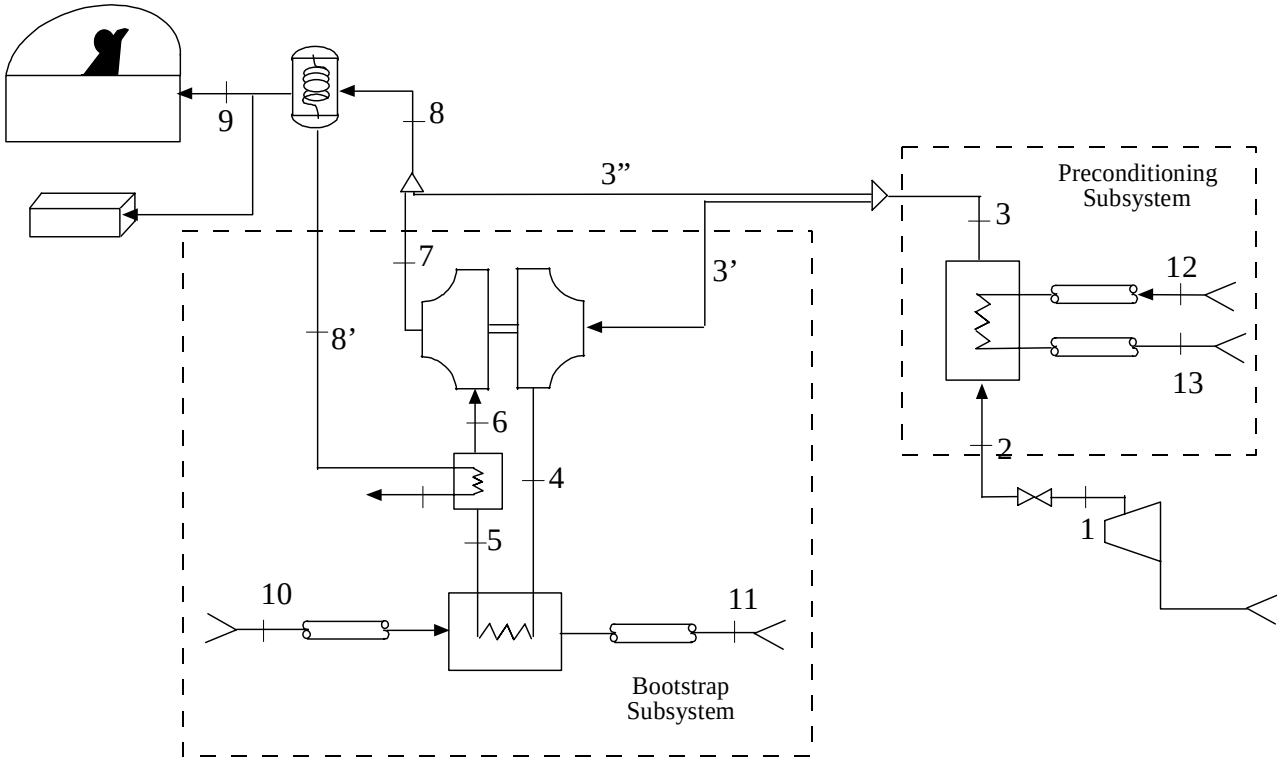

Figure 6.4. Sub-system definitions for the ECS of Figure 6.1.

6.3.1 Pre-conditioning Sub-system

The air pre-conditioning sub-system includes the primary heat exchanger, a ram inlet and exit, and the ducts that connect them. The optimization problem for this sub-system is defined as

$$\text{Minimize } \dot{C}_A = \lambda_{E_b} E_b + \lambda_{T_r} T_r + \lambda_{T_W} T_w \tag{6.8}$$

w.r.t. $\vec{x}_A$

subject to a set of primary and secondary constraints.

Since the bleed air is taken from a single high-pressure compressor stage, the exergy of bleed air and its cost are, for this case, fixed. With the additional equation (a reasonable approximation) that

$$\lambda_{T_r} = \lambda_{T_w} \tag{6.9}$$

and the assumption of constant marginal costs (justified given the results shown in Figure 6.3), the minimization problem for this case reduces to minimizing the mass and momentum drags for the subsystem, i.e.

Minimize $$\frac{\dot{C}_A}{\lambda_{T_r}} = T_r + T_w \tag{6.10}$$

w.r.t. $\vec{x}_A$

subject to:

$$\vec{h}(\vec{x}_A) = \vec{0} \tag{6.10.1}$$

$$\vec{g}(\vec{x}_A) \leq \vec{0} \tag{6.10.2}$$

The types of heat exchangers considered for the pre-conditioning sub-system (and later for the bootstrap sub-system) are compact heat exchangers. Due to their low weight to capacity ratio, these exchangers are commonly used in aircraft energy sub-systems. There is a wide range of available geometries and types of fins that can be used (see for example the classic book on compact heat exchangers by Kays and London, 1998). Here we arbitrarily select offset-strip fins for the design of the heat exchangers in the ECS since this is one of the most commonly used plate-fin geometries.

In general, once the particular type and geometry of the fin are selected, the only remaining degrees of freedom are the height, width and length of the heat exchanger core. It is assumed here that the design of the manifolds and other accessories has no effect on heat transfer performance. The model for estimating heat exchanger core mass developed by Muñoz and von Spakovsky (1999) was used. This model also uses a

linear least squares equation that relates core mass to total mass (i.e. core plus manifolds and insulation) to estimate the total heat exchanger weight. In all cases, the calculated weight correlates extremely well with observed values. The heat transfer and pressure drop models used are based on the work of Shah (1981), Shah and Webb (1982), and Kays and London (1998). Both sides of the heat exchangers have one pass unless stated otherwise.

To illustrate the benefits of decomposition, two design optimization cases (cases a and b) with different but overlapping sets of independent variables as given in Tables 6.1 and 6.2 were used. For case a, offset strip fins designated 1/9-25.01 were used for the bleed-air side of the heat exchanger and 1/8-19.86 for the ram-air side. The vector of decision (independent) variables $\vec{x}$ and the corresponding constraints, for case a, are summarized in Table 6.1. The vector of equality constraints, $\vec{h}$, is determined by the thermodynamic and heat transfer models. For case b, some of the geometric fin parameters on both sides of the heat exchanger are considered variable as shown in Table 6.2. Since the friction and Colburn factors are not known for case b, the predictive formulas developed by Manglik and Bergles (1990) are used. These authors report that the formulas have a minimum multivariate correlation coefficient of 0.923 in the laminar and turbulent flow regimes at a 99% confidence level. For consistency, the formulas of Manglik and Bergles were also used for case a.

As can be seen from Table 6.1, decision variables and constraints other than those for the heat exchanger are also considered in the design optimization, i.e. those for the ram air intake. For this component, it was assumed that the ECS uses scoop-type of ram air inlets.

Table 6.1. Decision variables and associated inequality constraints for the optimization of the pre-conditioning sub-system (case a). The ram-air side uses plate-fin strip fins designated 1/8-19.86. The bleed-air fin used is 1/9-25.01[32]

Component	Decision variable case a		Constraints
Primary Heat Exchanger	L_r	Length ram side (m)	$0.1<L_r<0.9$
	L_b	Length bleed side (m)	$0.05<L_b<0.9$
	L_n	Non flow length (m)	$0.1<L_n<0.9$
Ram Air Inlet	A_i	Area of inlet, outlet (cm^2)	$95<A_i<290$
	Derived variables		
Heat Exchangers	R_{er}	Reynolds number, ram air side	$R_{er}<5000$
	R_{eb}	Reynolds number, bleed air side	$R_{eb}<5000$

Table 6.2. Additional decision variables and associated inequality constraints to those given in Table 6.1 for the optimization of the pre-conditioning sub-system (case b).

Component	Additional decision variables for case b		Constraints[33]
Primary Heat Exchanger	s_r	Lateral fin spacing, ram side (mm)	$0.83<s_r<2.08$
	h_r	Height of the offset-strip-channel, ram side (mm)	$1.29<h_r<10.6$
	l_r	Length of fin, ram side (mm)	$2.40<l_r<6.35$
	s_b	Lateral fin spacing, ram side (mm)	$0.83<s_b<2.08$
	h_b	Height of the offset-strip-channel, ram side (mm)	$1.29<h_b<10.6$
	l_b	Length of fin, ram side (mm)	$2.40<l_b<6.35$

[32] From geometry data given in Kays and London (1998). performance data were calculated using the formulas given by Manglik and Bergles (1990).

[33] Offset-strip-fins with double sandwich construction were excluded.

As indicated in Tables 6.1 and 6.2 above, the number of independent variables for case a is 4. With a variable fin geometry, this number increases to 10 (case b). The temperature difference between the bleed air leaving and the ram air entering the heat exchanger's ΔT is also taken as a variable but outside the optimization for different values of the mass flow rate ratios of air. It was assumed that the flow rate of cooling air in the regenerative heat exchanger is fixed at 5% of the total bleed-air flow. Since the required mass flow rate to the cabin and avionics is known, this fixes the amount of bleed air in the pre-conditioning sub-system. Different ram-to-bleed mass flow rate ratios were investigated (ranging from 1 to 2.5) by varying the ram air inlet cross-sectional area. Note that a given mass flow rate ratio and a fixed desired outlet bleed-air temperature is equivalent to selecting a desired heat transfer effectiveness.

For each desired value of the coupling function, i.e. exit bleed temperature and mass flow rate ratio (which effectively fixes the heat transfer effectiveness), the pre-conditioning subsystem was optimized (Eq. (6.10)) using a commercial optimization program based on a Sequential Quadratic Programming algorithm. Results for cases a and b are shown in Figure 6.5 The curves represent the loci of optima for the desired difference between the exit bleed and inlet ram air temperature for a given mass flow rate ratio. In order to verify the quality of the results, an optimization with mass flow rate ratio as an independent variable was also performed and the results are shown in the same figure represented by the curve, which has no markers.

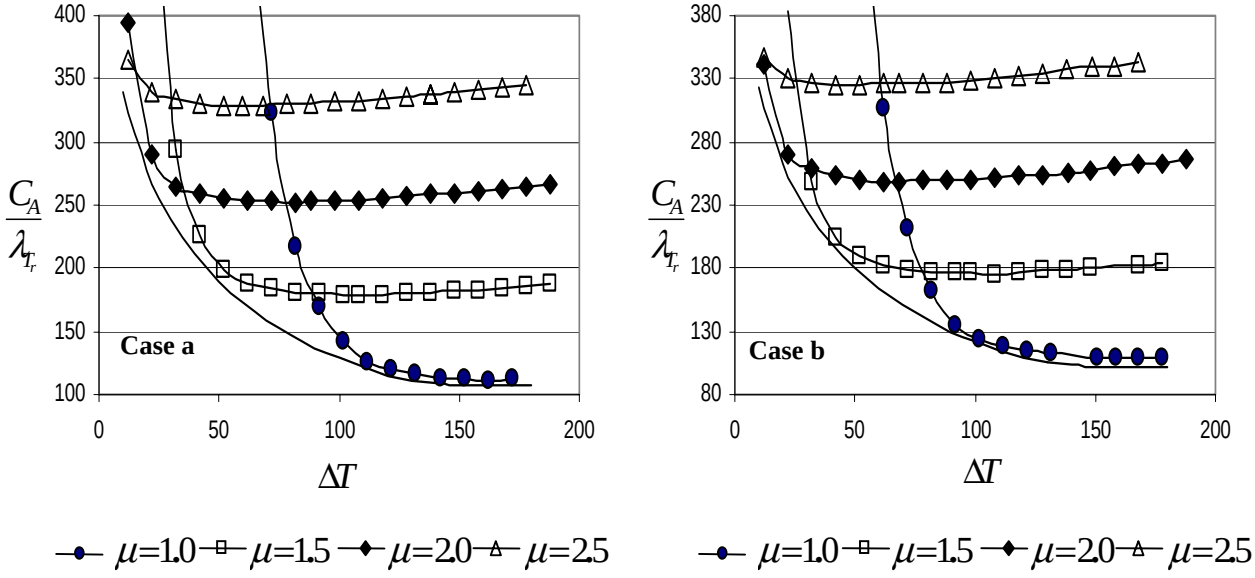

Figure 6.5 Local pre-conditioning sub-system cost as a function of the coupling function, i.e. the ram to bleed air temperature difference ($\Delta T \equiv T_{e_{bleed}} - T_{i_{ram}}$), and mass flow rate ratio ($\mu = \dot{m}_{ram} / \dot{m}_{bleed}$).

6.3.2 Bootstrap Sub-system

The bootstrap sub-system is composed of the air cycle machine (compressor and turbine assembly), the regenerative heat exchanger, the secondary heat exchanger, and its supersonic inlet, exit and ducts. The heat exchangers were designed for fixed fin geometries identical to those used in case a for the optimization of the primary heat exchanger (pre-conditioning sub-system). The decision variables, constraints and specifications for the bootstrap sub-system are given in Table 6.3. As indicated, the ram-to-bleed mass flow rate ratio is considered a variable.

A suitable objective function for this sub-system is

$$\text{Minimize} \quad \frac{\dot{C}_B}{\lambda_{T_r}} = T_r + T_w \tag{6.11}$$

w.r.t. $\vec{x}_B$

subject to:

$$\vec{h}(\vec{x}_B) = \vec{0} \tag{6.11.1}$$

$$\vec{g}(\vec{x}_B) \leq \vec{0} \tag{6.11.3}$$

The cost of the bleed air for the bootstrap sub-system is the cost of the product of the pre-conditioning sub-system and depends on the exergy of this connecting stream (stream (3) in Figure 6.4 above) between sub-systems. The product of the bootstrap sub-system is the required cold air (overall ECS product). The mechanical exergy (i.e. pressure component) of the connecting stream is a required value in the optimization of the bootstrap sub-system. This obviously implies that the pressure drop on the bleed-air side of the primary heat exchanger (pre-conditioning sub-system) is known or a reasonable value can be assumed. For this application, it is assumed that the pressure drop on the bleed-air side remains constant at about 5% of the inlet pressure. In addition, the effects of small variations in the pressure of the connecting stream on the design of the bootstrap sub-system were observed to be negligible; and, thus, this pressure was held constant at some appropriate value.

Table 6.3. The decision variables and associated inequality constraints used in the optimization of the bootstrap sub-system.

Component	Decision variable		Constraints
Air Cycle Machine	PR_{cp}	Design Pressure Ratio ACM Compressor	$PR_{cp}<3.0$
	PR_{tb}	Design Pressure Ratio ACM Turbine	$PR_{tb}<8$
Secondary Heat Exchanger	L_r	Length ram side (m)	$0.1<L_r<0.9$
	L_b	Length bleed side (m)	$0.05<L_b<0.9$
	L_n	Non flow length (m)	$0.1<L_n<0.9$
	μ	Ram to bleed mass flow rate ratio	$1<\mu<2.5$
Regenerative Heat Exchanger[34]	L_r	Length ram side (m)	$0.05<L_r<0.5$
	L_b	Length bleed side (m)	$0.05<L_b<0.5$
	L_n	Non flow length (m)	$0.05<L_n<0.5$
	Derived variables		
Heat Exchangers	R_{er}	Reynolds number, ram air side	$R_{er}<5000$
	R_{eb}	Reynolds number, bleed air side	$R_{eb}<5000$

The total number of independent (decision) variables for the optimization of the bootstrap sub-system is 9. The results of the optimization of the bootstrap sub-system are shown in Figure 6.6 as a function of the temperature difference between the bleed-air exit and ram-air inlet. Each point, as before, represents the optimum cost for each value of the air temperature difference in the primary heat exchanger (pre-conditioning sub-system).

[34] The cooling air side of the heat exchanger has 4 passes.

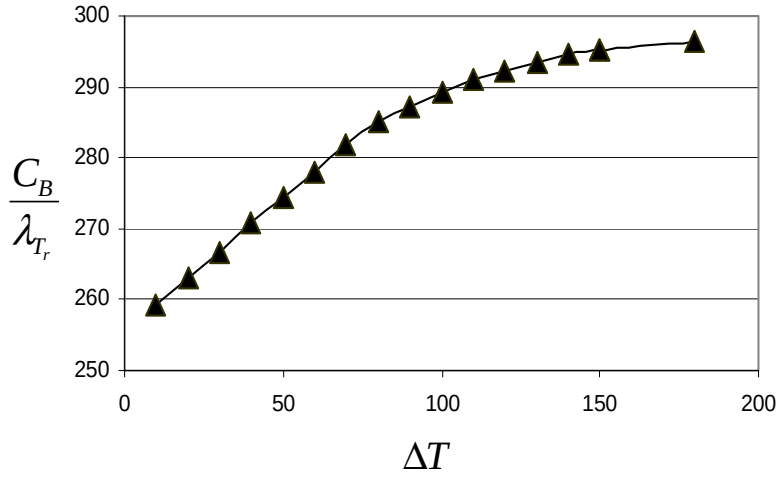

Figure 6.6. Local bootstrap sub-system cost as a function of the coupling function, i.e. the ram-to-bleed air temperature difference ($\Delta T \equiv T_{e_{bleed}} - T_{i_{ram}}$).

6.4 System-Level Problem

The optimum design for the ECS as a whole is the one that minimizes in an integrated fashion the total cost of both the pre-conditioning and bootstrap sub-systems. Since the level of feedback between these two sub-systems for the illustration as presented is fixed, the optimum design for the ECS is the sum of the optima for the objective functions given by equations (6.10) and (6.11). In other words, the total cost is the minimum cost of producing the connecting stream in the pre-conditioning sub-system plus the minimum cost of cooling the air coming out of the pre-conditioning sub-system to the desired temperature and pressure needed to meet the cooling load requirements for the aircraft. This sum when plotted against the coupling function (in this case the temperature of the bleed air leaving the pre-conditioning sub-system) as in Figure 6.7 constitutes the optimum response (ORS) of the problem. The system-level problem is then to find the value of the coupling function that minimizes the overall cost. This can be done by inspection of Figure 6.7. Thus, the optimum design is the one with the temperature difference that minimizes the total cost (≈ 150 K)

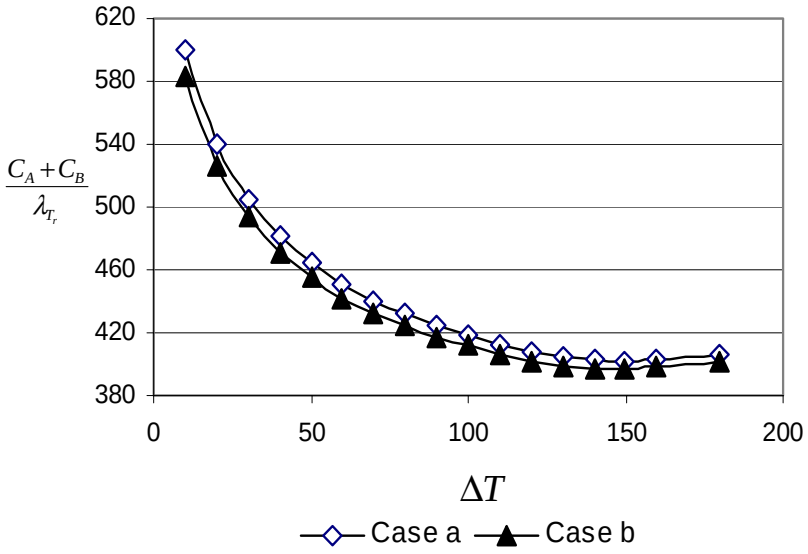

Figure 6.7. Optimum Response Surface for the ECS as a function of the ram-to-bleed air temperature difference (case a has 13 degrees of freedom, case b has 19 degrees of freedom, and in each case ΔT is varied parametrically).

The optimal solution, thus, is found by observing the behavior of the optimum total cost as a function of the temperature difference in the pre-conditioning sub-system. Quite clearly, some savings are achieved by increasing the number of independent variables in the primary heat exchanger (pre-conditioning sub-system). With reference to Figure 6.7, the fact that the mass flow rate of the cooling air (stream (8) in Figure 6.4 above) is assumed fixed and the bypass air is zero (stream (3") in Figure 6.4 above) effectively fixes the only possible feedback signal from the bootstrap sub-system to the pre-conditioning sub-system. This conveniently voids the necessity for iterating and dealing with convergence problems, i.e. a one-pass optimization was sufficient which, of course, generally will not be the case. The choice of temperature difference as an independent variable outside the optimization proved to be convenient as well since the total cost was fairly well behaved when plotted versus this difference. Note that one could have easily defined an additional system-level optimization problem for the entire

ECS in which the only independent variable at the system level would have been the temperature difference in the pre-conditioning sub-system. For this system-level problem, the decomposed local- or unit-level design optimizations of the pre-conditioning and bootstrap sub-systems would have taken place within that occurring at the system-level, i.e. a LGO approach. The total number of degrees of freedom involved would in this case have then been 14 for case a and 20 for case b.

Chapter 7

Applications of the Iterative Local Global Optimization Approach (ILGO)

Before attempting to apply the ILGO approach to a more complex system, the ECS design problem solved in the previous chapter is again considered. The most relevant results were *normalized* and are reproduced in Figure 7.1. The only coupling function present, u_{12}, is the temperature of the cool air leaving unit 1 (preconditioning sub-system) and entering unit 2 (bootstrap sub-system). It can be assumed that unit 1 acts as a provider of intermediate product p_1 (u_{12}) for unit 2. Unit 2 takes the intermediate product p_1 as intermediate resource r_1 and the external resource R_2 (fuel) to produce the system-level product P^o (i.e. the cool air for cabin and avionics). The overall system-level problem is to

Minimize $\quad C_T = k_1 R_1 + k_2 R_2 + Z_1 + Z_2$ (7.1)

w.r.t. $\quad \vec{X} = \{\vec{x}_1, \vec{x}_2\}, \quad \vec{Y} = \{\vec{y}_1, \vec{y}_2\}$

subject to

$$\vec{H} = \vec{0} \qquad (7.1.1)$$
$$\vec{G} \le \vec{0}$$

and $\quad k_1 = k_2 = 1$ (7.1.2)

The problem solved in the previous chapter was the minimization of the sum of external resources (fuel) used to operate the ECS as well as those used to fly (carry) the ECS. The latter is conceptually a cost associated with the capital function. However, for reasons of simplicity, Z will for this illustration be included within the resource term R.

The first step of the ILGO is the design of the units for a given value of the coupling function (intermediate product p_1). Therefore, the unit-level optimization problem for unit 1 is to

Minimize $C_1 = R_1$ (7.2)

w.r.t. $\vec{x}_1, \vec{y}_1$

subject to

$\vec{h}_1 = \vec{0}$ (7.2.1)

$\vec{g}_1 \leq \vec{0}$

and $p_1 - p_1^0 = 0$ (7.2.2)

For unit 2, the unit-level optimization problem is

Minimize $C_2 = R_2$ (7.3)

w.r.t. $\vec{x}_2, \vec{y}_2$

subject to

$\vec{h}_2 = \vec{0}$ (7.3.1)

$\vec{g}_2 \leq \vec{0}$

and $r_1 - p_1^0 = 0$ (7.3.2)

In the above equations, p_1^o is an arbitrary starting value for the intermediate product p_1 or intermediate resource r_1 (coupling function u_{12}). A value of $p_1^o = 0.5$ is chosen to

begin with. The marginal costs associated with this intermediate product (resource) are the slopes of the lines tangent to the curves at $p_1^o = 0.5$ as indicated in Figure 7.1b and Figure 7.1c. The solutions of the two local- or unit-level problems are, as indicated in Figure 7.1, C_1=0.70 and C_2=0.48 for unit 1 and unit 2, respectively. The marginal costs of the intermediate product are then calculated as

$$\lambda_{12}^1 = \frac{\partial R_1}{\partial p_1} \tag{7.4.1}$$

$$\lambda_{12}^2 = \frac{\partial R_2}{\partial p_1} \tag{7.4}$$

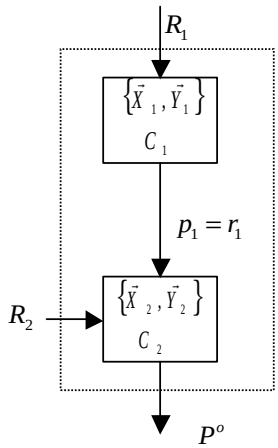

Fig. 7.1.a

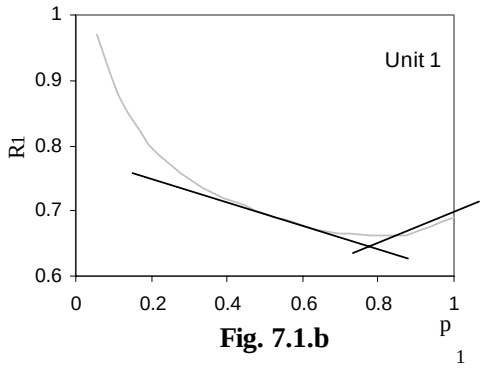

Fig. 7.1.b

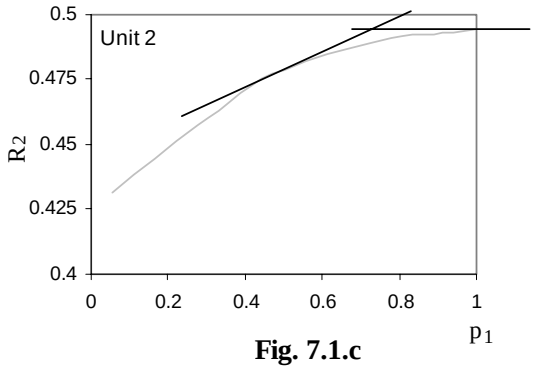

Fig. 7.1.c

Figure 7.1. Application of ILGO to the design optimization of an ECS (the curve in gray represents the 2-D projection of the problem's optimum response surface).

The numerical values of the marginal costs can also be estimated directly from Figure 7.1 as $\lambda_{12}^{1} = -0.20$ and $\lambda_{12}^{2} = +0.08$. With these marginal costs, a new value for the coupling function is chosen using the algorithm update expression

$$\left(p_1^o\right)_{new} = \left(p_1^o\right)_{old} - \varepsilon(-0.20) = 0.5 + 0.2\varepsilon \tag{7.5}$$

where ε is some small positive number and the marginal cost of the external resource of unit 1 was chosen because its absolute value is greater than that for unit 2.

Assuming complete ignorance of the optimum response surface for the problem, one supposes constant marginal costs over the entire range of the coupling function, so that the new value for p_1^o is the maximum possible according to equation (7.5). This new value is $p_1^o = 1.0$. In the second iteration, the marginal cost associated with C_2 is equal to zero and the sign of that for C_1 is positive. As a consequence, the second iteration will point towards a value of p_1 lower than 1.0. An intermediate point between the initial point (i.e. p_1=0.5) and the one obtained in the previous iteration is p_1=0.75. This last value is used in the next iteration. The correct solution ($p_1 \approx 0.85$) is obtained in three or four iterations. It is important to note that had the marginal costs been constant (i.e. $C_T = R_1 + R_2$ versus p_1 linear), a single iteration would have been required.

7.1 Synthesis / Design Optimization Problem Definition

ILGO will now be applied to a much more complex problem. The synthesis / design task at hand is to perform the integrated optimization of two sub-systems, which are part of an advanced military aircraft. The problem is to carry out the conceptual design of a low-bypass turbofan engine with afterburning (Propulsion Sub-system - PS) and the full synthesis / design optimization of an air-cycle Environmental Control Sub-system (ECS).

The PS provides the necessary thrust for the vehicle to carry out the desired mission. The mission[35] is the set of conditions under which the aircraft must be synthesized / designed. Here, the mission defined by the Request for Proposal for an Air-to-Air Fighter (AAF) given by Mattingly et al. (1987) is used. The mission has 14 different phases or legs. A general description of the mission is given in Figure 7.2 and Tables 7.1 & 7.2. In addition to providing the required rates of climb and acceleration and overcoming the aircraft's drag, the PS must provide the power required to operate all the remaining sub-systems.

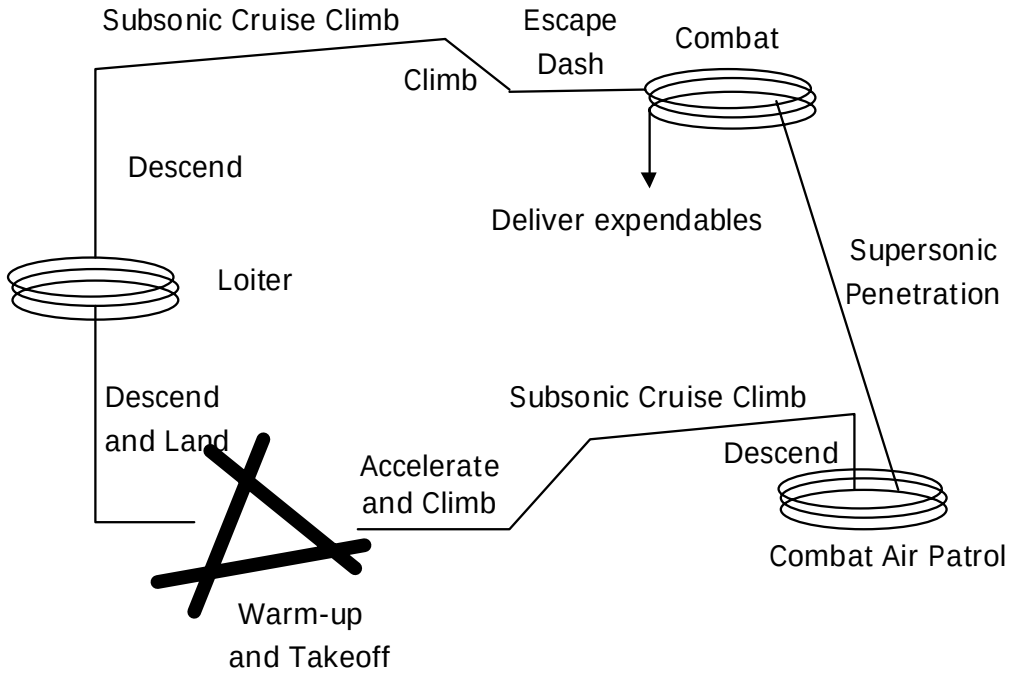

Figure 7.2. Mission profile by phase or leg (Mattingly et. al., 1987).

[35] The mission is equivalent to the load profile and set of environmental conditions in a stationary application.

Table 7.1. Mission Specifications.

Phase	Description
1	Warm-up and take-off, field is at 600 m pressure altitude with T=310 K. Fuel allowance is 5 min at idle power for taxi and 1 min at military power for warm-up. Take-off roll plus rotation must be $\leq$ 450 m on surface with friction coefficient = 0.05. $V_{TO} = 1.2V_{STALL}$
2	Accelerate to climb speed and perform a minimum time climb in military power to best cruise mach number and best cruise altitude conditions (BCM/BCA)
3	Subsonic Cruise Climb at BCM/BCA until total range for climb and cruise climb is 280 km
4	Descend to 9150 m
5	Perform combat air patrol loiter for 20 min at 9150 m and Mach number for best endurance.
6	Supersonic penetration at 9150 m and M=1.5. Range=185 km
7	Combat is modeled by the following: • Fire 2 AMRAAM missiles • Perform one 360 deg., 5g sustained turn at 9150 m, M=0.9 • Accelerate from M=0.8 to M=1.6 at 9150 m at max. power • Fire 2 AIM-9Ls and ½ ammo. Conditions at end of combat are M=1.5 at 9150 m
8	Escape dash, at M=1.5 and 9150 m for 46 km.
9	Using military power, do a minimum time climb to BCM/BCA
10	Subsonic cruise climb to BCM/BCA
11	Subsonic cruise climb at BCA/BCM until total range from the end of combat equals 278 km
12	Descend to 3000 m
13	Loiter 20 min. at 3000 m and Mach number for best endurance
14	Descend and land, field is at 600 m pressure altitude with T=310 K. A 2 s free roll plus breaking distance must be $\leq$ 450 m. Runway has a friction coefficient = 0.18. $V_{TD} = 1.15V_{STALL}$

The ECS provides the cooling necessary to dissipate the heat generated in the aircraft. A set of cooling requirements has been added to the mission according to design specifications given by Muñoz and von Spakovsky (1999). These requirements are shown in Table 7.2. The relationship between the different sub-systems that make up an aircraft is very complex. Before attempting to understand all of the factors involved in the problem, consider an aircraft system such as the one shown in Figure 7.3. An energy balance on the aircraft leads to the following expression:

$$\{T-(D+R)\}V = W\frac{dh}{dt}+W\frac{d}{dt}\left\{\frac{V^2}{2g}\right\} \tag{7.6}$$

Table 7.2. Performance Requirements / Constraints.

Item	Requirement
Payload	• 2 AMRAAM missiles (148 kg each) • 2 AIM-9L missiles (87 kg each) • 500 rounds of 25 mm ammo (522 fixed weight (cannon, ammo casings, etc), 125 kg spent ammunition)
Max Mach Number	2.0 @ 12200 m
Acceleration	$0.8 \rightarrow 1.6$ M/9150 m $t \leq 5$ s
Sustained g level	$n \geq 5$ at 0.9 M/9150 m, $n \geq 5$ at 1.6 M/9150 m
Crew	One (90 kg pilot plus equipment)
Fuel	JP-4
Cooling	Requirements as per cooling, temperature and pressure schedules given by Muñoz and von Spakovsky (1999)
Jet Engines	One or two engines. Bleed air flow rate and bleed port depend on ECS design.

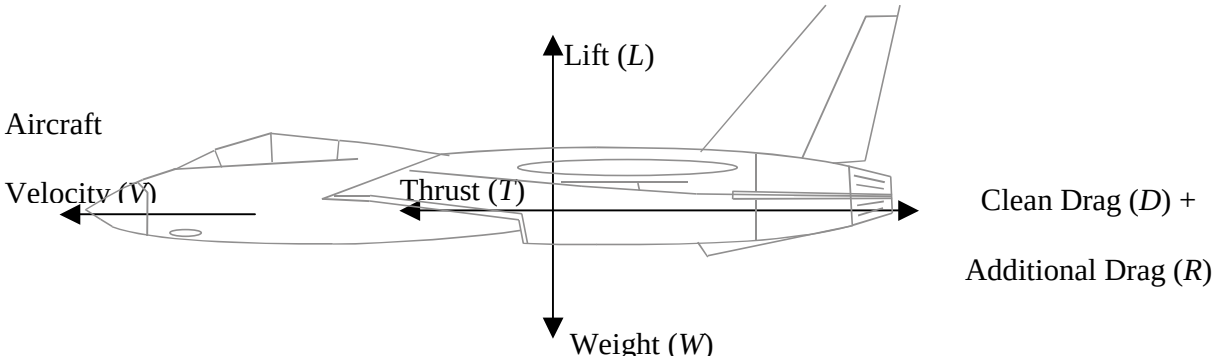

Figure 7.3. Force balance on an aircraft.

The term on the left-hand-side of equation (7.6) is the rate of mechanical energy input. The first and second terms on the right-hand-side represent the storage of potential and kinetic energy, respectively. Here the traditional aircraft lift and drag relationships

$$L = nW = qC_L S \tag{7.7}$$

and $D = qC_D S$ (7.8)

are used where n is the load factor, which is equal to the number of g's perpendicular to the direction of the velocity. A lift-drag polar relationship of the form (Mattingly et al., 1987)

$$C_D = K_1 C_L{}^2 + K_2 C_L + C_{D_0} \tag{7.9}$$

is assumed.

Equations (7.6) through (7.9) can be manipulated to produce the thrust equation for the i_{th} leg, namely

$$\frac{T_i}{W_i} = \frac{q_i S}{W_i}\left[K_1\left(\frac{n_i}{q_i}\frac{W_i}{S}\right)^2 + C_{D_0} + \frac{D_{ECS_i}}{q_i S}\right] + \frac{1}{V_i}\frac{d}{dt}\left(h_i + \frac{V_i^2}{2g}\right) \tag{7.10}$$

where the fact that $K_2 \approx 0$ for high performance aircraft (Mattingly et al, 1987) has been used. The only additional drag, R, being considered is the momentum drag created by the ECS (i.e. $R = D_{ECS}$). The drag-polar behavior used is shown in Figure 7.4 and is similar to that of current military aircraft.

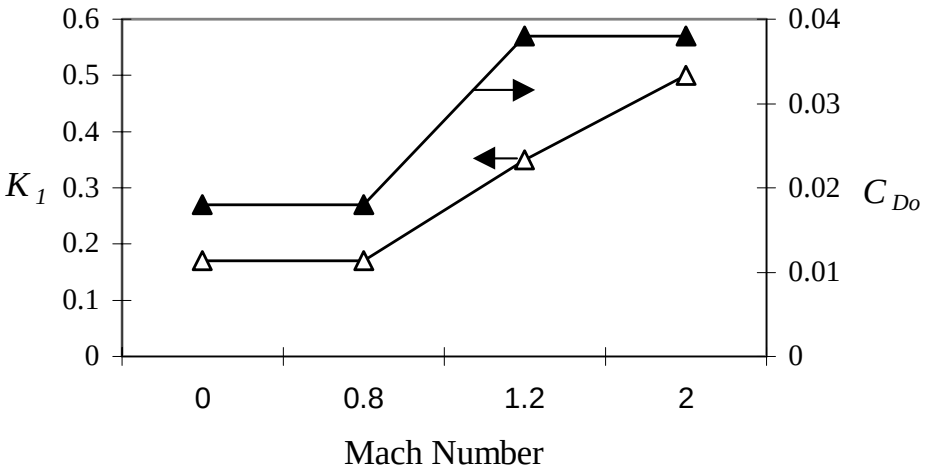

Figure 7.4. Typical drag-polar for military aircraft (Mattingly et al., 1987).

In equation (7.10), the velocity (V) and the rates of climb (dh/dt) and acceleration (dV/dt) are directly or indirectly given by the mission specifications (Table 7.1). The drag created by the ECS is also leg-dependent as will be discussed below.

An alternative version of equation (7.10) can be given as a function of the thrust at sea level take-off (T_{SL}) and gross take-off weight (W_{TO}), i.e.

$$T_i = \alpha T_{SL} = q_i S\left[K_1\left(\frac{n_i}{q_i}\frac{\beta_i W_{TO}}{S}\right)^2 + C_{D_0} + \frac{D_{ECS_i}}{q_i S}\right] + \frac{\beta_i W_{TO}}{V_i}\frac{d}{dt}\left(h_i + \frac{V_i^2}{2g}\right) \qquad (7.11)$$

where β_i is the fraction of the take-off weight at leg i and α is the fraction of the sea level take-off thrust. The take-off gross weight is given by

$$W_{TO} = W_{SS} + W_{PS} + W_{ECS} + W_{FUEL} + W_{PPAY} + W_{EPAY} \qquad (7.12)$$

where W_{SS} is the weight of the structures, which refers to all sub-systems present in the aircraft (wing, fuselage, hydraulics, power distribution, etc.) with the exception of the ECS, weapons and the PS. W_{PS} is the weight of the engine (propulsion sub-system), W_{ECS} is the weight of the ECS, W_{FUEL} is the weight of fuel necessary to carry out the mission, W_{PPAY} is the weight of the permanent payload (crew, equipment) and W_{EPAY} is the expendable payload (ammo and missiles).

An analysis of the constraints of the RFP will show a functional relationship between the minimum thrust-to-weight ratio or thrust loading at sea-level takeoff (T_{SL}/W_{TO}) and wing loading at take-off (W_{TO}/S). The construction of the resulting constraint diagram is beyond the scope of this work (the interested reader may consult the aircraft performance and design books of Nicolai (1975) or Anderson (1999)). The complete constraint diagram for the AAF is shown in Figure 7.5 (Mattingly et al., 1987). This diagram shows all the possible thrust and wing loading values that will lead to designs that comply with the requirements of the RFP. As indicated in Figure 7.5, the following ratios are arbitrarily set to the values indicated for the AAF:

$$\frac{T_{SL}}{W_{TO}} = 1.20 \tag{7.13}$$

and

$$\frac{T_{SL}}{S} = 3065 \ \text{N/m}^2 \tag{7.14}$$

Equations (7.11) through (7.14) hint at the tight integration issues associated with the design of an aircraft. The design and operation of any given sub-system is highly influenced by and in turn influences the synthesis / design and operation of all the others. Take the case of the ECS, for example. The ECS's weight and energy and extra thrust requirements affect the required total thrust which leads to higher fuel consumption and higher take-off gross weight. Equation (7.13) clearly shows that an increase in W_{TO} is associated with higher thrust, which in turns affects the size of the PS. The weight of the structures is also affected as indicated by equation (7.14)

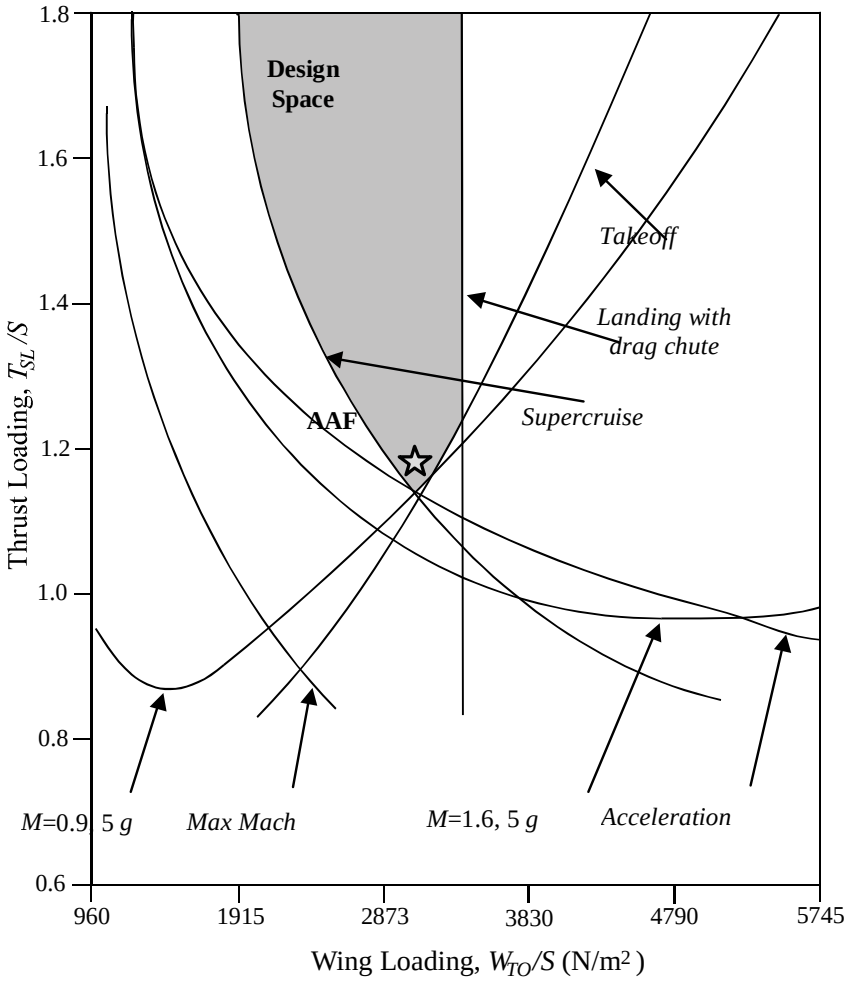

Figure 7.5. The complete AAF Constraint Diagram (Mattingly et. Al., 1987).

Based on the above, one can conclude that, in general, when any sub-system is installed in an aircraft, additional fuel (with the consequent effect on system weight) is required to

- provide the additional thrust associated with carrying the increased system mass
- overcome any additional drag, which may result from installing the sub-system in the aircraft
- carry the quantity of fuel required for the previous items.

- produce the power that some sub-systems may require. Power extractions from the PS cause increased fuel consumption and the associated larger weight discussed above.

Returning now to the weight equation, equation (7.12), the fuel weight is calculated based on engine performance and mission requirements and depends on the system synthesis / design and mission requirements. The weight of the ECS and the PS result from the sub-system optimization problems. The weight of the structures depends on a number of design considerations: materials used, aerodynamic performance, durability, strength and stability among many others.

The design of the structures is beyond the scope of this work. Here we consider the weight of the structures to correspond to values in agreement with existing design practices. To this end, consider the data given in Figure 7.6a, which shows the empty weight (structures plus PS plus ECS) for a number of high performance jet aircraft. The data were extracted from published information (Jane's All the World's Aircraft 1999-2000). A similar plot (see Figure 7.6b) indicates that a similar trend exists for the PS weight.

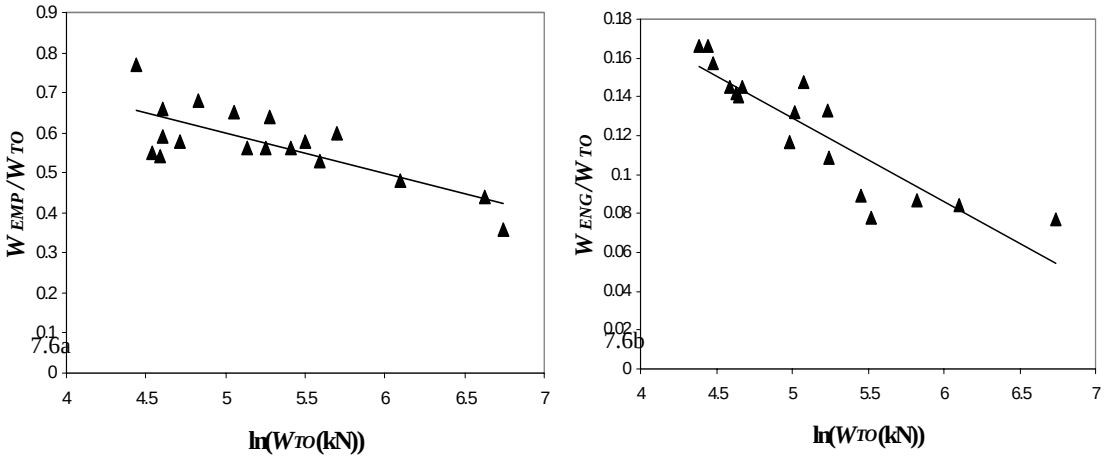

Figure 7.6. Empty weight (7.6a) and PS (7.6b) weight versus take-off weight for supersonic aircraft.

From Figure 7.6, it is possible to obtain the weight of the structures for a given value of the take-off weight. Thus, the weight of the structures sub-system is the empty weight (Figure 7.6a) minus the engine weight (Figure 7.6b) multiplied by a factor, k_{ecs}, to reflect the fact that the empty weight also includes the weight of the ECS. Based on the work of Muñoz and von Spakovsky (1999), $k_{ecs} = 0.975$ is used (i.e. the ECS mass is assumed to be 2.5 % of the structures mass).

As to the fuel weight in equation (7.12), it is a complex function of the thermodynamic performance of the engine, the mission requirements, the technology used and some stability considerations. In general, it is given by

$$W_{FUEL} = g \sum_{mission} \dot{m}_i \Delta t_i = g \sum_{mission} TSFC \cdot T \cdot \Delta t_i \tag{7.15a}$$

or

$$\text{Minimize} \qquad W_{FUEL} = w_{fuel}(W_{TO}, \vec{X}_{PS}, \vec{Y}_{PS,} mission) \tag{7.15b}$$

where the rate of fuel consumption has been written in terms of the thrust specific fuel consumption (*TSFC*).

Equation (7.15), however, is fairly inconvenient due to the fact that the specifications of each of the mission legs are given in terms of different parameters. As seen in Table 7.1, some of the legs have specified range, others specified duration, while still some others have specific maneuvers to be carried out. In addition, the duration of some of the legs changes as the decision variables are varied. Therefore, it is useful to employ a transformation, which puts all mission segments under a unified measure. Fuel consumed in each leg written in terms of the weight ratio is such a measure. The ratio of the final to the initial weight for leg *i* is defined as

$$\pi_i = W_{final} / W_{initial} \tag{7.16}$$

In order to proceed with the calculation of the weight ratios, consider the rate at which aircraft weight diminishes due to the consumption of fuel, namely

$$\frac{dW}{dt} = -TFSFC \cdot T \tag{7.17}$$

or $$\frac{dW}{W} = -TSFC\frac{T}{W}dt = -TSFC\frac{T}{W}\frac{dt}{ds}ds = -TSFC\frac{T}{W}\frac{ds}{V} \tag{7.18}$$

Equation (7.18) represents the weight-time and weight-velocity transformation that is used to unify the different requirements of the mission. The integration of equation (7.18) is done by breaking each mission segment into several (typically 5) intervals. The flight and operating conditions for each sub-segment are assumed to be constant at some representative value so that the integration can be accomplished explicitly. It was found that in most cases, five intervals are sufficient to ensure excellent accuracy. The resulting weight ratio relations for different cases are given in Table 7.3.

There is a special case, however, which deviates from the above calculations and corresponds to the mission segment when the expendable payload is delivered. If it is assumed that the delivery is done at some point *j* in the mission then

$$\frac{W_j - W_{EPAY}}{W_j} = 1 - \frac{W_{EPAY}}{W_j} \tag{7.19}$$

With equation (7.14) and the weight ratios and after some manipulation, the fuel consumption can be written as

$$W_{FUEL} = W_{TO}(1 - \prod_{i=1}^{n}\pi_i) - W_{EPAY}(1 - \prod_{i=j}^{n}\pi_i) \tag{7.20}$$

where *n* is the number of legs being considered.

The weight fractions depend on the design of the PS and other sub-systems, the thrust required, the afterburner setting and power requirements of the other sub-systems, ambient conditions, and a number of other factors. These complex set of factors are addressed by means of simulation as indicated below.

Table 7.3. Weight ratio calculations for different mission legs.

Case	$\pi = W_{final} / W_{initial}$
Constant speed climb	$\exp\left\{\frac{-TSFC}{V}\left[\frac{\Delta h}{1-\frac{D+D_{ECS}}{T}}\right]\right\}$
Horizontal Acceleration	$\exp\left\{\frac{-TSFC}{V}\left[\frac{\Delta\left(V^2/2g\right)}{1-\frac{D+D_{ECS}}{T}}\right]\right\}$
Climb and Acceleration	$\exp\left\{\frac{-TSFC}{V}\left[\frac{\Delta\left(h+V^2/2g\right)}{1-\frac{D+D_{ECS}}{T}}\right]\right\}$
Constant altitude/Speed cruise	$\exp\left\{\frac{-TSFC}{V}\left(\frac{D+D_{ECS}}{W}\right)\Delta s\right\}$
Constant altitude/Speed turn[35]	$\exp\left\{-TSFC\cdot n\cdot\left(\frac{D+D_{ECS}}{W}\right)\frac{2\pi NV}{g\sqrt{n^2-1}}\right\}$
Loiter	$\exp\left\{-TSFC\left(\frac{D+D_{ECS}}{W}\right)\Delta t\right\}$
Warm-up	$1-TSFC\left(\frac{T}{W_{TO}}\right)\Delta t$
Take-off Rotation	$1-TSFC\left(\frac{T+D_{ECS}}{W_{TO}}\right)\cdot t_R$

[36] N is the number of turns.

7.2 Propulsion Sub-system (PS)

The propulsion sub-system has eighteen components as indicated in Figure 7.7. The sub-system is a low-bypass turbofan engine with afterburning.

7.2.1 Thermodynamic Model

The on and off-design behavior of the engine is simulated using a modern performance code developed by an engine manufacturer for modeling any type of aircraft engine system. The model of the engine uses typical component maps (e.g., compressor, fan hub, fan tip, turbine, burner, and compressor maps) and functional relationships and numerical constants that modify the maps to make the simulation as realistic as possible. The component maps are chosen from several alternatives depending on the design pressure ratio. The computer program has its own set of solvers to carry out the mass, momentum, energy and shaft speed balances. Results from the simulation are the thermodynamic properties at each of the engine stations (pressure, temperature, Mach number, etc.), the inlet air flow rate, nozzle areas, and the fuel consumed in the combustor and afterburner adjusted to provide the thrust required by the mission (equation (7.11)) during the different segments of the mission.

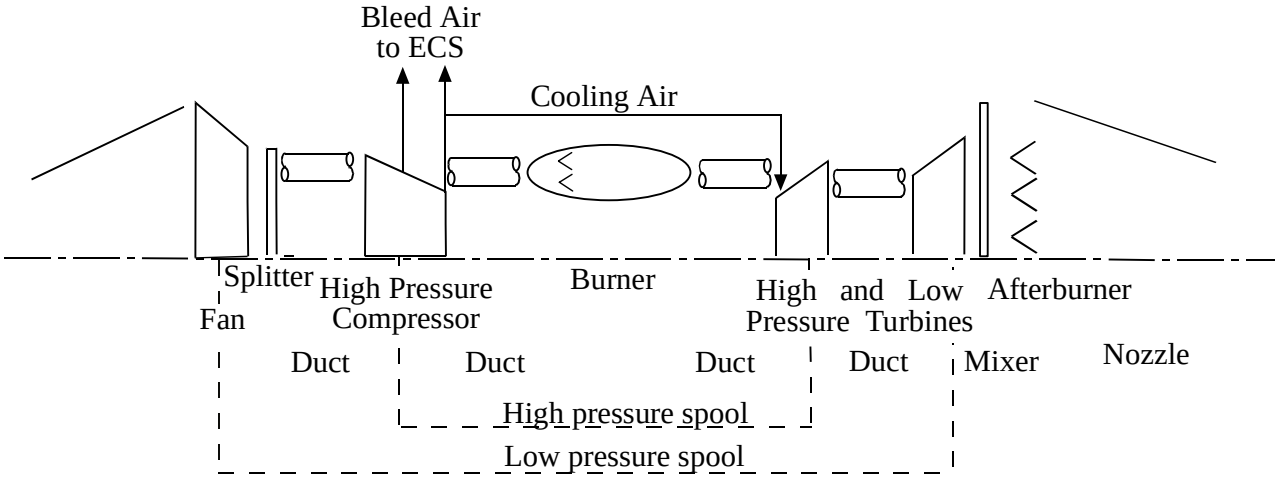

Figure 7.7. Turbofan engine components of the propulsion sub-system (PS).

7.2.2 Inlet and Nozzle Drag Models

The thrust provided by the engine simulator does not account for the drag created by the installation of the engine. This "uninstalled" thrust (F) must be adjusted for the drag created by the engine inlet and nozzle. Thus,

$$T = F - \phi_{inlet}F - \phi_{nozzle}F \tag{7.21}$$

The drag created by the inlet at subsonic conditions is approximated as the momentum drag created by an isentropic, one-dimensional flow of a perfect gas. Assuming massive separation and no recovery of the additional drag (i.e. the worst case scenario), the conservation of mass and perfect gas relationships lead to

$$\phi_{inlet} = \frac{\dfrac{M_0}{M_1}\sqrt{\dfrac{T_1}{T_0}}\left(1+\gamma M_1^2\right)-\left(\dfrac{A_1}{A_0}+\gamma M_0^2\right)}{\left(\dfrac{F}{m_0}\right)\left(\dfrac{\gamma M_0}{a_0}\right)} \tag{7.22}$$

For the supersonic case, a compressible model that uses a normal shock approximation and neglects internal friction and the disturbed pressure field on the cowl yields

$$\phi_{inlet} = \frac{\left(\dfrac{A_1}{A_0}-1\right)\left\{M_0-\left(\dfrac{2}{\gamma+1}+\dfrac{\gamma-1}{\gamma+1}M_0^2\right)^{1/2}\right\}}{\dfrac{F}{m_0 a_0}} \tag{7.23}$$

The computer program that simulates the PS cycle also provides the inlet and exit areas of the nozzle at various segments of the mission. The installation penalty due to the nozzle is given by

$$\phi_{nozzle} = \frac{M_0 \frac{C_{D_{nozzle}}}{2}\left(\frac{A_{exit} - A_{in}}{A_0}\right)}{\frac{F}{m_0 a_0}} \tag{7.24}$$

where the drag coefficient is a function of the Mach number as presented in Mattingly et al. (1987).

7.2.3 Physical Model

The weight and dimensions of the PS are calculated using the computer code Weight Analysis of Turbine Engines (WATE) (WATE User's Guide, 2000). WATE was originally developed by the Boeing Military Aircraft Company in 1979 and improved by NASA and the McDonnell Douglas Corporation. The original weight and dimensions were derived using a semi-empirical method obtained from analyzing a database of 29 engines. The improved code (used in this paper) is based on analytical and dimensional calculations (the primary method is to calculate material volume and then multiply by density). The new code also accounts for more of the individual parts that make up an engine component than the original empirical method.

7.2.4 Capital Cost Model

The capital cost model developed by Birkler et. Al. (1982) and appropriately adjusted for inflation is used. The model uses equations for estimating the development and production costs of military turbojet and turbofan engines. The model was obtained by applying regression analysis to available data. The cost includes the cost of development to meet the model qualification test (MQT), total development cost, and the cumulative average price at the 1000th production engine. The engine characteristics that best explain production as well as development cost with respect to MQT are the maximum thrust of the engine at sea-level-static conditions (an indicator

of engine size), Mach number (a measure of performance), and turbine inlet temperature (the dominant technical parameter in the engine cycle). The derived equation for total development cost includes a production quantity term as well as thrust and Mach number. This cost encompasses the expenses involved in developing a new engine to MQT specifications plus the cost to correct service related deficiencies and costs for continual performance and reliability improvements over time,.

7.3 Environmental Control Sub-system (ECS)

The ECS being synthesized / designed (Figure 7.8) is an improvement over the one in the previous chapter. As can be seen in Figure 7.8, a hot stream has been added to allow for better temperature control as well as an ejector for low speed, low altitude mission segments. There is no reason to claim that the regenerative heat exchanger should be placed after the secondary heat exchanger as opposed to before it. Thus, to solve this placement problem, the two heat exchangers are part of the "superconfiguration" (Olsommer et al., 1999) and each has an associated binary variable that determines its existence or non-existence. Naturally the sum of both binary variables should be equal to 1.

7.3.1 Thermodynamic Models

The thermodynamic models are given in great detail in Muñoz and von Spakovsky (1999). A brief description of the models follows beginning with the general atmospheric conditions, which correspond to the temperature of a standard hot day (MIL-STD-210B 10% risk) and the pressure and humidity ratios of the US Standard Atmosphere. Furthermore,

- The pressure and temperature schedules for the cabin and avionics are a function of altitude. The cooling load is a function of altitude and Mach number.

- All heat exchangers are plate-fin heat heat exchangers using offset-strip fins. The heat transfer and pressure drop models used are based on the work of Shah (1981) and Kays and London (1998). Both sides of the heat exchangers have one pass unless stated otherwise.
- The air cycle machine is modeled using compressor and turbine (both high-speed centrifugal) maps relating pressure ratio and isentropic efficiency to corrected flow rate and shaft speed. The maps used correspond to typical ECS air cycle machines.
- The water separator efficiency and pressure drop maps used correspond to a typical low- pressure water separator.
- For the supersonic inlet/exit, the pressure recovery and flow rate ratio correspond to those of a typical scoop-type ram-air inlet. The ducts and ram-air exit were modeled using a compressible flow model with a typical friction factor of 0.01. The momentum drag created by the ram inlet/exit was calculated neglecting the pressure and skin drags.

7.3.2 Physical Models

A detailed explanation of the physical models (mass and volume) used can be found in Muñoz and von Spakovsky (1999). A summary of the models used follows:

- Heat Exchangers: The mass of the heat exchanger core was calculated taking into account the geometry and materials of the fins and plate. All of the parts are assumed made of an aluminum alloy. The core mass was compared to that of existing heat exchangers and excellent agreement was found. Finally, the total mass was obtained by multiplying the core mass by an appropriate factor to include the mass of manifolds and other accessories. This factor was obtained through curve-fits of known data.

- Air Cycle Machine: The models of Baljé (1962) were used to estimate the necessary wheel diameter of the ECS turbo-machines. Curve-fits of existing data provided a correlation between wheel diameter and total mass.
- Water separator: A model based on existing data which gives the mass of the water separator as a function of the nominal air flow rate was used.
- Ram Inlet, Exit and Ducts: Models, which were developed using existing data, were employed. The models typically give the mass of the component as a function of the cross-sectional area, thickness, and density of the material used.
- The components not mentioned above were assumed to correspond to a typical ECS (Dieckmann et al., 1972).

7.3.3 Component Capital Cost Models

Two main sources of component capital cost information have been used to obtain ECS cost correlations. The first source is component data that is obtained directly from catalog data with corresponding costs estimated using the Federal Stock Number and cost databases. The second source of capital cost information is correlations, which were developed in the early 70's as part of the Integrated Environmental Control System program carried out under the sponsorship of the Air Force Flight Dynamics Laboratory (Dieckmann et al., 1972). These equations have been updated to reflect present dollars by using the Federal Stock Number and the Federal Cost Database. All of the correlations were obtained originally on the assumption that the costs are calculated based on quantity sets of 100. The information obtained from the catalog/FSN does not specify the quantity basis on which the cost was calculated and was thereby assumed to be 100 as well. In the case of compact heat exchangers, additional data have been included. This data was compiled recently by the Air Force Research Laboratory as part of their advanced heat exchangers program.

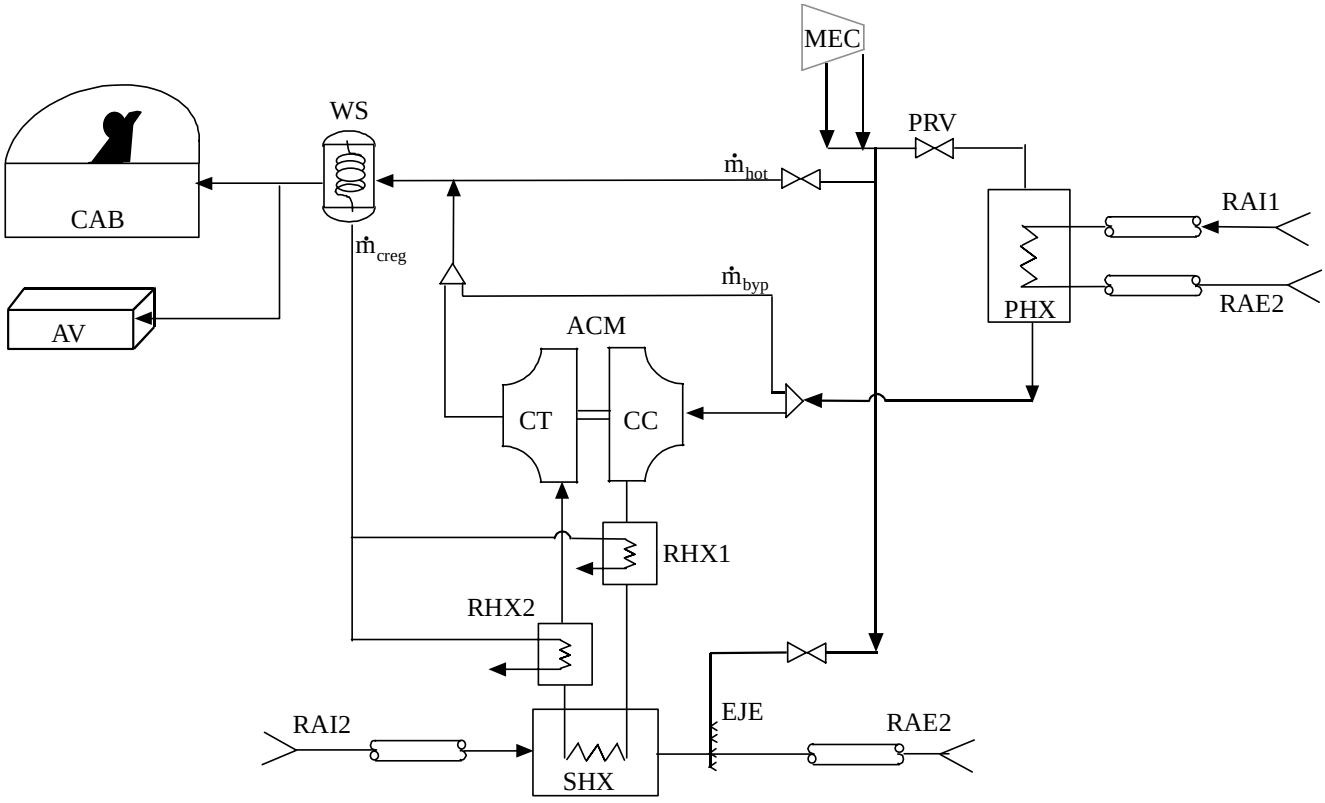

WS	Water separator	MEC	Main Engine Compressor	PRV	Pressure Regulating Valve	CAB	Cabin
PHX SHX	Primary and Secondary Heat Exchangers	CC CT	Centrifugal Compressor and Turbine	RAI1 RAI2	First and Second Ram Air Inlets	EJE	Ejector
RHX1 RHX2	1st and 2nd Regenerative Heat Exchangers	ACM	Air Cycle Machine	RAE1 RAE2	First and Second Ram Air Exits	AV	Avionics

Figure 7.8. Environmental Control Sub-system (ECS) and components.

In this work, research and development costs have not been included and, thus, the total cost merely reflects the replacement cost of the component when purchased in the quantity sets indicated above. At this time, catalog data with corresponding costs are only available for heat exchangers, water separators and air cycle machines. The

updated cost correlations developed by the Air Force Flight Dynamics Laboratory are used in the case of components for which no additional cost data is available.

The available data and equations relate cost to a characteristic size or geometric parameter (e.g., mass, diameter). The resulting cost-mass equations are updated to take into account the number of times the component is to be replaced throughout the ECS's lifetime. The capital costs are calculated for an estimated ECS lifetime of 8000 hours. This number is based on current military aircraft design practices (Tirpak, 2000).

The number of replacements for component *i* is NR_i and is calculated as

$$NR_i = round\left(\frac{8000}{MTBF_i} + 0.5\right) \tag{7.25}$$

where MTBF is the Mean Time Between Failures in operating hours. The MTBF is estimated from the reliability index of each component, which is defined as

$$RI = \frac{10^6}{MTBF\ k_1} \tag{7.26}$$

In the above equation, k_1 is a constant which for a typical ECS takes the value of 5730. Typical RI's for the ECS components (Dieckmann et al., 1972) were used.

7.4 Structures Sub-system (SS)

The aerodynamic model was presented in the first part of this chapter. A computer code was written to solve the equations given in Table 7.3. The resulting values for thrust for each of the legs is then used with the engine simulation code to estimate the fuel consumed in each of the mission legs.

The cost model used was developed by Resetar et al. (1991). The model provides separate costs for the following major cost elements: non-recurring engineering, non-recurring tooling, development support, flight test, recurring engineering, recurring

tooling, recurring manufacturing labor, recurring manufacturing material, and recurring quality assurance

The cost model was derived from a database consisting of 13 military aircraft with first flight dates ranging from 1960 to 1978: A-6, A-7, A-10, C-5, C-141, F-4, F-14, F-15, F-16, F-18, F-111, S-3A, and T-39. Empty weights for the sample aircraft range from under 10,000 lbm to over 300,000 lbm, while speeds range from 400 kn to over 1,300 kn.

The airframe cost refers to the cost of the assembled structural and aerodynamic components of the air vehicle that support sub-systems essential to a particular mission. It includes not only the basic structure (wing, fuselage, empennage, and nacelles) but also the air induction sub-system, starters, exhausts, fuel control subsystem, inlet control sub-system, alighting gear (tires, tubes, wheels, brakes, hydraulics, etc.), secondary power, furnishings (cargo, passenger, troop, etc.), engine controls, instruments (flight navigation, engine, etc.), environmental control, racks, mounts, intersystem cables and distribution boxes, etc. inherent to and inseparable from the assembled structure, dynamic sub-systems, and other equipment homogeneous to the airframe. Airframe costs also encompass the integration and installation of the propulsion, avionics, and armament sub-systems into the airframe but not those efforts directly related to their development and manufacture. The cost estimate does not include training, support equipment, data, and spares. Since the structures cost already includes the ECS cost, the former was multiplied by a factor of 0.975. This factor is obtained from assuming a linear relationship between cost and weight. This assumption proved to be valid as shown in the following sections.

For cost calculation purposes, it was assumed that 4 test and 350 production aircraft are built, respectively. These numbers agree with current military aircraft programs (Tirkap, 2000).

7.5 PS Decision (Independent) Variables

The design and operational independent variables for the PS are given in Table 7.4. Their ranges were selected based on existing engines with the proper thrust class. All of the components in the PS use current (year 2000) technology.

The following types were selected for various propulsion subsystem components:

- Inlet: 2D external compression
- Nozzle: 2-D convergent-divergent
- Combustor: single-dome
- Mixer: Forced mechanical mixer.

The fan and high-pressure compressor are designed with constant tip radius. Both of these components have inlet guide vanes (variable in the case of the HPC). The high-pressure turbine (HPT) and low-pressure turbine (LPT) have constant mean and tip radii, respectively. They use metallic blades. In addition, some important geometric, thermodynamic and aerodynamic decision variables not participating in the optimization for the rotating turbo-machinery are given in Table 7.5. The number of stages for the fan and HPC are calculated by the engine sizing code (WATE) based on the design pressure ratio. The HPT and LPT have one stage each.

Table 7.4. PS decision variables and constraints.

Component	Design Decision Variables		Constraints
Fan	α	Fan bypass ratio	$0.3 \leq \alpha \leq 0.6$
	PR_{fan}	Fan design pressure ratio (tip and hub)	$3.0 \leq PR_{fan} \leq 5.0$
Compressor	PR_{hpc}	High pressure compressor design pressure ratio	$4.0 \leq PR_{hpc} \leq 8.0$
Turbine	PR_{hpt}	High pressure turbine design pressure ratio	$1.8 \leq PR_{hpt} \leq 3.0$
	PR_{lpt}	Low pressure turbine design pressure ratio	$1.8 \leq PR_{lpt} \leq 3.0$
Mixer	M_{mixer}	Mixer Mach number	$M_{mixer}=0.4$
	Operational Decision Variables		
Compressor	BP_{low}	Low pressure bleed port[37]	$BP_{low}=0,1$
	BP_{high}	High pressure bleed port[37]	$BP_{high}=0,1$
Turbine	T_{it}	Turbine inlet temperature	$T_{it} \leq 1778$ K
	Dependent Variables		
Afterburner	T_{aft}	Afterburner temperature[38]	$T_{aft} \leq 2000$ K
Fan	φ_{hub}	Fan (hub) % stall margin[38]	$\varphi_{hub} > 10$
	φ_{tip}	Fan (tip) % stall margin[38]	$\varphi_{tip} > 10$
Fan and compressor	PR_{cp}	Overall pressure ratio	$17.0 \leq PR_{cp} \leq 32.0$
Compressor	φ_{hpc}	Compressor % stall margin[38]	$\varphi_{hpc} > 10$
	N/A	Bleed port selection[38]	$BP_{low}+BP_{high}=1$

[37] Binary variable: 0 means no bleed air is taken from the bleed port.

[38] This variable takes different values at different mission segments.

Table 7.5. Some important thermodynamic, geometric and aerodynamic parameter values for the PS optimization.

Parameter	fan	HPC	Parameter	HPT	LPT
$Mach_{in}$	0.50	0.45	$Mach_{in}$	0.20	0.17
$Mach_{exit}$	0.50	0.45	$Mach_{exit}$	0.30	0.32
Max. 1^{st} stage PR	1.80	1.40	Ratio of exit to entrance radius	1.20	1.00
Hub to tip ratio	0.40	0.46	Blade solidity	0.71	1.22
Blade solidity	1.10	0.84	Blade thickness ratio	0.20	0.20
Blade thickness ratio	0.10	0.08	1^{st} stage aspect ratio	1.20	1.20
1^{st} stage aspect ratio	2.00	1.00	Last stage aspect ratio	1.80	1.80
Last stage aspect ratio	1.50	1.00	Blade taper ratio	1.00	1.00
Blade taper ratio	0.556	0.83	Stator solidity	0.92	1.11
Stator solidity	0.80	0.75	Isentropic efficiency	0.90	0.90
Polytropic efficiency Hub Tip	 0.89 0.88	0.88	Turbine loading parameter	0.35	0.30

7.6 ECS Decision (Independent) Variables

The synthesis / design and operational independent variables for the ECS are given in Table 7.6. The range of the independent variables is based on existing designs and on the work of Muñoz and von Spakovsky (1999, 2000a).

Table 7.6a. ECS decision variables and constraints.

Component	Synthesis / Design Decision Variable			Constraints
Primary and secondary heat exchangers	L_c	Cold side length (m)		$0.5<L_c<0.9$
	L_h	Hot side length (m)		$0.06<L_h<0.9$
	L_n	Non flow length (m)		$0.5<L_n<0.9$
Air cycle machine	PR_{cp}	Compressor design pressure ratio		$1.8<PR_{cp}<3.0$
	PR_{tb}	Turbine design pressure ratio		$PR_{tb}<12$
First and second regenerative heat exchangers[39]	L_c	Cold side length (m)		$0.3<L_c<0.5$
	L_h	Hot side length (m)		$0.15<L_h<0.3$
	L_n	Non flow length (m)		$0.3<L_n<0.5$
	Reg_1	Existence-nonexistence of regenerative heat exchanger in configuration		$Reg_1, Reg_2 = 0,1$
	Reg_2			$Reg_1 + Reg_2 = 1$
Ram air inlet, outlet	A_1, A_2	Areas of inlet, outlet (cm^2)		$120< A_1, A_2<220$
Primary and secondary heat exchanger fin type: hot and cold sides[40,41]	Fin_{hot} Fin_{cold}	Fin No.	Surface designation [42]	R_{emax}
		1	¼(s)-11.1	8000
		2	1/8-15.2	6000
		3	1/8-13.95	6000
		4	1/8-15.61	6000
		5	1/8-19.86	5000
		6	1/9-22.68	5000
		7	1/9-25.01	4000
		8	1/9-24.12	4000
		9	1/10-27.03	4000
		10	1/10-19.35	4000

[39] The cooling air-side of the heat exchanger has 4 passes. The cold and hot side use fin numbers 4 and 8, respectively. The plate thickness is 0.254 mm.

[40] Discrete variable.

[41] The plate thickness is 0.254 mm.

[42] See Kays and London (1998).

Table 7.6b. ECS decision variables and constraints.

	Operational Decision Variables		
Pressure regulating valve	PR_{vv}	Pressure setting	PR_{vv}<6.0
Low pressure bleed port	BP_{low}	Low pressure bleed port[43]	BP_{low}=0,1
High pressure bleed port	BP_{high}	High pressure bleed port[43]	BP_{high}=0,1
Splitter	m_{byp}	Bypass air flow rate	m_{byp}<0.2 kg/s
Bleed port	m_{hot}	Hot air flow rate	m_{hot}<0.2 kg/s
Regenerative heat exchanger	m_{creg}	Cold air flow rate	m_{creg}<0.2 kg/s
	Dependent variables		
Cold and hot sides heat exchangers	Re_c [44]	Reynolds number, cold air side	$R_{ec/}$ R_{emax} <1
	Re_h [44]	Reynolds number, hot air side	$R_{eh/}$ R_{emax} <1
Cabin and avionics	T_{cold} [44]	Cooling air temperature	$\|T_{cold}-T_{sched}\|$< 3
	P_{cold} [44]	Cooling air pressure	P_{cold} = P_{sched}
	m_{cold} [44]	Cooling air flow rate	m_{cold} = m_{sched}
ACM	W_{cp},W_{tb} [44]	Compressor and turbine work	W_{cp}=W_{tb}

7.7 Optimization Problem Definitions

The sub-systems that make up the aircraft as well as their coupling functions are shown in Figure 7.9. As explained above, the interdependence between the two units being synthesized / designed (PS and ECS) is quite tight. Although the other units, namely the structures (SS) and payload (PAY) sub-systems, are not synthesized / designed, i.e. they do not have decision parameters which are being modified, their role is not strictly passive. Thus, for example, the SS sub-system's weight is affected by the synthesis / design decisions in all of the other units. The result is that the aircraft system

[43] Binary variable: 0 means no bleed air is taken from the bleed port.

[44] This variable takes different values at different mission segments.

at hand constitutes a typical case of a system in which “everything influences everything else”.

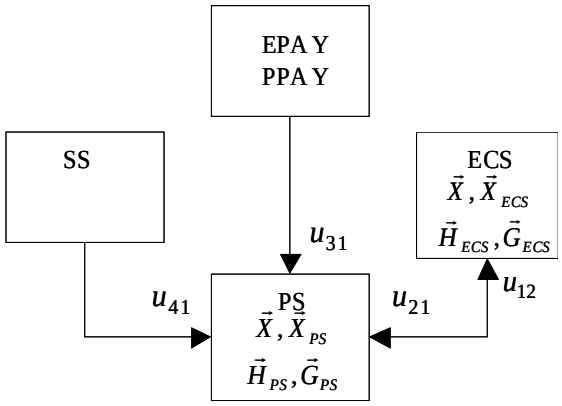

u_{12}	Bleed air temperature and pressure
u_{21}	Ram air momentum drag, ECS weight, bleed air requirement
u_{31}	Weight of the permanent and expendable payload
u_{41}	Drag and lift coefficients at different Mach numbers, weight of the structures

Figure 7.9 Sub-systems and sub-system coupling functions.

The nature of the simulation tools, the number and type of variables used in the synthesis / design and the resulting optimization algorithm choice as well as the selection of the objective function will dictate the type of optimization strategy used to solve the problem. What follows is a description of the take-off gross weight, total fuel consumption and total cost problem definitions alongside a presentation of results and a complete analysis.

7.7.1 Gross Take-Off Weight System-Level Optimization Problem Definition[45]

The first optimization problem formulated is that for the conceptual design optimization of a turbofan engine with afterburner and the synthesis / design optimization of the ECS for a military AAF using the mission given in Figure 7.2 and Table 7.1. The figure of merit employed is the gross take-off weight. Thus, the system-level optimization problem is to

$$\text{Minimize} \qquad W_{TO} = W_{SS} + W_{PS} + W_{ECS} + W_{FUEL} + W_{PPAY} + W_{EPAY} \tag{7.27}$$

w.r.t. $\left\{\vec{X}_{PS}, \vec{Y}_{PS}\right\}, \quad \left\{\vec{X}_{ECS}, \vec{Y}_{ECS}\right\}$

subject to

$$\vec{H}_{PS} = \vec{0}, \quad \vec{G}_{PS} \le \vec{0} \tag{7.27.1}$$

and $$\vec{H}_{ECS} = \vec{0}, \quad G_{ECS} \le \vec{0} \tag{7.27.2}$$

where the vectors of equalities $\vec{H}$ represent the thermodynamic and physical models (weight and volume) for each of the sub-systems. The vectors of inequalities $\vec{G}$ represent the physical limits for some of the variables or physical quantities.

It is important to note that although the minimization of weight is not a thermoeconomic problem, it shares many of its characteristics. For example, the synthesis / design and operation of any given sub-system forces the sub-systems with which it interacts to change their size. In the present problem, that change is reflected in different weights and in a thermoeconomic problem in different costs.

[45] W_{TO} is a figure of merit commonly used by the aircraft/aerospace community.

7.7.2 Fuel Consumption System-Level Optimization Problem Definition

The minimization of total fuel consumption is also a problem of great interest. This system-level optimization is defined as

$$\text{Minimize} \qquad W_{FUEL} = w_{fuel}(W_{TO}, \vec{X}_{PS}, \vec{Y}_{PS,} mission) \tag{7.28}$$

w.r.t. $\left\{\vec{X}_{PS}, \vec{Y}_{PS}\right\}, \quad \left\{\vec{X}_{ECS}, \vec{Y}_{ECS}\right\}$

subject to

$$\vec{H}_{PS} = \vec{0}, \quad \vec{G}_{PS} \le \vec{0} \tag{7.28.1}$$

and $$\vec{H}_{ECS} = \vec{0}, \quad \vec{G}_{ECS} \le \vec{0} \tag{7.28.2}$$

where n is the number of mission segments. In addition, the bleed pressures and temperatures in both sub-systems must match, i.e.

$$[P_{bleed}]_{PS} = [P_{bleed}]_{ECS} \qquad \text{and} \qquad [T_{bleed}]_{PS} = [T_{bleed}]_{ECS} \tag{7.28.3}$$

It is implicit in the formulation of the above problem that the fuel consumption over the entire mission is calculated using proper values for the intermediate products and feedbacks between the PS and the ECS.

7.7.3 Total Cost System-Level Optimization Problem Definition

Future air vehicles present a unique set of requirements not previously addressed. For example, future Uninhabited Air Vehicles (UAVs) must be substantially more affordable than comparable manned systems both in terms of acquisition and operational costs. Future UAVs will likely be high Mach, high performance vehicles. To permit an integrated approach to their optimal synthesis and design, it will, thus, be necessary to combine into a single comprehensive model both thermodynamic and cost

functions for these and other aerospace vehicles so that a large number of independent variables related to how different technologies optimally accommodate limited payload spaces can be investigated (Brown, 1999).

The minimization of capital cost at the system level is formulated as

$$\text{Minimize} \quad C_{\mathrm{T}} = C_{SS} + C_{PS} + C_{ECS} + C_{FUEL} \tag{7.29}$$

$$\text{w.r.t.} \ \left\{\vec{X}_{PS}, \vec{Y}_{PS}\right\}, \quad \left\{\vec{X}_{ECS}, \vec{Y}_{ECS}\right\}$$

subject to

$$\vec{H}_{PS} = \vec{0}, \quad \vec{G}_{PS} \le \vec{0} \tag{7.29.1}$$

$$\text{and} \ \vec{H}_{ECS} = \vec{0}, \quad \vec{G}_{ECS} \le \vec{0} \tag{7.29.2}$$

In addition, the bleed pressures and temperatures in both sub-systems must match, i.e.

$$[P_{bleed}]_{PS} = [P_{bleed}]_{ECS} \quad \text{and} \quad [T_{bleed}]_{PS} = [T_{bleed}]_{ECS} \tag{7.29.3}$$

For the above problem, the expendable payload is constant and, thus, is not part of the objective function. As with the previous problems, fuel consumption over the entire mission is calculated using proper values for the intermediate products and feedbacks between the PS and the ECS.

Now, in order to complete the definition of the optimization problem for any one of the three objectives given above, it is necessary to subdivide the mission of Figure 7.2 and Table 7.1 into segments (phases or legs). A preliminary analysis reveals that the mission segments and phases of Table 7.7 are the most critical ones, either because their fuel consumption is significant or the operating conditions are very stringent for the two sub-systems being synthesized / designed.

Table 7.7. AAF critical mission segments.

Mission segments		
No.	**Name**	
1	wup	Warm-up
2	tka	Take-off acceleration
3	tkr	Take-off rotation
4	clac	Climb/accelerate
5	scc	Subsonic cruise climb
6	cap	Combat air patrol
7	acc	Acceleration
8	pen	Penetration
9	ct1	Combat turn 1
10	ct2	Combat turn 2
11	cac	Combat acceleration
12	esc	Escape dash
13	scc_2	Subsonic cruise climb 2
14	loi	Loiter
15	mmn	Maximum Mach number

From Table 7.4 one sees that the total number of design variables for the PS is five. Of the mission legs in Table 7.7, six have specified turbine inlet temperature (because military[46] or maximum thrust is specified), so that the total number of continuous independent operational variables is nine (T_{it} for the nine remaining legs) The number of binary variables is two per leg (bleed port selection). Therefore, the total number of independent variables for the PS design optimization problem is forty-four (thirty binary). The total number of constraints is seventy six.

For the ECS synthesis / design optimization, the number of synthesis / design decision variables is nineteen including two binary (existence or non-existence of either

[46] Military thrust is defined as the thrust obtained with no afterburning and max. T_{it}

one of the regenerative heat exchangers) and two discrete (type of fin for both sides of the primary and secondary heat exchangers from a set of ten). The operational variables include four continuous variables and two binary (bleed port choice) per segment so that the total (i.e. for the entire mission) number is ninety. Therefore, the ECS synthesis / design optimization problem uses one hundred nine independent variables. The number of constraints is one-hundred and eighty.

Given the nature of the simulation and the number and type of variables and constraints, one can clearly see that one is confronted with a very complex, large-scale mixed integer non-linear optimization problem. The difficulties associated with solving this problem are exacerbated by the following:

- There is a need to iterate until proper convergence of the take-off weight is achieved.
- The engine simulation tool was not specifically written for optimization purposes. Each time a simulation is run, it is necessary to launch the program and read the necessary software licenses. This difficulty added to the previous item makes the take-off weight calculation (for any given values of the independent variables) very expensive computationally. The ECS simulation code does not have this drawback since it was developed in-house.
- The presence of both binary and discrete variables makes it necessary to use a heuristic approach: either a genetic algorithm or a simulated annealing optimization algorithm. There are no general gradient-based methods able to solve the mixed integer non-linear programming (MINLP) problem. However, heuristic algorithms impose a significant time penalty in terms of solution time.

With the comments given above, it becomes clear that decomposition is not only advisable but desirable. Quite naturally, two problems, one for the PS and another for the ECS, can be defined. In the presentation that follows, the terminology used is consistent with that of the previous chapters

7.8 Unit-Level Optimization Problems

7.8.1 PS Unit-Level Design Optimization Problem Definition

The boundaries of the two units (sub-systems) are clearly seen in Figure 7.10. The resource used to produce the system-level product (thrust) is fuel. An intermediate product/feedback is the bleed air for the ECS. The ECS in turns has an associated drag penalty, which must be overcome by additional thrust. Other information from the ECS to be used in the PS design is the ECS mass and the bleed port selection. Thus, the PS, i.e. power plant, unit-level design optimization problem is to

$$\text{Minimize} \qquad W_{TO} = w_{SS}(W_{TO}) + W_{PS} + W_{ECS} + W_{FUEL} + W_{PPAY} + W_{EPAY} \tag{7.30}$$

w.r.t. $\left\{\vec{X}_{PS}, \vec{Y}_{PS}\right\}$

subject to

$$T_i = \alpha T_{SL} = q_i S\left[K_1\left(\frac{n_i}{q_i}\frac{\beta_i W_{TO}}{S}\right)^2 + C_{D_0} + \frac{D_{ECS_i}}{q_i S}\right] + \frac{\beta_i W_{TO}}{V_i}\frac{d}{dt}\left(h_i + \frac{V_i^2}{2g}\right) \tag{7.30.1}$$

where it should be pointed out that for the unit-level optimization (as opposed to the system-level optimization, equations (7.27)), W_{ECS} is held constant, i.e.

$$W_{ECS} - W_{ECS}^o = 0 \tag{7.30.2}$$

In addition, the following constraints are also imposed:

$$\dot{m}_{bleed\,i} - \dot{m}_{bleed\,i}^o = 0 \tag{7.30.3}$$

$$BP_{low\,i} - BP_{low\,i}^o = 0 \tag{7.30.4}$$

$$BP_{high_i} - BP^{o}_{high_i} = 0 \tag{7.30.5}$$

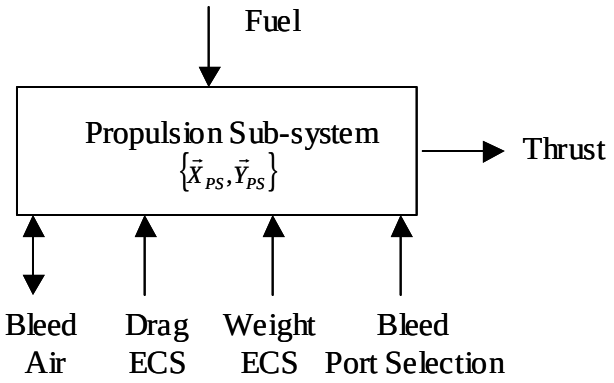

Figure 7.10. PS (power plant) intermediate product and feedbacks.

Constraints (7.30.2) through (7.30.5) indicate that the weight of the ECS, the bleed air flow rate, and the bleed port from which it is taken are set equal to the values indicated with the superscript *0*. These values are set externally. The necessary initial estimates of the weight fractions β_i are given by Nicolai (1975) or Mattingly et.al. (1987).

The minimization of total fuel consumption is also a problem of great interest. This optimization is defined for the PS as

$$\text{Minimize} \qquad W_{FUEL} = w_{fuel}(W_{TO}, \vec{X}_{PS}, \vec{Y}_{PS,} mission) \tag{7.31}$$

$$\text{w.r.t.} \ \{\vec{X}_{PS}, \vec{Y}_{PS}\}$$

subject to

$$\vec{H}_{PS} = \vec{0}, \quad \vec{G}_{PS} \le \vec{0} \tag{7.31.1}$$

It is implicit in the formulation of the above problem that the fuel consumption over the entire mission is calculated using proper values for the products and feedback of the ECS.

The PS design optimization based on capital cost is formulated as

$$\text{Minimize} \quad C_{\text{T}} = C_{SS} + C_{PS} + C_{ECS} + C_{FUEL} \tag{7.32}$$

w.r.t. $\left\{\vec{X}_{PS}, \vec{Y}_{PS}\right\}$,

subject to

$$\vec{H}_{PS} = \vec{0}, \quad \vec{G}_{PS} \leq \vec{0} \tag{7.32.1}$$

7.8.2 ECS Unit-Level Synthesis / Design Optimization Problem Definition

The only PS product being used directly by the ECS is the bleed air. However, this bleed air and the ECS drag penalty also represent feedbacks to the PS as do the ECS weight and the choice of bleed port for each of the legs. Each translates into excess thrust.

Let us now define the marginal costs of the intermediate feedback (bleed air) and products (ECS weight and drag) for a given selection of the bleed port at different mission legs. The marginal costs based on the optimum fuel weight for a given leg *i* are given by

$$\lambda_{bleed\,i} = \frac{\partial W_{FUEL\,i}^{*}}{\partial Bleed} \tag{7.33}$$

$$\lambda_{decs\,i} = \frac{\partial W_{FUEL\,i}^{*}}{\partial D_{ECS}} \tag{7.34}$$

and

$$\lambda_{wecs\,i} = \frac{\partial W_{FUEL\,i}^{*}}{\partial W_{ECS}} \tag{7.35}$$

where the weight of the fuel at the i_{th} leg is given by

$$W_{FUEL\,i} = W_{TO}\left(1 - \pi_i\right) \cdot \prod_{1}^{i-1} \pi \tag{7.36}$$

and the fuel consumed due to the ECS can then be written as

$$W_{FUEL_{ECS}} = \sum_{i=1}^{n} \left(\lambda_{bleed\,i} Bleed_i + \lambda_{decs\,i} D_{ECS\,i} + \lambda_{wecs\,i} W_{ECS} \right) \tag{7.37}$$

It has been assumed in equation (7.37) that the marginal costs are constant over the range of bleed, drag, and weight of the ECS.

Equation (7.37) can be disaggregated even further to account for the additional fuel consumption due to each of the different intermediate feedbacks (i.e., bleed, ECS drag and weight) from the ECS. The resulting fuel consumptions are

$$W_{FUEL_{bleed}} = W^o_{FUEL} + \sum_{i=1}^{n} \left(\lambda_{bleed\,i} Bleed_i \right) \tag{7.38}$$

$$W_{FUEL_{decs}} = W^o_{FUEL} + \sum_{i=1}^{n} \left(\lambda_{ecs_i} D_{ECS_i} \right) \tag{7.39}$$

$$W_{FUEL_{wecs}} = W^o_{FUEL} + \sum_{i=1}^{n} \left(\lambda_{wecs_i} W_{ECS} \right) \tag{7.40}$$

where the reference fuel weight W^o_{FUEL} has been set to correspond to the case with no bleed air, ECS drag or weight.

To obtain the impact of these factors on the overall objective function, namely the gross take-off weight, equation (7.27) is solved (i.e. iterated on WTO until convergence is achieved) with the fuel weight values given by equations (7.38) to (7.40). Thus, the increase in the gross take-off weight due to the ECS products and feedback are given by

$$\Delta W_{TO_{bleed}} = W_{TO}(W_{FUEL_{bleed}}) - W_{TO}(W^o_{FUEL}) \tag{7.41}$$

$$\Delta W_{TO_{decs}} = W_{TO}(W_{FUEL_{decs}}) - W_{TO}(W^o_{FUEL}) \tag{7.42}$$

and

$$\Delta W_{TO\,wecs} = W_{TO}(W_{FUEL\,wecs}) - W_{TO}(W^{o}_{FUEL}) \tag{7.43}$$

Thus far bleed and drag have been referred to in general terms and no mention of what properties should be used to represent them has been made. In the case of bleed air, options are energy, exergy (or other thermodynamic properties) or air flow rate. Drag can be represented as a force or a form of energy (i.e. propulsive power loss). The work of Muñoz and von Spakovsky (2000b) indicates that there is a mathematical advantage with the use of properties that make the marginal costs monotonic and, ideally, linear. In a different paper, the same authors (Muñoz and von Spakovsky, 2000a) found a linear relationship between fuel consumption and bleed air flow rate as well as between fuel consumption and drag force. These findings constitute a good choice for the property to represent bleed and drag. In addition, there is an intrinsic practical advantage with the use of these two properties. The engine simulator can be easily adjusted to provide variable air flow rates at the high and low bleed ports. It is also easy to increase or decrease the necessary thrust according to the drag penalty created by the ECS.

One problem arising from the use of bleed air flow rate is the need for "matching" the bleed port temperatures and pressures in both sub-systems for all mission legs. The PS is designed with assumed values for the drag, bleed air flow rate, and weight of the ECS. If the overall system is optimized without decomposition, the values used by the PS and obtained from optimizing the ECS are identical. However, the iterative version of the decomposition approach used (ILGO) makes it necessary in the ECS synthesis / design to use the temperature and pressure of the bleed port obtained from running the PS in the previous iteration. Therefore, it is necessary to check that in addition to flow rate, the bleed thermodynamic conditions are consistent. Although this potentially poses a problem in terms of convergence, the expected low variability of the bleed port conditions after a few iterations should render this problem insignificant.

With the above comments and taking into account that there is no external resource being used by the ECS, the unit-level synthesis / design optimization problem is set up as follows:

$$\text{Minimize} \quad \Delta WTO_{ECS} = \Delta W_{TObleed} + \Delta W_{TOdecs} + \Delta W_{TOwecs} \tag{7.44}$$

w.r.t. $\left\{\vec{X}_{ECS}, \vec{Y}_{ECS}\right\}$

subject to the constraints given in Table 7.4, as well as

$$[P_{bleed}]_{PS} = [P_{bleed}]_{ECS} \quad \text{and} \quad [T_{bleed}]_{PS} = [T_{bleed}]_{ECS} \tag{7.44.1}$$

i.e. the bleed pressures and temperatures must match.

For the ECS the fuel consumption problem is defined as

$$\text{Minimize} \quad \Delta W_{FUEL\,ECS} = \sum_{i=1}^{n} \left(\lambda_{bleed\,i} \dot{m}_{bleed\,i} + \lambda_{decs_i} D_{ECS\,i} + \lambda_{wecs_i} W_{ECS}\right) \tag{7.45}$$

w.r.t. $\left\{\vec{X}_{ECS}, \vec{Y}_{ECS}\right\}$

Subject to the same constraints as problem (7.44).

The capital cost minimization for the ECS is written as

$$\text{Minimize} \quad \Delta C_{T\,ECS} = C_{ECS} + \left(\Delta C_{FUEL} + \Delta C_{SS} + \Delta C_{PS}\right)_{ECCS} \tag{7.46}$$

subject to the same constraints as problem (7.44).

where the $\Delta C_{T\,ECS}$ is increase in the system's capital due to the ECS. In the above equation, C_{ECS} is the capital cost; $\Delta C_{FUEL\,ECS}$ is the cost of the extra fuel due to the ECS penalties (bleed air, ram drag, and ECS weight); and $\Delta C_{SS\,ECS}$ and $\Delta C_{PS\,ECS}$ are the extra cost of the structures and propulsion subsystems, respectively.

7.9 Solution Approach

One of the options available to solve the optimization problems defined above is to use the local-global optimization (LGO) decomposition technique presented by Muñoz and von Spakovsky (2000b). In order to do this, the design of the PS (problem (7.32)) would need to be carried out for multiple bleed air flow rates, ECS drags and ECS weights, and bleed port selections. This would mean that a number of unit-level optimization runs with respect to the PS design and operational variables would have to be solved for innumerable combinations of values of the constraints (7.32.2) to (7.32.5). A similar number of unit-level optimizations would have to be done for the ECS. The results would then be used to generate the optimum response surface (ORS) of the system, which in this case would be in the WTO versus ECS drag, bleed, and weight domain. If this off-line version of the method (OL-LGO; see Muñoz and von Spakovsky (2000b)) is to be used, the results would have to be stored for later use in the system-level optimization problem for the PS and ECS combined. The latter problem involves finding the combination of bleed air, ECS drag, and weight that minimizes the system-level objective function.

From a practical viewpoint, there are a number of difficulties associated with the implementation of the OL-LGO technique in its general form for this case. These difficulties are summarized as follows:

- The calculation of the take-off gross weight involves "flying" the engine on paper over the entire mission to obtain the fuel consumption. The process is repeated a number of times until convergence on the take-off weight is achieved. The resulting W_{TO} value can then be sent to the optimizer for analysis.
- The process described in the previous item requires different computer codes. First, there is a computer program that calculates the necessary thrust for each of the mission legs by solving the differential equations (7.11) and (7.18) (flight dynamics code). The thermodynamic engine simulation follows. This step is particularly slow

due to the fact that the engine performance code in use is not 'persistent', i.e. it is necessary to launch the program every time the engine is 'flown' over the mission. The thrust obtained from the engine simulator is adjusted by a different computer code to account for inlet and nozzle losses, i.e. equations (7.21) to (7.24). Some of the outputs of the thermodynamic simulation added to aerodynamic, materials and other design variables are used by WATE (NASA's engine weight code) to calculate the weight of the engine. The final step is the post-processing of all of the codes' results. The entire process just described makes the simulation very expensive computationally. For reference, the calculation of a single value for the take-off gross weight takes on average about 55 seconds on a current PC workstation, a duration which can be prohibitive for large-scale optimization.

The previous discussion points to the need for the iterative version of the LGO technique, i.e. ILGO, presented in Muñoz and von Spakovsky (2000b). Of the two versions of ILGO presented in the same reference, version A requires that both PS and ECS be synthesized / designed for arbitrary values of the intermediate products and feedbacks (i.e. ECS bleed, drag, and weight). Such a constraint is easy to meet in the PS design. However, the ECS synthesis / design would unnecessarily be constrained by this requirement. In fact, arbitrary combinations of the connecting functions between PS and ECS may not necessarily lead to feasible solutions for the ECS. Therefore, version B of ILGO, which does not have these shortcomings, is used for the ECS synthesis / design optimization while version A is retained for the PS.

The implementation of ILGO requires the following steps:

1. The first step is to design the PS (i.e. perform optimization problem (7.30)) for an initial estimate of the necessary amount of bleed air and ECS drag and weight. Since no information about the ECS exists at this stage of the design process, estimates are used based on Muñoz and von Spakovsky (2000a). Thus, the initial amount of bleed air is estimated as 120% of the amount of air required to cool the load (cabin and avionics). The ECS drag is initially estimated at 1200 N for each of the legs. An initial estimate for the ECS weight is 410 kg (900 lbm). To begin with, it is assumed

that the bleed air is taken from the high-pressure bleed port at all points of the mission. Once the bleed port has been chosen and the amount of bleed air and ECS drag and weight are fixed, the number of independent variables is effectively reduced from 44 to 14 at the unit-level, none of which is an integer.

2. After completing the PS design, the bleed port thermodynamic conditions are calculated at all operating conditions (mission segments). The fuel-based marginal costs for each of the mission legs are calculated as well in this step. The entire modeling/optimization process for the PS design optimization is depicted in Figure 7.11.

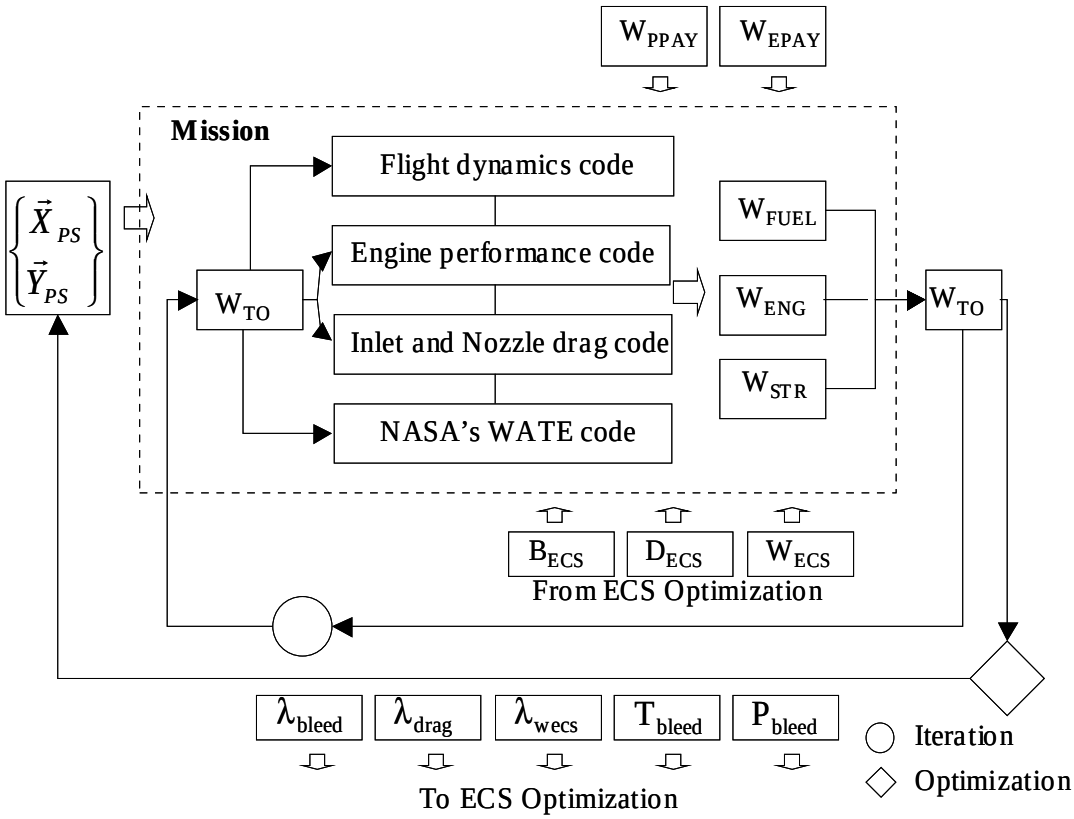

Figure 7.11. The PS unit-level modeling and optimization procedure.

3. The bleed and pressure values for each of the mission legs along with the marginal costs are used to carry out the synthesis / design optimization of the ECS (problem (7.44)). Based on the previous work of Muñoz and von Spakovsky (2000a), the

marginal costs are assumed constant over the synthesis / design space. This assumption is equivalent to saying that the response surface is in fact a hyper-plane. With the previous supposition, the intermediate products and feedbacks are allowed to take arbitrarily large or small numbers. To begin the solution of problem (7.44), the bleed pressure and temperature maps presented by Muñoz and von Spakovsky (1999) are used. The total number of variables is 109. Given the large number of variables and the fact that 4 of them are integer for the ECS problem, time decomposition is used in the manner described in Muñoz and von Spakovsky (2000b). The work of Muñoz and von Spakovsky (1999) shows that the most demanding operating condition for the ECS corresponds to the mission segment with high altitude and subsonic speed. This point is critical because of a combination of relatively low bleed pressures, high cooling temperatures, and low ram air availability. Thus, the selected synthesis / design or reference condition corresponds to the second subsonic cruise climb leg (scc_2) of Table 7.7.

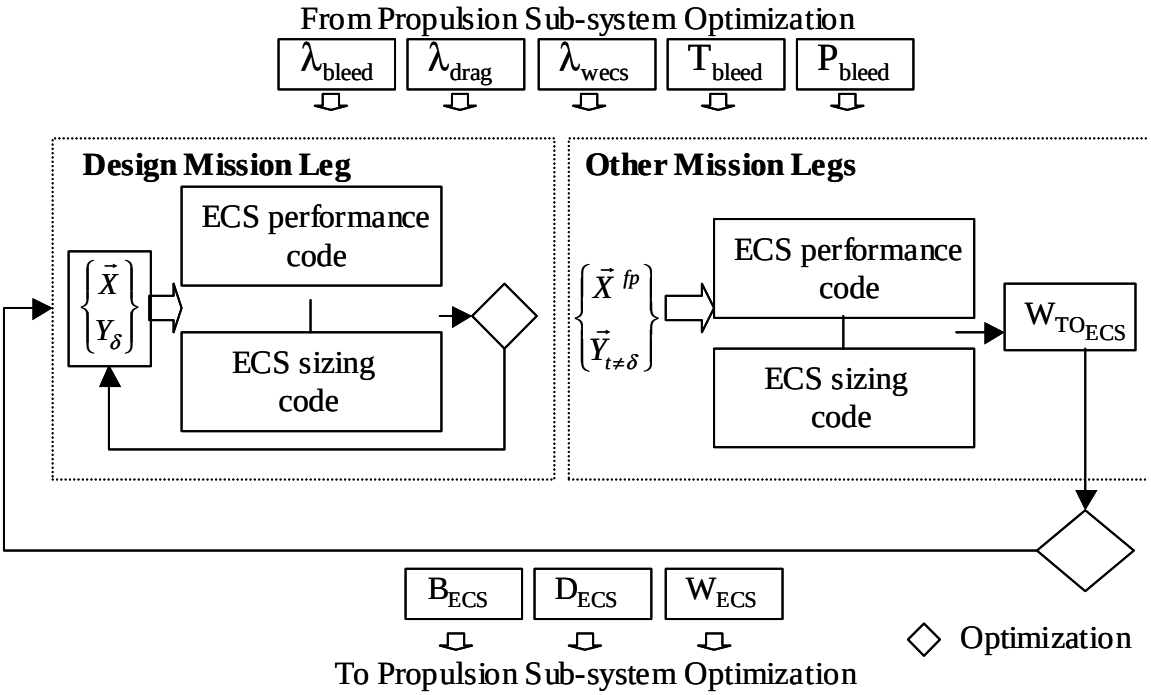

Figure 7.12. ECS unit-based system-level modeling and optimization procedure.

4. The second subsonic cruise climb leg is used to obtain a set of the most promising solutions. Each of these (typically 5) provides constant values for the ECS synthesis / design decision variables, which are then used in the off-design optimization. At the operational-level, fourteen problems are resolved each with respect to the operational decision variables for each leg. The optimization procedure for the ECS is shown in Figure 7.12.

5. Once completed, the ECS synthesis / design provides updated values for the products and feedbacks of the ECS. These values are used in step 1 to redesign the PS. The iterative process continues until no improvement in the system-level objective function is observed.

6. An additional consideration is that the bleed pressure and temperature for the optimized PS should be equal to those used in the optimization of the ECS. The final match between bleed air properties is to be verified.

The procedure described above is the same regardless of whether the objective function is the total take-off gross weight (equation 7.27)) or the fuel consumed to carry out the mission (equation (7.28)) or the total cost (equation (7.29)).

All of the optimization problems are solved using the commercial optimization package iSIGHT (1999). Each optimization iteration typically consists of two steps. The first uses a Genetic Algorithm (GA) in order to effectively deal with the mixed integer variables and possible local minima problems in each of the sub-system (unit-level for the PS and unit-based system-level for the ECS) optimizations. Each GA optimization run has a minimum population size equal to three times the number of variables with a minimum of 50. The minimum number of iterations for the GA is set to 100 and 1000 times the population size for the PS and ECS optimization problems, respectively. In the first step, the convergence criterion for the calculation of the take-off gross weight is set at 0.2 %. This means that the value of W_{TO} sent to the optimization algorithms has an error of approx. ±200 N. The second step uses the top two or three solutions obtained with the GA to narrow down the best solutions using a gradient-based algorithm

(Method of Feasible Directions). For the second step, the convergence criterion on the take-off gross weight calculation is set at 0.1 %.

7.10 Results

An optimum value for the gross take-off weight was found in 4 iterations of ILGO. Figure 7.13 shows the evolution of the take-off gross weight and the weight of the PS and ECS for the different runs. It is clearly evident that in every run some improvement was achieved in the system-level objective function (gross take-off weight) and the weight of both sub-systems. The flat behavior of W_{TO} for the last two iterations indicates that the overall iterative optimization scheme converged, i.e. no improvement is achieved after iteration 4. This observation was verified by running the problem a fifth time with no observable change in the independent variables or the system-level objective function.

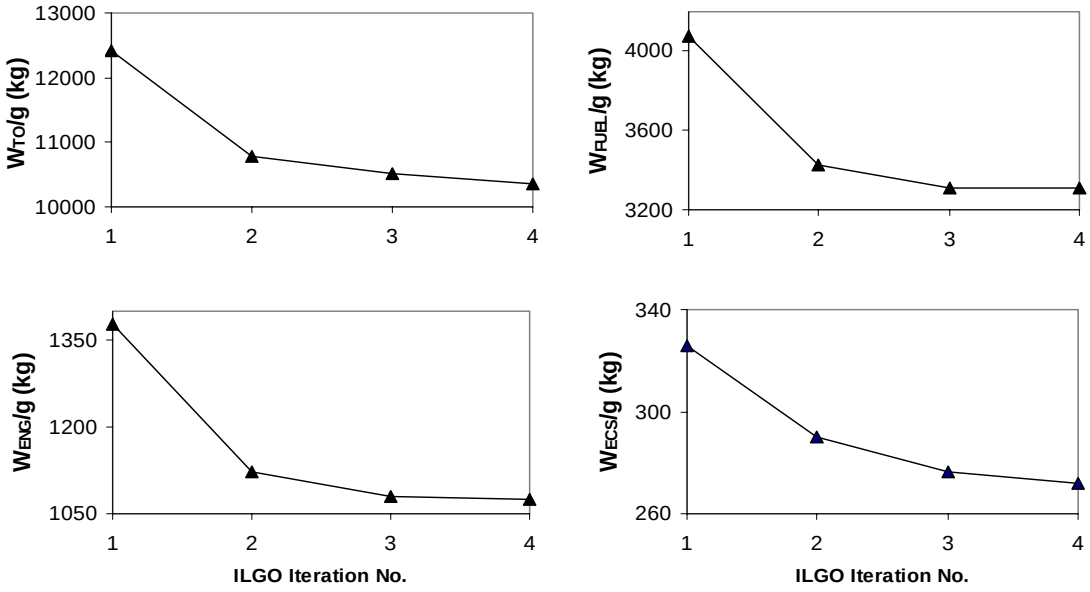

Figure 7.13. Evolution of the take-of gross weight, fuel, and ECS and engine weight at different points of the iterative local-global optimization (ILGO) approach.

Table 7.8. ECS and PS optimum values for the operational variables

Leg	PR_{vv}	m_{creg}	m_{byp}	m_{hot}	BP_{low}[47]	BP_{high}[47]	T_{it}
tkr	1.406	0.0174	0.000	0.000	0	1	1778
tka	2.193	0.0349	0.200	0.000	0	1	1778
wup	1.845	0.001	0.063	0.000	0	1	1778
clac	3.440	0.056	0.101	0.000	1	0	1778
scc_1	2.459	0.104	0.002	0.000	1	0	1355
cap	1.380	0.200	0.002	0.000	0	1	1090
acc	4.029	0.101	0.001	0.044	1	0	1778
pen	5.564	0.062	0.001	0.000	1	0	1588
ct1	6.000	0.069	0.016	0.000	1	0	1778
ct2	4.229	0.087	0.032	0.000	1	0	1778
cac	5.885	0.058	0.016	0.000	1	0	1778
esc	5.287	0.086	0.032	0.000	1	0	1574
mmn	4.229	0.137	0.024	0.000	1	0	1636
scc_2	1.463	0.088	0.000	0.000	1	0	1275
loi	2.115	0.015	0.048	0.000	1	0	1113

Optimum results for the PS and ECS independent operational and synthesis / design variables appear in Tables 7.8 and 7.9, respectively. Optimum objective function values and weights appear in Table 7.10. The change of selected independent variables for both the PS and the ECS for the different optimization runs is shown in Figure 7.14. The evolution of the ram air scoop inlets and the core dimensions of the primary heat

[47] This variable is common to the ECS and PS optimization problems.

exchanger are shown as well as the fan bypass and pressure ratio, the high pressure compressor's design pressure ratio, and the low and high pressure turbines' design pressure ratios. All of the variables have been non-dimensionalized by dividing them by the minimum allowable value found in Tables 7.4 and 7.6.

Table 7.9. PS and ECS optimum values for the synthesis / design variables. The same results were obtained by using as the system-level objective either the take-off gross weight, the fuel weight, or the total cost.

L_h (Prim HX)	0.500	α	0.563
L_c (Prim HX)	0.060	PR_{fan}	4.997
L_n (Prim HX)	0.500	PR_{hpc}	5.140
L_h (Sec. HX)	0.500	PR_{hpt}	2.907
L_c (Sec. HX)	0.060	PR_{lpt}	1.814
L_n (Sec. HX)	0.508	PR_{cp}	2.60
L_c (Reg. HX)	0.300	PR_{tb}	8.56
L_c (Reg. HX)	0.150	Fin_{hot}	4
L_n (Reg. HX)	0.300	Fin_{cold}	4
A_1	120.0	Reg_1	0
A_2	120.0	Reg_2	1

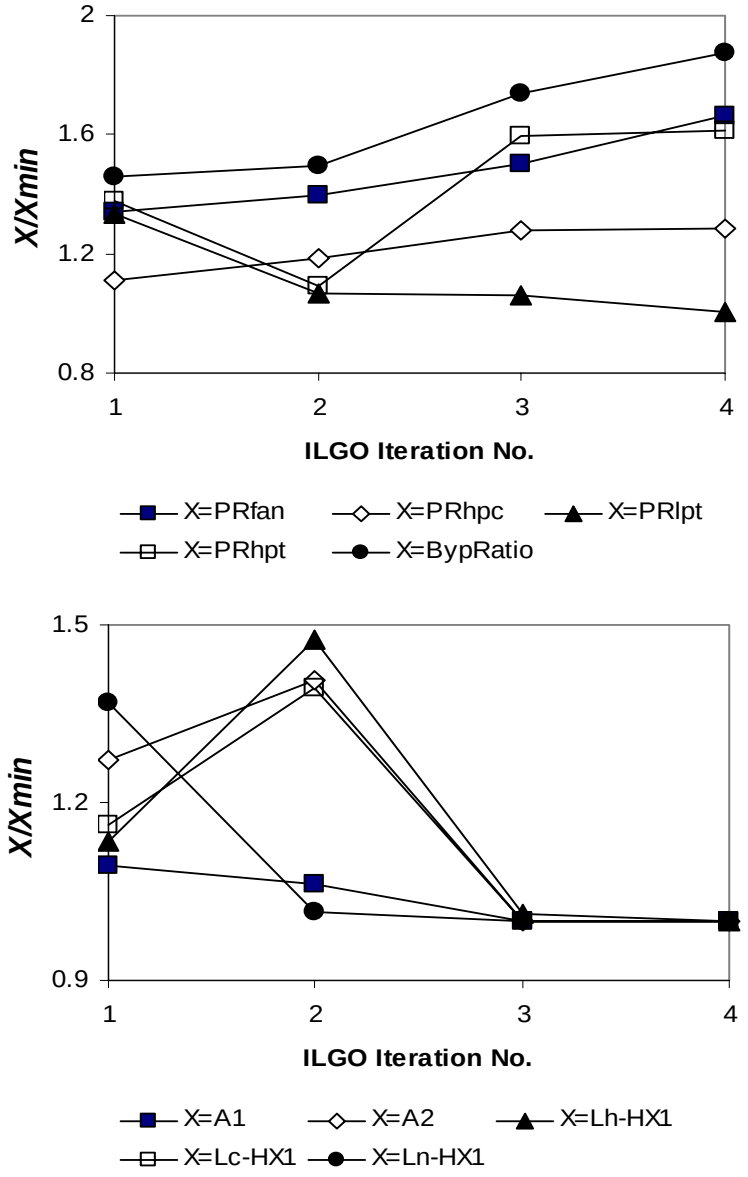

Figure 7.14. Change of select independent variables for the ECS and PS synthesis / design as the ILGO scheme progressed.

Table 7.10. ECS and PS optimum objective function values and weights.

ΔW_{TOECS}/g (kg)		852
$\Delta W_{FUELECS}$/g		551
$\Delta W_{FUELbleed}$/g		79
$\Delta W_{FUELdecs}$/g		52
$\Delta W_{FUELwecs}$/g		420
W_{ECS}/g[48]		272
	Prim HX	24
	Sec. HX	24
	Reg. HX	11
	ACM	12
	Ram Inlets	11
	Ram exits	9
	Ducting[49]	129
	Other[49]	17

W_{TO}/g (kg)		10364
W_{FUEL}/g		3308
W_{SS}/g		4526
W_{ENG}/g		1075
	fan	229
	hpc	121
	hpt	142
	lpt	243
	noz	52
	other	288

The marginal costs (the slopes of the curves) at the optimum for select mission legs are given in Figure 7.15. The linear behavior of the marginal costs for both design and off-design conditions is clearly evident. This behavior is observed even though no energy or exergy quantities were used. The fact that the marginal costs represented by the slope of the curves in Figure 7.14 are constant most likely helped the relatively fast overall convergence of the ILGO scheme used. In Muñoz and von Spakovsky (2000b), it was theorized that constant marginal costs would lead to the final solution in only one

[48] Includes 15% additional mass for packaging and installation. All of the component weights include accessories.

[49] Not participating in the optimization.

iteration. This was not the case in this application, primarily due to the initial mismatch between bleed conditions used in the ECS optimization and those obtained from running the PS optimization.

The marginal costs are indicative of the relative importance of the intermediate products going from the PS to the ECS and the feedback coming from the ECS back to the PS. A first order approximation using the allowable ranges for the ECS independent variables of Table 7.4 reveal that the variability of bleed air flow rate, ECS drag and weight are approximately 0.75 ± 0.2 kg/s, 350 ± 300 N and 700 ± 300 kg, respectively. With these values and the marginal costs of Figure 7.16 one can readily conclude that the effect of the ECS weight is significantly higher than that of bleed air flow rate and momentum drag. Thus, the optimum ECS solution is expected to have the smallest possible weight value. The fact that all of the marginal costs have positive values indicates that a solution with lower bleed and drag will be preferred for a given value of ECS weight.

Figure 7.17 shows the change in pressure and temperature bleed for all of the mission segments as a function of the system-level optimization iteration number. Quite clearly the bleed properties stabilized after a few runs and, thus, a final match was achieved.

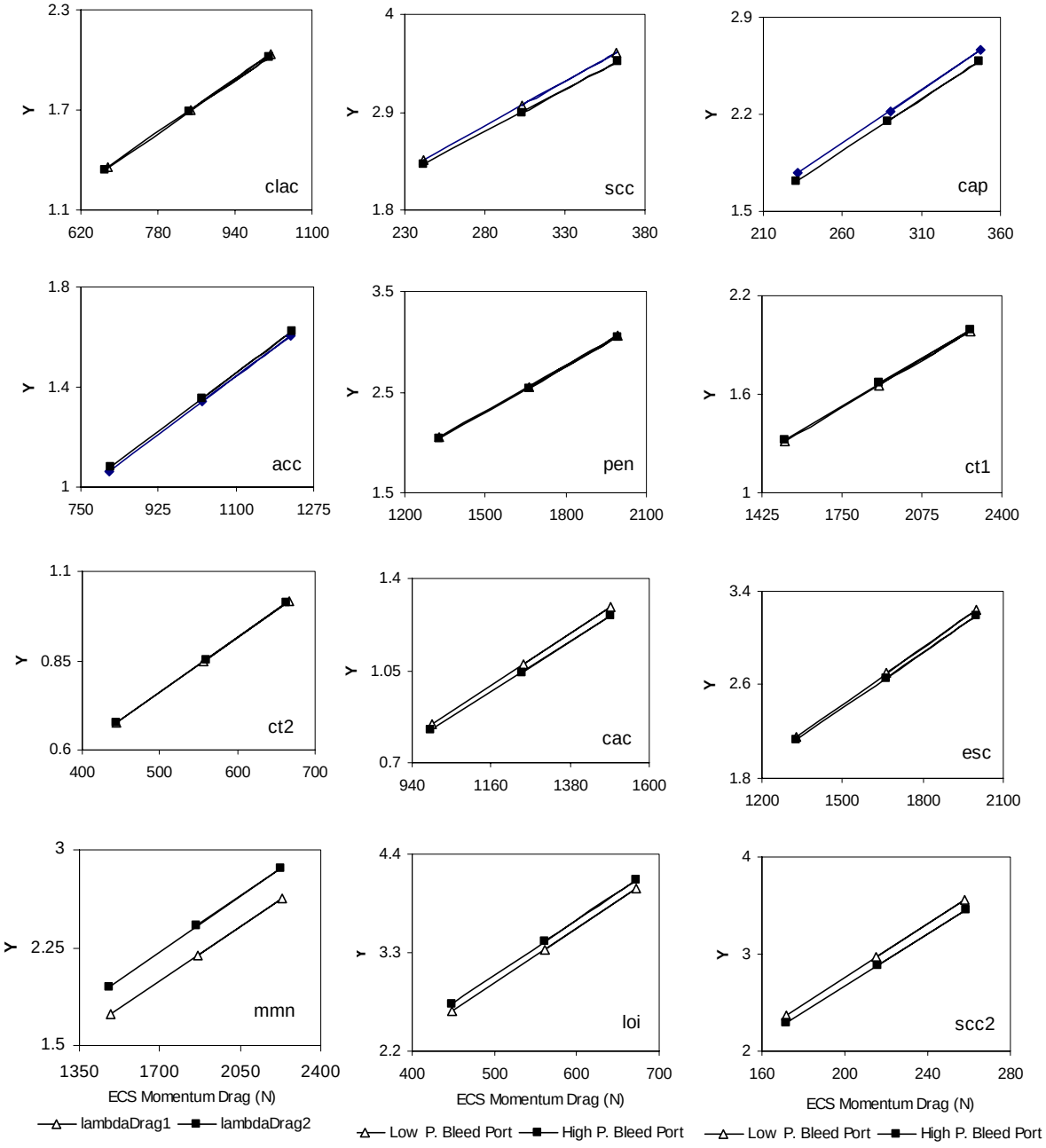

Figure 7.15a. Incremental fuel consumption *Y* due to ECS momentum drag at different mission legs. The slopes of the curves are the drag marginal cost based on fuel.

$$Y \equiv \frac{W_{FUEL}(bleed, D_{ESCS}) - W_{FUEL}(bleed, 0)}{W_{FUEL}(bleed, 0)} x100$$

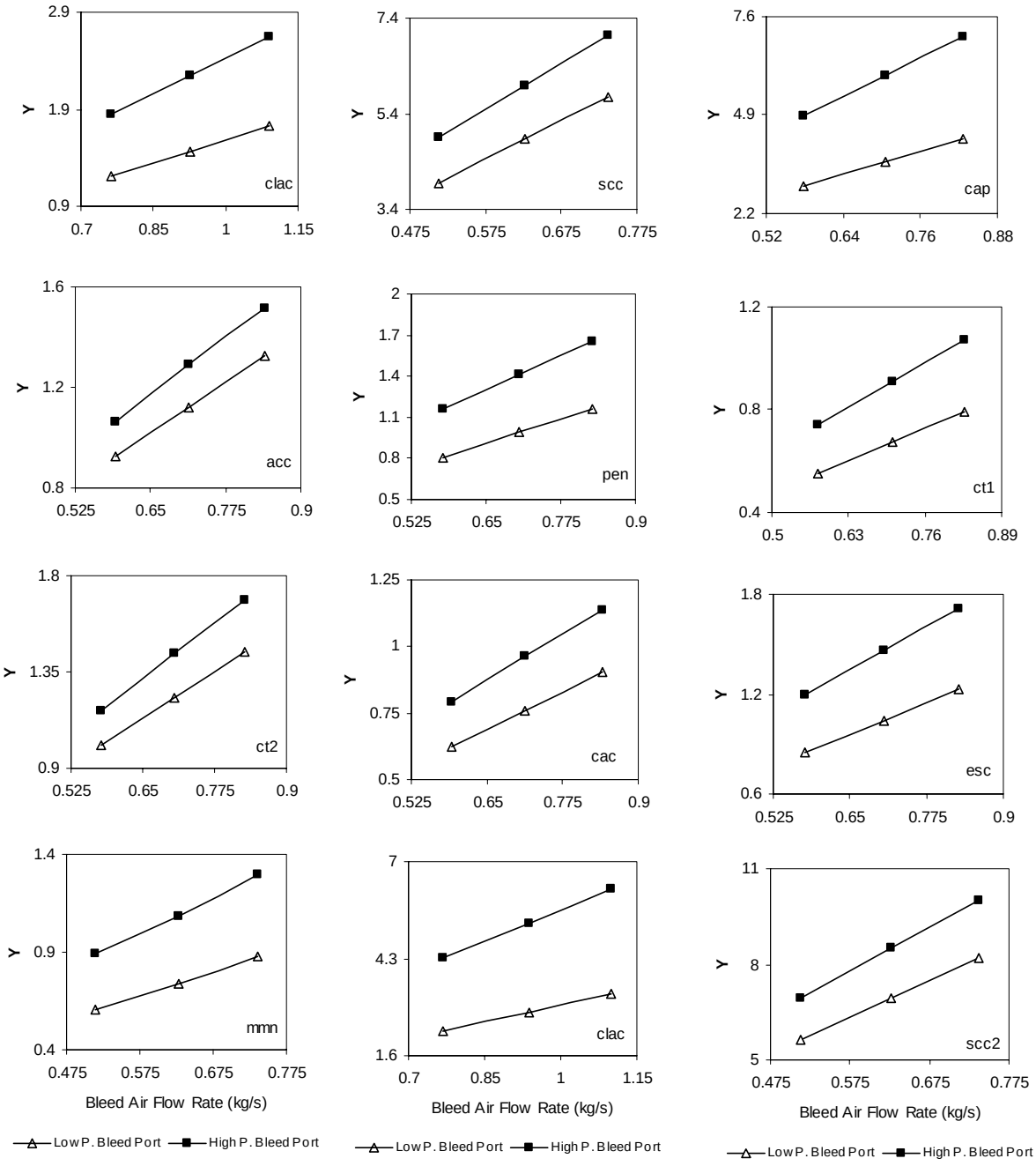

Figure 7.15b. Incremental fuel consumption *Y* due to ECS bleed air extraction at different mission legs. The slopes of the curves are the bleed air marginal cost based on fuel. $Y \equiv \frac{W_{FUEL}(bleed, D_{ECS}) - W_{FUEL}(0, D_{ECS})}{W_{FUEL}(0, D_{ECS})} x100$

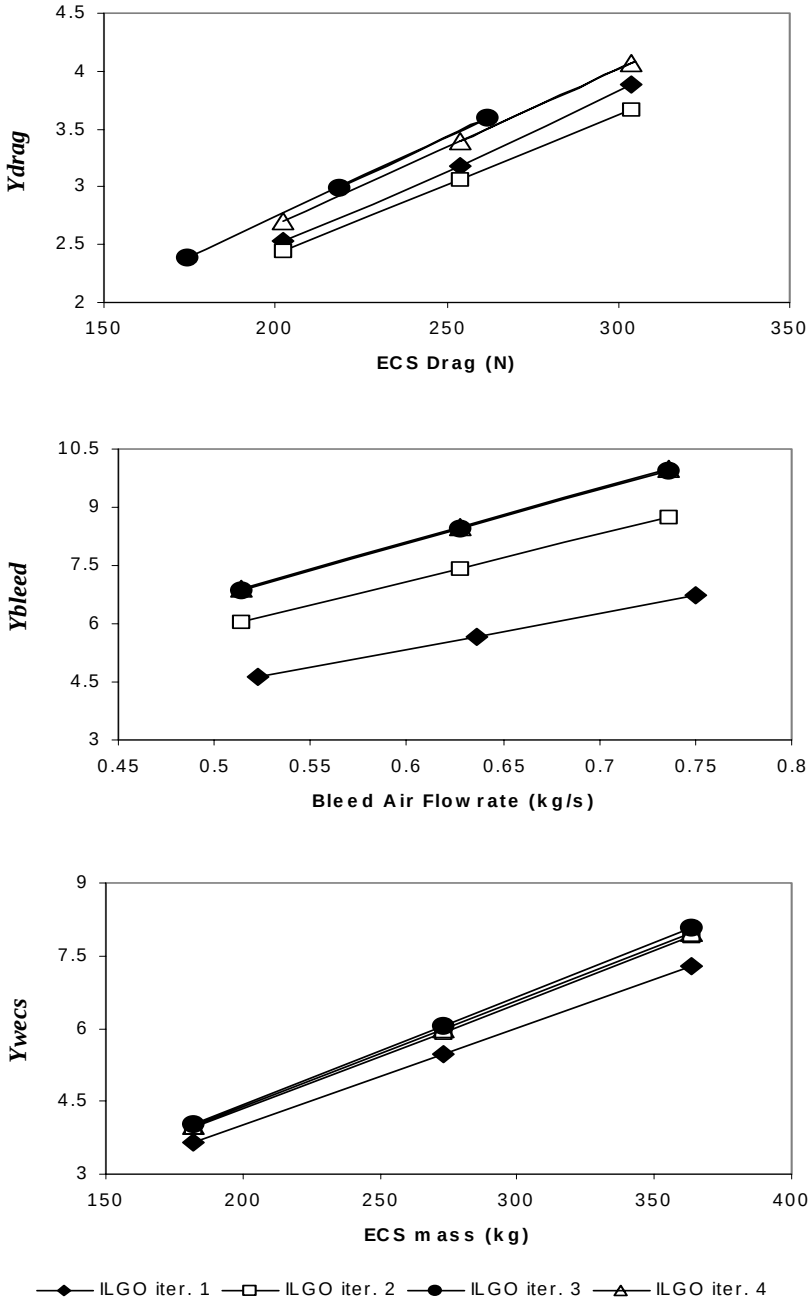

Figure 7.16. ECS drag, mass and bleed air marginal costs at the design point (scc_2) for different iterations of ILGO. The marginal costs are the slopes of the curves. The fact that the marginal costs are constant indicate that the ORS is a hyper-plane.

$$Y_{drag} \equiv \frac{W_{FUEL}(bleed, D_{ECS}, W_{ECS}) - W_{FUEL}(bleed, 0, W_{ECS})}{W_{FUEL}(bleed, 0, W_{ECS})} x100 \; ; \; Y_{bleed} \equiv \frac{W_{FUEL}(bleed, D_{ECS}, W_{ECS}) - W_{FUEL}(bleed, 0, W_{ECS})}{W_{FUEL}(bleed, 0, W_{ECS})} x100$$

$$Y_{wecs} \equiv \frac{W_{FUEL}(bleed, D_{ECS}, W_{ECS}) - W_{FUEL}(bleed, D_{ECS}, 0)}{W_{FUEL}(bleed, D_{ECS}, 0)} x100$$

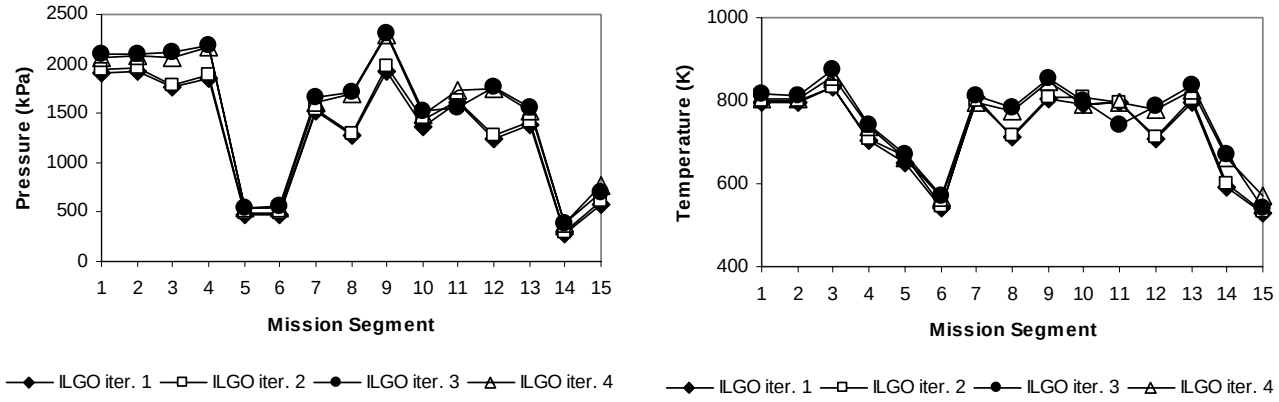

Figure 7.17. High pressure bleed port temperature and pressure for the mission legs given in Table 7.5 at each iteration of the system-level optimization.

The fact that the optimum solutions for the gross take-off weight, fuel consumption, and total cost minimization problems are identical (see Table 7.9 above) can be explained by the near linear relationship between W_{TO} and W_{FUEL} shown in Figure 7.18. Furthermore, the marginal costs show that weight is the most important of the intermediate products and feedbacks going to and coming from the ECS. Table 7.10 above indicates that the heat exchangers have the biggest contribution to weight among the components participating in the optimization. With these last two observations in mind, it comes as no surprise that the optimum solution found for the ECS corresponds to the synthesis / design with the lowest possible heat exchanger core dimensions. Additionally, since ram air has an incremental impact on fuel consumption (and hence on WTO) due to the extra thrust needed (via momentum drag) and mass required (that of the ram air inlet and exit), the minimum ram air inlet areas are also what would be expected.

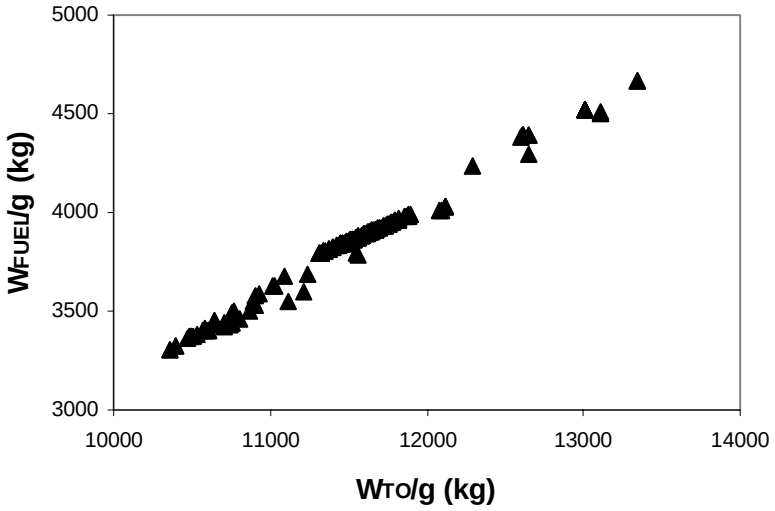

Figure 7.18 Fuel weight versus take-off gross weight corresponding to feasible solutions obtained at different iterations of the overall (system-level) optimization.

On the PS side, the optimizer found an optimum solution with the highest possible turbine inlet temperatures. Again, this is an expected result due to the fact that it is much more efficient to burn fuel in the combustor than in the afterburner.

As indicated above, the solution of the total cost minimization problem was also identical to the ones obtained for total take-off gross weight and fuel consumption as objective functions. The optimum costs for the different sub-systems are given in Table 7.11.

Table 7.11 Optimum cost results given in thousands of 1999 US dollars. The cost of fuel and the ECS are based on 8000 flight hours. A constant fuel price of $0.2/lbm was assumed.

Cost-Fuel	7778
Cost-ECS	541
Cost-PS	5642
Cost-SS	14140

The fact that the solution with minimum total cost is the same as the one with minimum weight comes as no surprise in the ECS problem since the cost functions of the major components are directly proportional to their mass. As to the PS, the cost correlations have the form

$$C_{PS\,i} = \left(a_{0\,i} + a_{1i}T_{SL} + a_{2i}M + a_{3i}T_{it}\right)_{\max} \tag{7.47}$$

where C_{PS_i} are the components of the capital cost (i.e. development and production costs) and $a_{0\,i}, a_{1_i}, a_{2\,i},$ and a_{3_i} are constants. Since the maximum Mach number and maximum turbine inlet temperature are fixed in this work and the maximum sea-level thrust is directly proportional to the take-off weight by virtue of equation (7.13) one can then conclude that the PS cost is in fact linearly dependent on W_{TO}. Figure 7.19 serves as a confirmation of this.

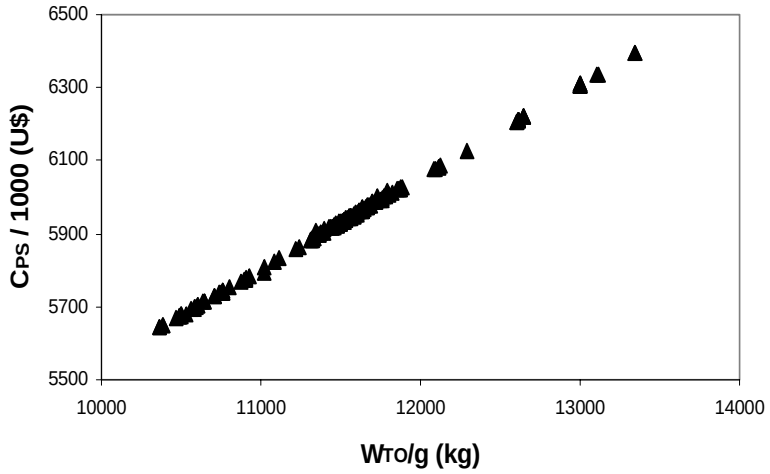

Figure 7.19. Propulsion sub-system capital cost vs. take-off gross weight.

The models for the capital cost components (i.e. engineering, tooling, manufacturing, etc.) that make up the total airframe have the following general form:

$$C_{SS_i} = a_{0_i} W_{EMP}^{a_{1i}} Sp_{\max}^{a_{2i}} N_{test}^{a_{3i}} \tag{7.48}$$

where $a_{0_i}, a_{1_i}, a_{2_i}$, and a_{3_i} are constants, W_{EMP} is the empty (structures plus ECS plus PS) weight, $Sp_{\max}$ is the maximum speed and N_{test} is the number of test aircraft. The last two factors are constant in this case and, thus, the cost of the structures is a function of the empty weight only. In turn, the relationship between empty weight and take-off gross weight is logarithmic (see Figure 7.6). The behavior of the structures cost with respect to WTO was plotted for the feasible solutions obtained from the last ILGO iteration for the complete (system-level) problem. The results are shown in Figure 7.20. This figure shows that, all factors included, the cost of the airframe is linear with respect to the take-off gross weight in the feasible range. When all of the costs are combined, the total system cost has the linear behavior plotted against WTO as shown in Figure 7.21, which explains the fact that the optimum solution is unaffected by the choice of either WTO or total system cost as the objective function.

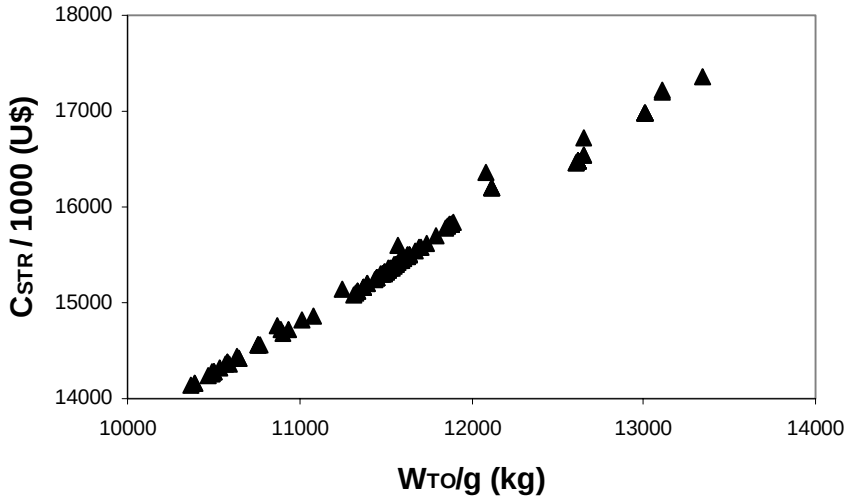

Figure 7.20. Airframe cost versus take-off gross weight.

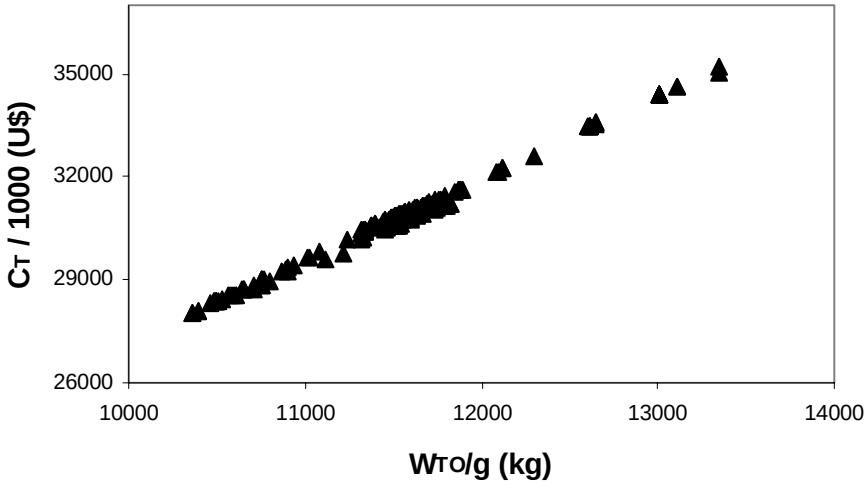

Figure 7.21 Aircraft System cost (excluding payload) vs. take-off gross weight

.

7.11 Comments/Discussion

7.11.1 The Global Optimality of the Solution

In order to study the global characteristics of the ILGO approach from a purely numerical standpoint [50], the solution results for ILGO were compared to those obtained without decomposition, i.e. when the optimization problem is treated as a whole. The objective function used was gross take-off weight. Obviously the number of independent variables had to be reduced to facilitate the solution of the system-level problem when taken in its entirety. Thus, the problem was solved with and without decomposition using the reduced variable set.

The PS design variables chosen were fan bypass ratio and fan and high pressure compressor pressure ratio. The low and high pressure turbine design pressure ratios were set at 2.0 and 2.2 respectively. The operational variables are given in Table 7.5 with one exception: the bleed port from which air for the ECS is taken at different mission segments were fixed at the values given in Table 7.9.

The number of ECS design and operational variables was also reduced. All of the integer variables were fixed by selecting the second regenerative heat exchanger in Figure 7.8 and choosing fins No. 5 and 7 for the cold and hot sides of the primary and secondary heat exchangers. The air cycle machine (ACM) compressor design pressure ratio was chosen to be 2.6. The core dimensions of the regenerative heat exchanger were fixed at 0.4, 0.2 and 0.4 m for the cold, hot and non-flow sides, respectively. The only ECS operational variables used were the valve pressure setting and bypass air flow rate. This selection of operational independent variables fixed the amount of bleed air taken from the main engine compressor (the amount of cooling air required in the cabin and avionics is a function of altitude and Mach number). The regenerative heat exchanger's cold air flow rates were set at 0.05 kg/s and no hot air was allowed .

Table 7.12. Comparison of decision variable results for the overall synthesis / design optimization problem with and without decomposition.

	Decomposition (ILGO)	**No Decomposition**
L_h (Prim HX)	0.500	0.500
L_c (Prim HX)	0.060	0.060
L_n (Prim HX)	0.500	0.500
L_h (Sec. HX)	0.500	0.501
L_c (Sec. HX)	0.060	0.060
L_n (Sec. HX)	0.500	0.500
A_1	120	121
A_2	120	120
PR_{tb}	5.08	5.21
α	0.398	0.393
PR_{fan}	4.50	4.45
PR_{hpc}	5.66	5.67

The number of iterations required for ILGO to obtain a solution for the reduced problem was again 4. The final results are given in Tables 12 to 14. Quite clearly, the solutions obtained from both methods are basically identical. The decomposed solution is well within 0.5 % of the solution obtained without decomposing the problem. It is important to note that the solution without decomposition took more than ten thousand iterations to converge. Thus, the optimization took six and a half days running on two PC workstations each with dual state of the art processors running in parallel. The time for the decomposed optimization was about two and a half days. Obviously, the decomposition approach required a lot more human intervention, which in fact mirrors the discipline-oriented nature of existing engineering practice and, thus, conceptually derives another advantage in terms of implementation for the ILGO approach over that with no-decomposition.

Table 7.13. ECS and PS optimum operational variables (case with no decomposition)

Leg	PR_{vv}	m_{byp}	T_{it}
tkr	1.643	0.060	1778
tka	1.736	0.039	1778
wup	1.715	0.008	1778
clac	2.572	0.030	1778
scc1	2.016	0.000	1341
cap	1.978	0.001	1056
acc	5.545	0.000	1778
pen	2.016	0.000	1528
ct1	2.426	0.000	1778
ct2	1.819	0.000	1778
cac	5.631	0.000	1778
esc	2.616	0.000	1517
mmn	3.270	0.000	1600
scc2	1.153	0.194	1354
loi	1.431	0.200	1005

Table 7.14. ECS and PS optimum total take-off gross weight objective function results.

	Decomposition (ILGO)	**No Decomposition**
W_{TO}	11526	11466
W_{FUEL}	3776	3734
W_{ENG}	1295	1299
W_{ECS}	314	314

The behavior of the marginal costs for this simplified problem were similar to those shown in Figures 7.15 and 7.16. The fact that the marginal costs are of the same sign (in fact are approximately constant) for all iterations is believed to be a major contributing factor to the global convergence of the ILGO approach as shown in previous chapters. These conditions are believed to be indicative of the convexity of the optimum value of the objective function with respect to the intermediate products and feedbacks, which in this case are bleed air and ECS drag and weight.

The very large number of iterations required to solve the problem without decomposition led to a set of about fifteen hundred feasible solutions of which half were distinct. This relatively large number of solutions and the fact that the bleed air flow rate is fixed allowed us to create a representation of the feasible synthesis / design space shown in Figure 7.22.

In order to verify some of the theoretical foundations for the ILGOmethod and the reasons for its global convergence, the Optimum Response Surface for the reduced problem was constructed using twenty uniformly distributed points across the synthesis / design space given in Figure 7.22. A cubic interpolation routine was used to obtain a smooth surface of the take-off gross weight versus ECS drag (at the synthesis / design point) and weight. The resulting surface plot is shown in Figure 7.23a. Figure 7.23.b shows the same plot as seen from above (in 2-D).

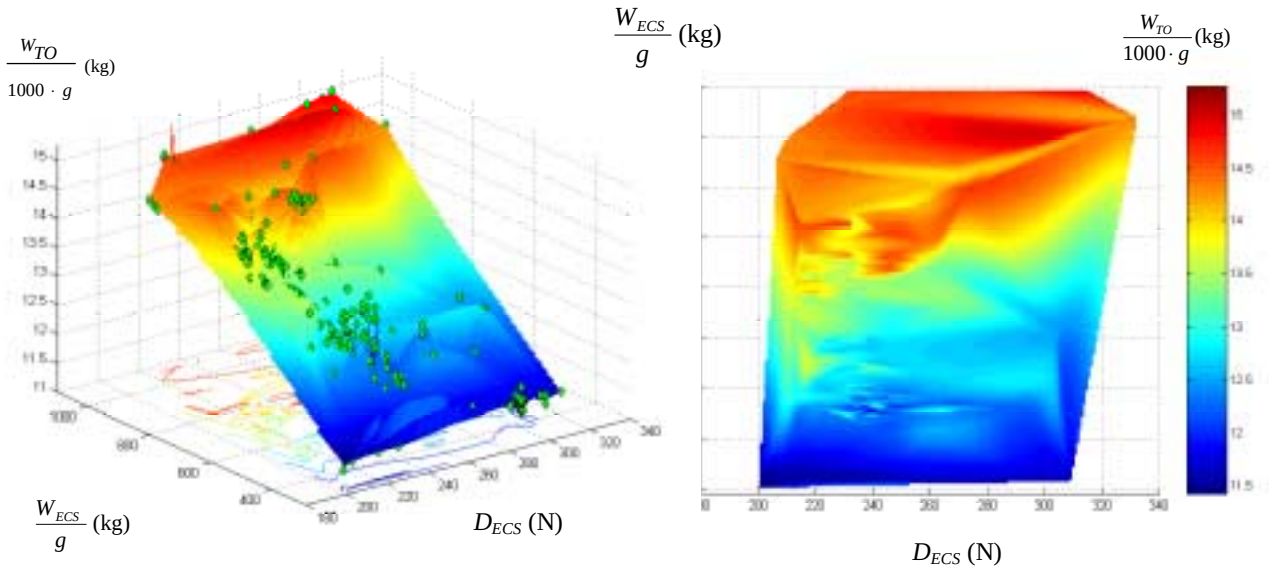

Figure 7.22. Restricted synthesis / design space for the take-off gross weight problem.

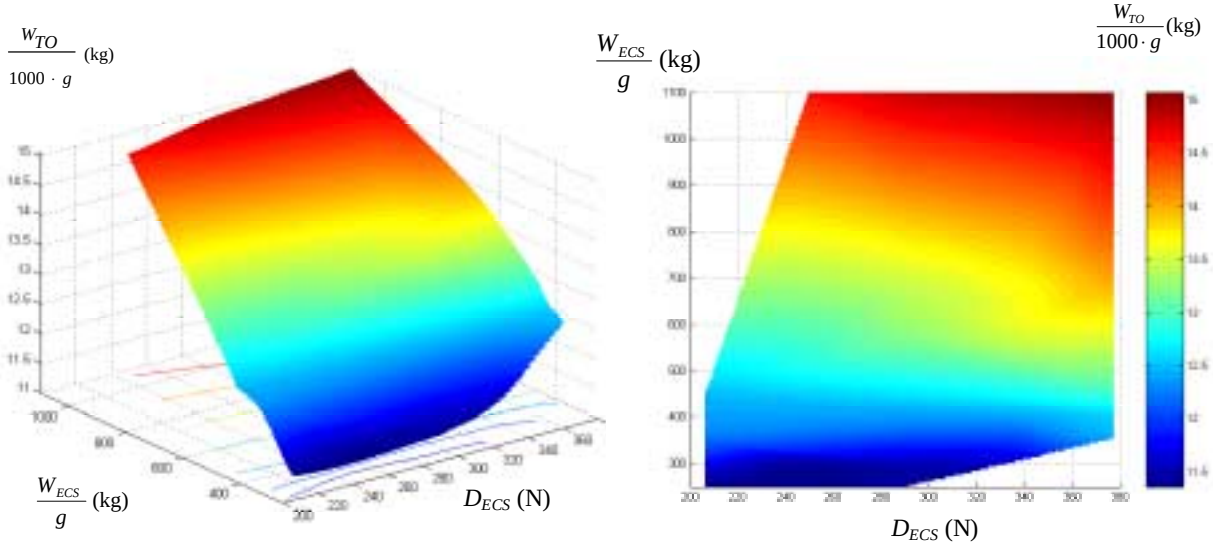

Figure 7.23. Optimum Response Surface for the take-off gross weight minimization problem.

Figure 7.23 has several interesting features. The first is that the synthesis / design space in ECS drag and weight is not only convex but shows an almost flat behavior, typical of a linear system. This is to be expected since the partial derivatives of the objective function (W_{TO}) with respect to the intermediate products and feedbacks (i.e. the marginal costs) are basically constant throughout the entire optimization process. The second important feature is that Figure 7.23 shows the great impact of the ECS weight on the objective function. The best solution is the one with the lowest possible weight. This, again, is to be expected given the large value of the weight marginal cost when compared to that of bleed and drag. This may explain the relatively minor effect of ECS drag, although there is clearly a tendency to have smaller W_{TO} values with low drag for a given weight. The effect of drag is not completely independent of weight, however, since ECS drag implies the need for a bigger and, therefore, heavier ram air scoop inlet. Furthermore, a larger ram air duct leads to increased ram air flow and possibly larger heat exchangers.

It is important to note that the linearity mentioned above was obtained by representing the intermediate products and feedbacks with properties that were non-exergy or even non-energy-based. The properties used resulted not only in linear behavior but also eased calculation of the marginal costs and in the future may provide the possibility of linking the sub-systems synthesized / designed to non-energy based sub-system syntheses / designs (e.g., the aircraft structure, etc.).

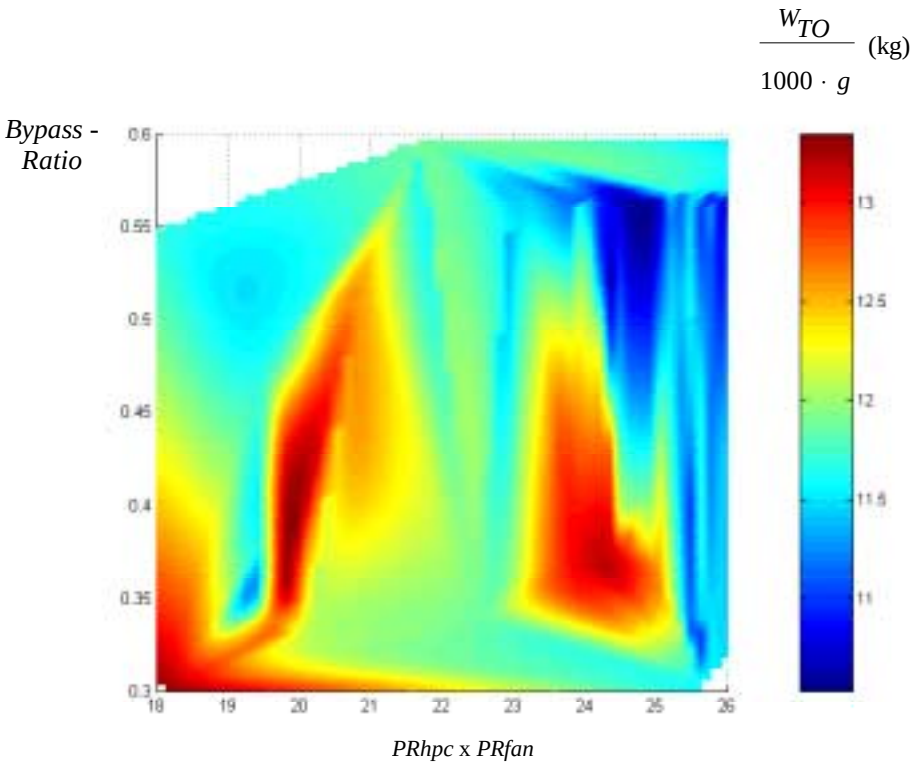

Figure 7.24. Take-off gross weight versus design bypass ratio and overall design pressure ratio.

Once more it should be stressed that the convergence of the algorithm depends on the convexity of the Optimum Response Surface independently of whether the actual synthesis / design space for each of the units, i.e. the behavior of the objective function with respect to the local decision variables, is convex or not. To better observe this, consider Figure 7.24, which shows the behavior of the take-off gross weight as a function of the overall compressor pressure ratio and bypass ratio for the optimum ECS weight, drag and bleed air. This figure was constructed with all of the feasible solutions found during the last iteration of ILGO for the complete problem. This figure, of course, is not a complete representation of the synthesis / design space because it does not contain all of the synthesis / design and operational variables. Obviously, a graphic representation in nine dimensions is impossible to create. However, Figure 7.24 hints at the possible non-convexity of the objective function with respect to the synthesis / design variables. The rapid convergence of the algorithm was not compromised by the apparent non-convexity of this synthesis / design space

The apparent non-convexity observed above underscores the importance of the choice of optimization algorithm(s) used to solve the problem. As indicate in earlier chapters, a genetic algorithm was used in this work followed by a gradient-based algorithm. Genetic algorithms are classified among the so-called global optimization methods because of their ability to escape local minima when properly conditioned (Olsommer el al., 1999a). To study the effect that the choice of optimization algorithm has on the solution, the complete problem was solved (for the optimum ECS feedbacks) using a gradient-based algorithm (Method of Feasible Directions) and three different starting points. The starting points have the minimum and maximum allowable, and the mean values of the design variables. The operational variables used were the optimum found previously in the complete solution. The optimization results are shown in Table 7.15.

Table 7.15. Optimum design variable values for different starting points. A gradient-based algorithm was used in all cases.

X_0=	X_{min}	X_{mean}	X_{max}
PR_{fan}	3.617	4.290	5.000
PR_{hpc}	4.760	6.080	5.232
PR_{hpt}	2.572	2.644	3.000
PR_{lpt}	2.596	2.630	3.000
α	0.455	0.529	0.600
W_{TO}/g	11505	11336	10916

From the results in the previous table, it becomes clear that a gradient-based algorithm alone may make finding the global optimum difficult. These results clearly show the tendency that gradient-based algorithms have of getting trapped in local minima. Additionally, the hypothesis that the synthesis / design space is non-convex is somewhat substantiated by this result.

7.11.2 The Marginal Costs as Indicators of the Importance of Off-Design Conditions

The type of time decomposition that is proposed and used in this work involves two steps. As indicated above, in the first step, a synthesis / design point is chosen to guarantee that the most demanding conditions are met. A preliminary synthesis / design optimization for that point yields a set of feasible solutions which can then be evaluated at all of the other operating conditions. Based on the instantaneous objective function value at the synthesis / design point, a ranking of feasible solutions can be created. In general, however, the best solutions at the synthesis / design point do not necessarily lead to the lowest overall objective function value when all of the operating conditions are taken into account.

The basis of the ILGO approach (A and B) is to find values of the coupling functions that lead to a decrease in the overall objective function - i.e. in a dynamic problem, a time-integrated value for the cost function. In the discretized version of the problem, which has been used throughout this work, the latter quantity is the sum of the individual impacts of the coupling function changes (in rate form) in terms of the objective function rate multiplied by the length of time during which that varitation takes place. Understanding these ILGO features is important for assessing which of the feasible solutions can be considered “promising” and, therefore, suitable for the time-integrated optimization with respect to the operational variables. Based on these comments, it becomes clear that various considerations as given below need to be taken into account in order to make such a selection:

- The time length of the design versus that of the off-design segments. Naturally, the shorter the operation under the most demanding conditions is, the least likely it is for the best solutions at the synthesis / design point to lead to an optimum synthesis / design when all time segments are taken into account.

- The instantaneous impact that changes in the coupling functions have in terms of the overall objective. This impact is in turn the product of two quantities: the marginal cost and the change in the coupling function (intermediate product or feedback). As mentioned above, once the optimization at the synthesis / design point has been carried out and a number of candidate solutions has been identified it is possible in most cases to have a good estimate of what the intermediate product / feedback (coupling function) changes are at all operating conditions. With this information and the marginal costs, it is then a straightforward matter to rank the feasible solutions based on their time-integrated behavior.

A graphical representation of the impact of the coupling functions such as that given in Figure 7.15 becomes very important for identifying promising solutions. Figure 7.15 shows the change in the overall objective function that can be achieved by varying the intermediate products at various instants of time. Once a potential synthesis / design has been identified (by solving the optimization problem at the synthesis / design point, for example), one could take the intermediate products / feedbacks (ECS weight and drag and bleed air in this case) and easily evaluate their individual contributions to, say, W_{TO}, in figure 7.15. In the case of the ECS-PS, once a synthesis / design is given, the weight and drag are known and the only remaining degree of freedom is the amount of bleed air, which is known with a maximum error of 10%. This information is sufficient to evaluate *all* of the potential solutions very inexpensively, if desired. This is not necessary, however, because of the information inherent in the marginal costs. To begin with, the marginal cost associated with ECS weight is much higher than that of drag and bleed. This true in all time segments. Thus, a candidate solution with high weight would be considered promising only if it has a low momentum drag. In turn, the greatest contributor to momentum drag is the inlet area. Based on this analysis, a synthesis / design with a comparatively large weight could potentially lead to the best possible solution only if it has low inlet area. The amount of bleed air remains within tight ranges and, therefore, need not be studied.

Table 7.16 shows the top five solutions of the synthesis / design segment (scc2). Table 7.17 shows how these solutions perform when the complete (i.e. integrated over the entire mission) is carried out. The ranking remains invariant due to the fact that the best solution at the synthesis / design point has both the lowest possible weight and inlet areas.

Table 7.16. Top five solutions based on the synthesis / design segment (scc_2).

	Solution Ranking				
	1	2	3	4	5
L_h (Prim HX)	0.500	0.511	0.504	0.503	0.500
L_c (Prim HX)	0.060	0.063	0.064	0.060	0.084
L_n (Prim HX)	0.500	0.508	0.500	0.502	0.500
L_h (Sec. HX)	0.500	0.500	0.525	0.501	0.500
L_c (Sec. HX)	0.060	0.066	0.062	0.060	0.077
L_n (Sec. HX)	0.508	0.500	0.523	0.503	0.500
L_c (Reg. HX)	0.300	0.300	0.300	0.302	0.302
L_c (Reg. HX)	0.150	0.151	0.154	0.181	0.165
L_n (Reg. HX)	0.300	0.300	0.309	0.309	0.310
A_1	120	135	133	135	135
A_2	120	165	170	172	165
PR_{cp}	2.8	2.8	2.7	2.8	2.8
PR_{tb}	11.6	7.9	6.5	6.4	7.3
Fin_{hot}	14	14	19	19	14
Fin_{cold}	14	16	16	17	16
W_{ECS}/g	272	284	296	300	301

Table 7.17. ECS optimum results.

Design point Rank	Mission Rank	ΔW_{TOECS}/g (kg)	$\Delta W_{FUELECS}$/g (kg)	$\Delta W_{FUELbleed}$/g (kg)	$\Delta W_{FUELdecs}$/g (kg)	$\Delta W_{FUELwecs}$/g (kg)	W_{ECS}/g (kg)
1	1	852	551	79	51	420	592
2	2	906	587	81	64	444	625
3	3	938	606	79	64	462	651
4	4	950	613	82	65	468	660
5	5	951	613	80	64	470	662

7.11.3 The Relationship Between Aerospace and Energy Optimization Methods: Conditions for Total Aircraft System Synthesis / Design

The similarities between the methods presented here and some of the methods used by the aerospace multi-disciplinary optimization community are evident. For example, the use of piece-wise linear approximations of system behavior in the vicinity of a design point are commonalties of ILGO and some of the leading MDO methods (e.g., CCSO (Sobieszczanski-Sobieski, 1989)). The marginal costs for the coupling functions and the independent variables are mathematical representations of the interdependence of the different units or technologies that comprise a system. They also serve as indicators of the relative importance of the decision variables and of the effects that changes in values of the coupling functions may have in terms of the overall objective function. Therefore, the marginal costs commonly used in stationary system synthesis / design optimization are seen to be mathematically and conceptually similar to the partial derivatives associated with Global Sensitivity Theory (Sobieszczanski-Sobieski, 1990) and the MDO methods that make use of them.

The similarities between approaches mentioned above may open the door for possible combined efforts in which the entire system may be synthesized / designed concurrently. The success of such a large multi-disciplinary effort depends a great deal

on the ability of the different specialty groups to closely interact and interdepend upon each other. The necessary common mathematical framework and understanding that is necessary to achieve this goal exists.

As indicated above, the relationship between the structure sub-system (SS) and the energy-based sub-systems (in this case the PS and ECS) is given explicitly by the thrust equation (equation (7.11)). This correlation also brings the external requirements (the mission) into the picture. In this work, the role of the SS is not exactly passive as its weight is affected by the decisions made in the rest of the system. This impact is made via the historical data of Figure 7.6. Although the SS is not being synthesized / designed and, thus, has no parameter values which are optimized, it is assumed that it reflects existing design trends. These trends, however, do not necessarily imply the SS is optimized for the given WTO weight. Of course, it would not be expected that the SS would be optimized for the particular PS and ECS that were synthesized / designed here. This larger optimization problem could be defined for the case of take-off gross weight as follows:

$$\text{Minimize} \qquad W_{TO} = W_{SS} + W_{PS} + W_{ECS} + W_{FUEL} + W_{PPAY} + W_{EPAY} \tag{7.49}$$

w.r.t. $\left\{\vec{X}_{PS}, \vec{X}_{PS}, \vec{X}_{SS}\right\}, \quad \left\{\vec{Y}_{ECS}, \vec{Y}_{PS}, \vec{Y}_{SS}\right\}$

subject to

$$\vec{H}_{PS} = \vec{0}, \quad \vec{G}_{PS} \le \vec{0} \tag{7.49.1}$$

$$\vec{H}_{ECS} = \vec{0}, \quad \vec{G}_{ECS} \le \vec{0} \tag{7.49.2}$$

$$\text{and } \vec{H}_{SS} = \vec{0}, \quad \vec{G}_{SS} \le \vec{0} \tag{7.49.2}$$

where the analysis system of equations (equation 7.49.2) for the structure sub-system is composed of a number of disciplines, most notably aerodynamics, structural analysis and controls. Other objective functions could also be used to formulate the system-level problem.

The above problem could be tackled with the tools developed here. It is, therefore, conceivable to have different groups of specialists tackling different aspects of the problem. An iterative procedure would be required in which a feasible solution is found, perhaps based on previous experience. The problem would then be set up so as to improve upon this solution. From the viewpoint of energy system synthesis / design, it is clear that a structures weight value and its derivatives with respect to the functions that couple them to the energy-based sub-systems would be enough information to make synthesis / design changes in the PS and ECS in order to benefit the entire system. The coupling functions are shown in Figure 7.9. The tradeoff between light bodies with high drag and those with high drag but large weight will not only be translated into decisions made by the aerostructures / control specialists but also by the PS and ECS groups. The latter effects would be measured by the competing impact that lift, drag and structures weight have in terms of the thrust equation. This equation, as seen above, is the basis for all the energy-based sub-system synthesis / design.

Chapter 8

Conclusions

The methods presented in this work constitute a natural way for carrying out the decomposed synthesis / design optimization of highly coupled, highly complex energy systems. These methods were developed with the fundamental goal of *enhancing* current engineering design practices and processes, not of *replacing* them. In addition, they were developed to support the use of existing codes that use common engineering concepts. The result is that relatively unfamiliar concepts are not required to formulate any of the parts of the problem with consequent ease of implementation and minimal expense (i.e. no new simulation, sizing or cost models or codes are needed if they already exist). In addition to the above, all of the methods presented here do not pose any additional cultural and logistical obstacles that may result from the integration of different technologies, codes, or disciplines possibly coming from dissimilar sources. On the contrary, the decomposed optimization schemes are designed to *thrive* in such environments by encouraging autonomous technology or disciplinary syntheses / designs and limiting the information flow between units to a local contribution to the objective function and its marginal costs with respect to the coupling functions. Therefore, any one group does not need to have access to the other groups' tools or technologies making the method suitable for large projects in which proprietary or intellectual authority issues are important. Furthermore, the models are not sensitive to how any given unit is optimized. That decision is completely autonomous to the particular group in charge of that unit's design. The methods are robust enough so that

starting with any solution they are guaranteed to provide at the very least an equally good or slightly better solution. The more iterations that are allowed, the greater the potential improvements are.

In particular, the Local-Global Optimization method in any of its forms (Real-time or Off-line) with its associated Optimum Response Surface (ORS) constitutes a powerful way of not only obtaining a global optimum solution but of gaining an enormous amount of insight as to the relative effect that each unit has in terms of the overall objective. Part of the analysis and results obtained from an application of LGO given by Muñoz and von Spakovsky (1999, 2000a) was used here to show the inner workings of the method.

The potentially large investment required for LGO is addressed by the iterative version of the method (ILGO). ILGO uses a close approximation of the ORS to reduce the number of unit optimizations required. The effect of the different units' independent variables is assessed in terms of the unit's (local) cost *and* their effect on the rest of the system. Thus, in ILGO, unit-based system-level optimization sub-problems (as opposed to purely local objective functions) are defined. Each of these sub-problems while using strictly local (unit) independent variables approximates the system-level optimum cost. The approximation of the ORS leads to the definition of marginal costs based on optimum costs and the functions coupling the units.

Incidentally, the methods presented shed some light on the on-going controversy as to the importance and usefulness of Second-Law based methods *for the synthesis / design optimization* (as opposed to analysis) of energy systems. There is no doubt that Second-law methods as *analysis* tools are superior to First Law approaches. However, when it comes to *optimization*, this is not necessarily true. Once the optimization problem is defined, there is only one global optimum and whether or not the problem is represented in Second or First Law terms has no effect on this optimum. Thus, the question becomes: is a Second Law *decomposition* approach superior to a First Law approach in arriving at the optimum? Again, the answer is: not necessarily. Whether or not one defines the problem in terms of the Second or First law should depend on what

effect the "properties of choice" for representing intermediate products and feedbacks has on the mathematical behavior of the ORS. Thus, properties that lead to monotonic and, in the ideal case, linear behavior of the optimum cost in the intermediate products / feedbacks domain are preferred, whether they are exergy-based or not. As was seen above and in Muñoz and von Spakovsky (2000b) where the ILGO approach was applied to a large-scale optimization problem, the desirable "properties of choice" were *not* Second Law based.

In addition to being a more intelligent way than LGO of applying decomposition, ILGO was also specifically developed keeping in mind a number of practical considerations, i.e. to mimic and enhance current engineering practice such that

- The analysis and optimization of each unit (sub-system) is modular and divided into clearly separated tasks. In industry these tasks are performed by specialized groups.
- The unit optimizations may be carried out concurrently.
- Human intervention is supported.
- Advanced, high-fidelity tools for the sub-systems and load simulations can be used.
- Sub-system optimizations are kept at the minimum possible.
- In each iteration of ILGO, improvements in the objective functions are achieved. In the event of a halt in the synthesis / design process due to extraneous reasons, an improved synthesis / design over that of the starting or reference synthesis / design will already have been achieved.

In support of the above practical features, a number of theoretical issues were also addressed. First, the MINLP for the entire system was solved and the global convergence of the method was verified. Additionally, fast convergence was achieved. Both of these results are due to the high linearity of the ORS. The latter finding was initially hypothesized based on the observed constant behavior of the marginal costs and later graphically verified.

Finally, it is important to note that the linearity mentioned above was obtained by representing the intermediate products and feedbacks with properties that were non-exergy or even non-energy-based. The properties used resulted not only in linear behavior but eased as well the calculation of marginal costs which in the future may provide the possibility of linking the sub-systems synthesized / designed to non-energy based sub-system syntheses / designs (e.g., the aircraft structure, etc.). A discussion on the latter was provided.

Chapter 9

Recommendations for Future Work

There are a number of additional issues that may be considered the natural "next steps" to this work. Some of these issues are listed below

- It is believed that among the methods developed here, ILGO is the most suitable for large synthesis / design problems. The complex application used here to demonstrate ILGO involves two large units. It would be desirable to employ the method for systems with three or more sub-systems. An ideal problem is the integrated synthesis / design of the Thermal Management Sub-system (TMS) along with the PS and ECS for advanced military aircraft. It is recommended that existing simulation tools such as Lockheed Martin's ITMS software be used.
- Inevitably, when dealing with problems such as the one mentioned above, the issue of dependence among time steps will start playing an important role. The use of transient modeling for such problems will certainly pose an additional challenge to any of the methods presented here. It is believed, however, that the formulation given here is sufficiently general and robust to tackle such problems. Examination of any of the formulas in chapter 7 reveals that in all cases the coupling functions, analysis system of equations, and constraints are time-dependent. Thus, no new methods are needed. In fact, in the application of ILGO to transient problems, the only major addition is the use of transient models instead of steady state ones for the units.

- The ever increasing complexity of systems and simulators and the need to account for transient behavior create a serious computational burden for simulation and consequently for optimization. To alleviate this problem, two possible solutions are suggested. The first is the use of models of different complexity for the modeling of the different units. The second is the use of approximations that could replace the actual modeling at certain stages of the optimization. Consider, for example, the case of the PS simulator employed here. The extreme expense resulting from the use of this tool combined with a global search type of optimization algorithm, e.g., a GA, could be alleviated a great deal by any or both of the schemes proposed. In the first case, a simple model that contains most of the thermodynamic features of the problem along with simplified sizing functions (such as the ones implied by Figure 7.6) could potentially aid in the search of the synthesis / design space. Once a few "promising areas" are found one could switch to an inexpensive gradient-based algorithm that uses the actual PS model. The second suggestion is to use actual simulation results to generate a model of the system. This model is known as the response surface of the system. This technique replaces the objective and/or the constraints with relatively simple functions, which are typically polynomials. Neural networks trained for the same purpose are also an alternative.

- Ideally other synthesis / design considerations such the trade-off between performance and manufacturing cost could be incorporated into the problem formulation. Such an undertaking would nicely complement other ongoing research efforts at Virginia Tech. In addition, more advanced simulation tools that interface operational variables with Life Cycle Cost would be highly desirable.

- Finally, the solution of a large-scale test problem that incorporates various research groups with relatively dissimilar techniques will greatly increase the awareness of the methods used by all of the communities involved. The conceptual synthesis / design of an aircraft system including the major sub-systems is believed to be an ideal candidate.

References

Ahrendts, 1980, Reference States, *Energy-The International Journal*, Vol. 5, pp. 667-677.

Anderson, J.D. Jr., 1999, Aircraft Performance and Design, WCB/McGraw-Hill

Baljé, O.E., 1962, A Study on Design Criteria and Matching of Turbo-machines, Parts A and B, *Journal of Engineering for Power*, pp 83-114.

Balling R.J.and Sobieszczanski-Sobieski, J, 1996, Optimization of Coupled Systems: A Critical Overview of Approaches, *AIAA Journal*, Vol. 34, No. 1, January

Bejan, A., 1995, Entropy Generation Minimization, CRC Press, Boca Raton, Florida.

Bejan, A., R., A Role for Exergy Analysis and Optimization in Aircraft Energy-System Design, AIAA Paper No. 2000-4855, *8th AIAA/USAF/NASA/ISSMO Symposium on Multidisciplinary Analysis and Optimization*, Long Beach, California, September 6-8, 2000.

Bejan, A., Tsatsaronis, G., et al., 1996, Thermal Design and Optimization, John Wiley and Sons, New York.

Birkler, J. L., Garfinkle, J. B., and Marks, K. E., Development and Production Cost Estimating Relationships for Aircraft Turbine Engines, Rand, N-1882-AF, Oct. 1982.

Boland, D. and Linnhoff, B., 1979, The Preliminary Design of Networks for Heat Exchange by Systematic Methods, *Chemical Engineer*, pp 222-228.

Brown, D.A., Integrated Energy Management System for Uninhabited Combat Air Vehicles (UCAVs), *IECEC 1999*, Paper No.249. Vancouver, 1999.

Bruno, J.C., F. Fernandez, F. Castells and I.E. Grossmann, MINLP Model for Optimal Synthesis and Operation of Utility Plants, *Transaction of the Institution of Chemical Engineers*, 76, pp.246-258 (1998).

Chong, E.K.P., and Zak, S.H., 1996, An Introduction to Optimization, Wiley-Interscience, New York, New York.

Curti, V., von Spakovsky, M.R., Favrat, D., 2000, An Environomic Approach for the Modeling and Optimization of a District Heating Network Based on Centralized and Decentralized Heat Pumps, Cogeneration and/or Gas Furnace (Part I: Methodology), *International Journal of Thermal Sciences*, vol. 39, no. 6, June, Elsevier, France.

Curti, V., von Spakovsky, M.R., Favrat, D., 2000, An Environomic Approach for the Modeling and Optimization of a District Heating Network Based on Centralized and Decentralized Heat Pumps, Cogeneration and/or Gas Furnace (Part II: Application), *International Journal of Thermal Sciences*, vol. 39, no. 6, June, Elsevier, France.

Dieckmann, R.R, Watson, A.C. and Glover, S.F., 1972, Development of Integrated Environmental Control Systems for Aircraft, Report No. AFFDL-TR-72-9, Air Force Flight Dynamics Laboratory, WPAFB, OH.

El-Sayed Y., 1989, A Decomposition Strategy for Thermoeconomic Optimization, *ASME Journal of Energy Resources Technology*, vol. 111, pp 1-15

El-Sayed Y., 1996, A Second-Law-Based Optimization: Part I Methodology & Part 2, *ASME Application, Journal of Energy Resources Technology*, Vol. 118, pp. 693-703.

El-Sayed, Y.M. and Evans, R.B., 1970, Thermoeconomics and the Design of Heat Systems, *Journal of Engineering for Power*, ASME Transactions, Vol. 92, 27, Jan.

El-Sayed, Y.M., 1996, A Second-Law-Based Optimization: Parts 1 and 2, *Journal of Engineering for Gas Turbines and Power*, ASME Transactions, vol. 118, October, N.Y.

Evans, R.B. and Tribus, M., 1962, A Contribution to the Theory of Thermoeconomics, UCLA Dept. of Engineering: Report No. 62-63, Los Angeles, CA, August.

Evans, R.B. and von Spakovsky, M.R., 1993, Engineering Functional Analysis (Parts II), *Journal of Energy Resources Technology*, ASME transactions, Vol. 115, No. 2, N.Y., N.Y., June.

Evans, R.B. and von Spakovsky, M.R., 1993, Engineering Functional Analysis (Parts II), *Journal of Energy Resources Technology*, ASME transactions, Vol. 115, No. 2, N.Y., N.Y., June.

Evans, R.B., 1980, Thermoeconomic Isolation and Essergy Analysis, *Energy: The International Journal*, Vol. 5, Nos. 8-9, 805-821.

Evans, R.B., and von Spakovsky, M.R., 1993, Engineering Functional Analysis (Part II), *Journal of Energy Resources Technology*, ASME Transactions, Vol. 115, No. 2, N.Y., June.

Floudas, A., 1995, Nonlinear and Mixed-Integer Optimization, Oxford University Press, New York.

Frangopoulos, C. A., 1994, Application of the Thermoeconomic Functional Approach to the CGAM Problem, *Energy-The International Journal*, Vol. 19, No. 3, pp. 323-342.

Frangopoulos, C.A., 1983, Thermoeconomic Functional Analysis: A Method for Optimal Dsign or Improvement of Complex Thermal Systems, School of Mechanical Engineering, Georgia Institute of Technology, Ph.D. Dissertation.

Frangopoulos, C.A., 1984, Thermoeconomic Functional Analysis: An Innovative Approach to Optimal Design of Thermal Systems, Second Law Aspects of Thermal Design. HTD Vol. 33, ASME, N.Y., N.Y., August.

Frangopoulos, C.A., 1989, Optimal Synthesis and Operation of Thermal Systems by the Thermoeconomic Functional Approach, *ASME Winter Annual Meeting*, AES 10-3, 49.

Frangopoulos, C.A., 1994, Application of Thermoeconomic Optimization Methods to the CGAM Problem, *Energy: The International Journal*, special edition, Vol. 19, No. 3, pp. 323-342, Pergamon Press, Great Britain.

Frangopoulos, C.A., and von Spakovsky, M.R., 1993, The Environomic Analysis and Optimization of Energy Systems (Part I*), Proceedings of the International Conference on Energy Systems and Ecology: ENSEC'93,* Vol. I, pp. 123-132, ASME, Cracow, Poland, July.

Frangopoulos, C.A., Evans R.B., 1984, Thermoeconomic Isolation and Optimization of Thermal System Components, Second Law Aspects of Thermal Design. HTD Vol. 33, ASME, N.Y., N.Y., August.

Fratzcher, W. and Gruhn, G., 1965, The Meaning and Definition of A Environment State for Exergetic Investigations (in German), Brennstoff-Warme-Kraft, Vol. 17, No. 7, pp. 337-341.

Gaggioli R. and El-Sayed Y., 1989, A Critical Review of Second Law Costing Methods, *Journal of Energy Resources Technology*, ASME Transactions, vol. 111, pp 1-15.

Gaggioli, R., Sama, D.A., Qian, S., and El-Sayed, Y. M., 1991, Integration of a New Process into an Existing Site: A Case Study in the Application of Exergy Analysis, *Journal for Engineering for Gas Turbines and Power*, ASME Transactions, vol. 113, no. 2.

Goldberg, D. E., 1989, Genetic Algorithms in Search, Optimization and Machine Learning, Addison Wesley, Reading, MA.

Hajek B., 1988, Cooling Schedules for Simulated Annealing, *Mathematics of Operations Research*, Vol. 13, No. 4, pp. 563-571.

Hajela P., 1999, Nongradient Methods in Multidisciplinary Design Optimization-Status and Potential, *Journal of Aircraft*, Vol. 36, No.1, Jan-Feb.

iSIGHT version 5 User's Guide, 1999, Engineous Software Inc., Morrisville, N.C.

Jane's All the World's Aircraft 1999-2000, 1999, Jane's Information Group, Couldson, UK

Kays, W.M. and London, A.L., 1998, Compact Heat Exchangers, Krieger Publishing Company, Malabar, FL.

Kestin, J., 1980, Availability: The Concept and Associated Terminology, *Energy-The International Journal*, Vol. 5, pp. 679-692.

Kirkpatrick S., Gelatt, C.D., and Vecchi, M.P., 1983, Optimization by Simulated Annealing, *Science*, Vol. 220, pp. 671-680.

Lazzaretto, A. and Andreatta, R., 1995, Algebraic Formulation of a Process-Based Exergo-economic Method, *Thermodynamics and the Design, Analysis and Improvement of Energy Systems*, AES-Vol. 35.

Le Claire, R., 1975, Evaluation of the Overall Fuel Mass Penalty of an Aircraft System, *Aeronautical Journal*, May, pp 225-228.

Letton, Jr, G., 1976, Avionics Cooling on USAF Aircraft, *AGARD Conference Proceedings on Avionic Cooling and Power Supplies for Advanced Aircraft*, The Hague, Netherlands, June.

Linhoff, B., 1989, Pinch Technology for the Synthesis of Optimal Heat and Power Systems, *Journal of Energy Resources Technology*, ASME Transactions. Vol. 111, pp. 137-147.

Linhoff, B. and Alanis, F.J., 1991, Integration of a New Process Into an Existing Site: A Case Study in the Application of Pinch Technology, *Journal of Engineering for Gas Turbines and Power*, ASME Transactions, Vol. 113, pp. 159-169.

Linnhoff, B., 1993, Pinch Technology for the Synthesis of Optimal Heat and Power Systems, *Journal of Energy Resources Technology*, ASME Transactions, vol. 111.

Lykins, R et al., 1998, Preliminary Thermodynamic Analysis of Power System Impact on Tactical Aircraft Performance, *Proceedings of the Aerospace Power Systems Conference*, SAE 981288.

Manglik, R.M. and Bergles, A.E., 1990, The Thermal-Hydraulic Design of the Rectangular Offset-Strip-Fin Compact Heat Exchanger in Compact Heat Exchangers, R.K. Shah, A.D. Kraus, and D. Metzger editors, Hemipshere Publishing Corporation, pp 123-149.

Mattingly, J.D., Heiser,W.H. and Daley, D.H., 1987, Aircraft Engine Design, AIAA Education Series, New York, New York.

Moran, M. J., 1982, Availability Analysis. A Guide to Efficient Energy Use, Prentice Hall, Englewood Cliffs, N.J.

Muñoz J. R., von Spakovsky M.R., 1999, A Second Law Based Integrated Thermoeconomic Modeling and Optimization Strategy for Aircraft / Aerospace Energy System Synthesis and Design (Phase I - Final Report), final report, Air Force Office of Scientific Research, New Vista Program, December.

Muñoz, J.R. and Michaelides, E.E., 1999, The Effect of the Model of the Environment on Exergy Analyses, *Journal of Energy Resources Technology*, ASME Transactions. Vol. 121. No. 4, pp. 268-276

Muñoz, J.R. and von Spakovsky, M.R., 2000a, An Integrated Thermoeconomic Modeling and Optimization Strategy for Aircraft / Aerospace Energy System Design, *Efficiency, Costs, Optimization, Simulation and Environmental Aspects of Energy Systems* (ECOS'00), Twente University, ASME, Netherlands, July 5-7.

Muñoz, J.R. and von Spakovsky, M.R., 2000b, The Use of Decomposition for the Large Scale Synthesis/ Design Optimization of Highly Coupled, Highly Dynamic Energy Systems: Part I - Theory, *2000 ASME International Mechanical Engineering Congress and Exposition*, Orlando, FL, Nov 5-10.

Muñoz, J.R. and von Spakovsky, M.R., 2000c, The Use of Decomposition for the Large Scale Synthesis/ Design Optimization of Highly Coupled, Highly Dynamic Energy Systems: Part II - Applications, *2000 ASME International Mechanical Engineering Congress and Exposition*, Orlando, FL, Nov 5-10.

Newberry, C.F., Exergy - The Aircraft Design Variable of Choice?, AIAA Paper No. 2000-4851, *8th AIAA/USAF/NASA/ISSMO Symposium on Multidisciplinary Analysis and Optimization*, Long Beach, California, September 6-8, 2000.

Nicolai, L., 1975, Fundamentals of Aircraft Design, published by the author.

Olsommer, B., von Spakovsky, M.R., Favrat, D., 1999a, An Approach for the Time-dependent Thermoeconomic Modeling and Optimization of Energy System Synthesis, Design and Operation (Part I: Methodology and Results), *International Journal of Applied Thermodynamics*, Vol. 2, No. 3.

Olsommer, B., von Spakovsky, M.R., Favrat, D., 1999b, An Approach for the Time-dependent Thermoeconomic Modeling and Optimization of Energy System Synthesis, Design and Operation (Part II: Reliability and Availability), *International Journal of Applied Thermodynamics*, Vol. 2, No. 4.

Paulus, D. and Gaggioli, R., Rational Objective Functions for Vehicles, AIAA Paper No. 2000-4852, *8th AIAA/USAF/NASA/ISSMO Symposium on Multidisciplinary Analysis and Optimization*, Long Beach, California, September 6-8, 2000.

Rao, S. S., 1996, Engineering Optimization-Theory and Practice, John Wiley and Sons, N.Y.

Resetar, S.A., Rogers, J.C., and Hess, R.W., Advanced Airframe Structural Materials: A Primer and Cost Estimating Methodology, RAND, R-4016-AF, Jan 1, 1991.

SAE Aerospace Applied Thermodynamics Manual, 1969, Society of Automotive Engineers, New York.

SAE AIR 1168/8, 1989 Aircraft Fuel Weight Penalty Due to Air Conditioning SAE Aerospace Applied Thermodynamics Manual, Warrendale, PA.

Sama D. A., 1995, Second Law Insight Analysis Compared with Pinch Analysis as a Design Method, *Second Law Analysis of Energy Systems: Towards the 21st Century*, University of Rome, Rome Italy, July.

Sama D. A., 1995, Differences Between Second Law Analysis and Pinch Technology, *Journal of Energy Resources Technology*, ASME Transactions. Vol. 117, pp. 186-190

Sama, D.A., Qian, S., Gaggioli, R., 1989, A common Sense Second Law Approach for Improving Process Efficiencies, *International Symposium on the Thermodynamic Analysis and Improvement of Energy Systems*, ASME, Pergamon Press, Beijing.

Sciubba E., 1999, Extended Exergy Accounting: Towards an Exergetic Theory of Value, *Efficiency, Costs, Optimization, Simulation and Environ-mental Aspects of Energy Systems* (ECOS'99), Tokyo Institute of Technology, ASME, Tokyo, June.

Sciubba, E., 1995, Artificial Intelligence Applications to the Synthesis of Thermal Processes, *Second Law Analysis of Energy Systems: Towards the 21st Century*, ASME, Univ. di Roma.

Sciubba, E., 1998, Artificial Intelligence in Thermal Systems Design: Concepts and Applications, Nova Science Publishers, Commack, N.Y.

Shah, R.K. and Webb, R.L., 1982, Compact and Enhanced Heat Exchangers, in Heat Exchangers: Theory and Practice, J. Taborek, G.F. Hewitt, and N. Agfan editors, Hemisphere Publishing Corporation, pp 435-468

Shah, R.S., 1981, Compact Heat Exchanger Design Procedure, in Heat Exchangers, Thermal-Hydraulic Fundamentals and Design, S. Kakac, A.E. Bergles and F. Matinger editors, Hemisphere Publishing Corporation, pp 495-536.

Sobieszczanski-Sobieski, J, 1989, Optimization by Decomposition: A step from Hierarchic to Non-hierarchic Systems, NASA CP-3031, Part 1.

Sobieszczanski-Sobieski, J, 1990, Sensitivity of Complex, Internally Coupled Systems, *AIAA Journal*, Vol. 28, pp.153-161, January.

Sobieszczanski-Sobieski, J. and Haftka, 1997, Multidisciplinary Aerospace Design Optimization: Survey of Recent Developments, *Structural Optimization*, Vol. 14, No. 1, pp 1-23.

Szargut, J. and Petela, R., 1965, Exergy (in Polish), Warsaw.

Szargut, J., Morris, D. R., et al., 1988, Exergy Analysis of Thermal, Chemical, and Metallurgical Processes, Hemisphere Publishing Company, New York.

Tirpak, J.A., 2000, Can the Fighter Force Hold its Edge?. *Air Force Magazine*, Vol. 83, pp. 24-31

Tsatsaronis, G. and Pisa, J., 1994, Exergoeconomic Evaluation and Optimization of Energy Systems-Application to the CGAM Problem, *Energy-The International Journal*, Vol. 19, No. 3, pp. 287-321.

Tsatsaronis, G. and Winhold, M., 1984, Thermoeconomic Analysis of Power Plants, EPRI AP-3651 Project 2029-8, Palo Alto, California, Electric Power Research Institute.

Tsatsaronis, G., 1985, Thermoökonomische Analzse von Energieumwandlungs-prozessen, Dr. Habilitatus Thesis, Dept. of Mechanical Engineering, Technical University of Aachen, West Germany.

Tsatsaronis, G., and Pisa, J., 1994, Exergoeconomic Evaluation and Optimization of Energy Sytsems: Application to the CGAM Problem, *Energy: The International Journal*, Vol. 19, No. 3, pp. 287-321, Pergamon, Great Britain.

Tsatsaronis, G., Pisa, J., et al., 1989, Thermodynamic Analysis and Improvement of Energy Systems, *Proceeedings of the International Symposium, Beijing, China*, Pergamon Press, pp. 195-200.

Valero, A., Lozano, M., et al., 1994, Application of the Exergetic Cost Theory to the CGAM Problem, *Energy-The International Journal*, Vol. 19, No. 3, pp. 365-381.

Valero, A., Lozano, M., et al., 1994, CGAM Problem: Definition and Conventional Solution, Ener*gy-The International Journal*, Vol. 19, No. 3, pp. 279-286.

Valero, A., Lozano, M.A., and Muñoz, M., 1986, A General Theory of Exergy Savings (Parts I, II, and III), *Computer-Aided Engineering of Energy Systems*, ASME, AES-Vol. 2-3, pp. 1-21.

Valero, A., Serra, L., Lozano, M.A., 1993, Structural Theory of Thermoeconomics, *Thermodynamics and the Design, Analysis and Improvement of Energy Systems, ASME*, AES-Vol. 30, N.Y., N.Y..

Valero, A., Serra, L., Lozano, M.A., and Torres, C., 1994, Application of the Exergetic Cost Theory to the CGAM Problem, *Energy: The International Journal*, Vol. 19, No. 3, pp. 365-381, Pergamon, Great Britain.

von Spakovsky M.R., 1986, A Practical Generalized Analysis Approach for the Optimal Thermoeconomic Design and Improvement of Real-World Thermal Systems, School of Mechanical Engineering, Georgia Institute of Technology, Ph.D. Dissertation.

von Spakovsky M.R., Evans R.B., 1984, Detailed Second Law Design of Components in Complex Thermal Systems, *Second Law Aspects of Thermal Design*. HTD Vol. 33, ASME, N.Y., N.Y., August.

von Spakovsky M.R., Frangopoulos, C.A., 1994, The Environomic Analysis and Optimization of a Gas Turbine Cycle with Cogeneration, *Thermodynamics and the Design, Analysis and Improvement of Energy System*s, ASME, AES-Vol. 33, N.Y., N.Y., November.

von Spakovsky, M., 1994, Application of the Functional Analysis to the Analysis and Optimization of the CGAM Problem, *Energy-The International Journal*, Vol. 19, No. 3, pp. 343-364.

von Spakovsky, M.R., 1994, Application of Engineering Functional Analysis to the Analysis and Optimization of the CGAM Problem, *Energy: The International Journal*, Vol. 19, No. 3, pp. 343-364, Pergamon, Great Britain.

von Spakovsky, M.R., and Evans, R.B., 1993, Engineering Functional Analysis (Part I), *Journal of Energy Resources Technology*, ASME Transactions, Vol. 115, No. 2, N.Y., June.

von Spakovsky, M.R., and Frangopoulos, C.A., 1993, The Environomic Analysis and Optimization of Energy Systems (Part II), *Proceedings of the International Conference on Energy Systems and Ecology*: ENSEC'93, Vol. I, pp. 123-132, ASME, Cracow, Poland, July.

WATE User's Guide, 1999, NASA Lewis Research Center.

Wepfer, W. and Gaggioli, R., 1978, Reference Datums for Available Energy. ACS Symposium Series 122, Washington, D.C., American Chemical Society.

Zimering, B. et al, 1999, Gas Turbine Power Generation System Configuration Study and Optimization, *1999 International iSIGHT Users Conference*, Chapel Hill, N.C., Oct 4-6.

Vita

Jules Ricardo Muñoz Guevara was born in Paz de Ariporo, Colombia on September 10, 1971. After graduating with honors from Colegio Nacional de Sugamuxi he served as a soldier in the Colombian Army. He then attended Universidad del Valle in Cali, Colombia, and in early 1995 he received his Bachelor of Science degree with honors in Mechanical Engineering. After graduation he worked for Carvajal S.A. a Colombian paper and publishing company as a project engineer. In 1995 he was awarded with the first Tulane ESL fellowship. In 1996 he initiated his graduate studies at Tulane University and received a Master of Science degree in Mechanical Engineering in 1997. Upon completion of his Ph.D. he will work as research engineer in the energy systems division of United Technologies Research Center in East Hartford, CT.